# UNIVERSITA' DEGLI STUDI DI PADOVA


**DIPARTIMENTO DI SCIENZE ECONOMICHE ED AZIENDALI "M. FANNO"**

**CORSO DI LAUREA MAGISTRALE IN ECONOMICS AND FINANCE**


**TESI DI LAUREA**

## "THE IMPACTS OF UNCERTAINTY SHOCKS ON THE GLOBAL FINANCIAL CYCLE: A MULTIPERSPECTIVE SVAR ANALYSIS"


**RELATORE:**

**CH.MO PROF. EFREM CASTELNUOVO**

**LAUREANDO: RUGGERO PITTINI**

**MATRICOLA N. 2023146**


**ANNO ACCADEMICO 2022 – 2023**

Dichiaro di aver preso visione del "Regolamento antiplagio" approvato dal Consiglio del Dipartimento di Scienze Economiche e Aziendali e, consapevole delle conseguenze derivanti da dichiarazioni mendaci, dichiaro che il presente lavoro non è già stato sottoposto, in tutto o in parte, per il conseguimento di un titolo accademico in altre Università italiane o straniere. Dichiaro inoltre che tutte le fonti utilizzate per la realizzazione del presente lavoro, inclusi i materiali digitali, sono state correttamente citate nel corpo del testo e nella sezione 'Riferimenti bibliografici'.

*I hereby declare that I have read and understood the "Anti-plagiarism rules and regulations" approved by the Council of the Department of Economics and Management and I am aware of the consequences of making false statements. I declare that this piece of work has not been previously submitted – either fully or partially – for fulfilling the requirements of an academic degree, whether in Italy or abroad. Furthermore, I declare that the references used for this work – including the digital materials – have been appropriately cited and acknowledged in the text and in the section 'References'.*

Firma (signature)

**ABSTRACT**

This thesis aims to investigate the role of global uncertainty shocks in affecting the Global Financial Cycle (GFC). Three kinds of uncertainty are considered: financial uncertainty, the uncertainty surrounding economic policies and the geopolitical uncertainty. The contribution and the impact of each uncertainty shock is assessed through a SVAR analysis, that employs multiple sets of identification strategies and estimation techniques. Specifically, the uncertainty shocks are identified alternatively with the Cholesky decomposition technique and with the Penalty Function Approach, whereas the VAR models are estimated by means of OLS and Bayesian estimations. We find that the three uncertainty measures have heterogenous effects on GFC, which are substantially negative and depend on the underlying econometric specification. However, financial uncertainty, as measured by the Global Financial Uncertainty indicator, proves to be the most important driver of GFC, since its shock explains the highest percentage of variance of GFC and triggers the most relevant reaction in GFC in every econometric specification.

**CONTENTS**

*LIST OF FIGURES*

**LIST OF TABLES**

**LIST OF EQUATIONS**

## INTRODUCTION

Globalization is a phenomenon that has affected our world since the first decades from the end of World War II, becoming more and more evident over the course of the years. It involves many aspects of our reality, ranging from society to economics, and, in a simple way, it could be defined as the process of increasing worldwide integration from a political, social, cultural, and economic standpoint (Cambridge Dictionary). In particular, financial globalization concerns the increasing volume of cross-border financial flows among economies from many different areas of the world, facilitated by technical advances and financial market deregulation (Kose et al., 2006). Consistently with this framework, Helene Rey documented the existence of the Global Financial Cycle, the phenomenon representing the high degree of co-movement in risky asset prices, capital flows, leverage, and financial aggregates around the world (Miranda - Agrippino and Rey, 2021).

The aim of this thesis is to investigate the role of global uncertainty in affecting the Global Financial Cycle, by examining the contribution of several sources of uncertainty. Overall, three kinds of uncertainty are considered: geopolitical uncertainty, the uncertainty surrounding economic policies, and financial uncertainty.

Each type of uncertainty will be proxied by a specific index. The geopolitical uncertainty will be measured by the Geo-Political Risk (GPR) index, the economic policies' uncertainty by the Global Economic Policy Uncertainty (GEPU) index and, finally, the financial uncertainty by the Global Financial Uncertainty (GFU) index.

The first chapter will introduce the Global Financial Cycle and it will briefly explain why uncertainty could be a determinant for the Global Financial Cycle. In addition, it provides a definition of the three measures of uncertainty, i.e., GEPU, GPR, and GFU, and a brief literature review of their effects on some of the most important macroeconomic aggregates.

Chapter 2 details the state of the art of the econometric techniques employed to carry out the empirical research by providing a brief dissertation on Structural Vectorial Auto Regressive (SVAR) models, Impulse Response Functions (IRFs), Forward Error Variance Decompositions (FEVDs), Bayesian econometrics, Cholesky decomposition, and the Penalty Function Approach (PFA).

Chapter 3 describes the econometric framework and the identification strategies employed to carry out the analysis. To sum up, a specific SVAR model is implemented for each kind of

uncertainty and, for every model, three strategies are taken into account to identify the structural uncertainty shock. The first one consists just of zero-restrictions on the Cholesky decomposition of the variance-covariance matrix of the reduced form VAR model. By construction, it provides a lower bound estimate of the effects of uncertainty shocks. The second one follows the Penalty Function Approach, elaborated by Uhlig (2005), and assumes the Minnesota prior distribution for the reduced form parameters. More precisely, it coincides with the identification strategy used by Caldara et al. (2016). Notice that, by construction, the PFA estimates the effects of uncertainty shocks at their maximums. The third and last identification strategy follows the PFA as well, but it imposes the Conjugate Gaussian Inverse-Wishart prior distribution for the reduced form parameters. It aims mainly at testing whether the results coming from the second specification change with varying the prior for the reduced form parameters.

Chapter 4 outlines a preliminary analysis of the uncertainty measures with respect to the business cycle and the GFC, focusing on pairwise correlations and Granger causalities. These instruments will be used also to analyse the relationships between the three kinds of uncertainty. By considering the Granger causality tests, GFC seems to be steadily predated by movements in the GFU index. In addition, the three uncertainty measures do not exhibit significant pairwise correlations and, hence, each of them should convey a distinct type of information.

The results of the analysis will be illustrated in the fifth and last chapter. The role of each kind of uncertainty in determining the GFC is evaluated through the Impulse Response Function of GFC to the uncertainty shock and through the relevance of the GFC in the Forward Error Variance Decomposition of each uncertainty shock. It emerges that both GEPU and GFU shocks impact significantly on the GFU and, in particular, GFU provides the most remarkable contribution in terms of IRF and FEVD, regardless of the selected identification strategy.

# 1.THE GLOBAL FINANCIAL CYCLE AND GLOBAL UNCERTAINTY MEASURES: A BRIEF LITERATURE REVIEW

This chapter will be devoted to briefly review the literature concerning the Global Financial Cycle and uncertainty, with a focus on the measures of global uncertainty that will be used for the empirical analysis, i.e., the GEPU, GFU and GPR indexes. More specifically, the first part of this chapter will concern the definition and the facts related to the Global Financial Cycle and economic uncertainty, whereas the second one will be about the documented effects of the three overmentioned measures of global uncertainty.

## *1.1 The Global Financial Cycle: definition and linked global factors*

Helene Rey (2013) documented that the time series of capital inflows, capital outflows, credit growth, leverage, and risky assets prices from many areas of the world follow the same common cyclical pattern synchronized with the VIX index. The latter is a measure of the realized volatility of the U.S. stock market based on the prices of the S&P 500 index call and put options. She called this phenomenon "Global Financial Cycle" (Rey, 2013).

More specifically, she firstly reported a negative correlation of VIX with gross capital flows, credit growth and the levels of leverage observed in the main financial centres. Secondly, by employing a dynamic factor model on a large cross section of 858 risky assets coming from all around the world, she showed that about a quarter of the variance of risky returns is explained by one single global factor, that exhibits a strong negative correlation with VIX (Rey, 2013). The sample of risky assets covers commodity prices, corporate bonds and the components of the equity indices traded in the largest markets worldwide, considering a period from 1990 to 2010 (Miranda - Agrippino and Rey, 2021).

The latter result has been confirmed more recently by Miranda - Agrippino, Nenova and Rey in an analysis which has been extended over the sample and enriched in variety with respect to the original one. This study also reports a negative correlation between the global factor and VIX which amounts to -0,649 (see Miranda - Agrippino and Rey, 2021).

In addition, Miranda - Agrippino and Rey (2021) documented the existence of two global factors for worldwide gross capital inflows and outflows, using a dynamic factor model similar to the one exploited to estimate the global factor for risky assets' prices. These two global

factors together account for about thirty five percent of the variance of gross capital flows and the first one is highly correlated with the global factor in asset prices - the pairwise correlation amounts to 0,815. The latter result led the authors to interpreting the global factor in risky assets prices and the first global factor in gross capital flows as the factors that reflect GFC. Since both factors explain a significant share of variation of the respective data, they concluded that GFC plays an important role in characterizing fluctuations in world risky assets prices and international gross capital flows.

As previously mentioned, the global factors are estimated using Dynamic Factor Models (DFM). The authors assumed that the cross-section of data $x_t$ – whether asset prices, capital flows, or private credit – can be represented as the sum of two orthogonal components, as in:

$$x_t = \Lambda f_t + \kappa_t \qquad (1.1)$$

where $f_t$ and $\kappa_t$ are vectors which collect the common factors and the idiosyncratic terms specific to $x_t$, respectively. Each factor loading represent the extent to which each variable in $x_t$ loads on the common factors and is stored in the matrix $\Lambda$ (Miranda - Agrippino and Rey, 2021).

For further technical details about the dynamic factor model, see Miranda - Agrippino and Rey (2020).

It is important to disclose that our empirical research will focus just on the global factor related to risky assets prices, which will be denoted by GFC for simplicity. The related time series is illustrated by *Figure 1*, which considers a time window which spans from January 1990 to April 2019.

### *1.2. Uncertainty*

The modern definition of uncertainty was provided by the notorious economist Frank Knight (1921). According to him, uncertainty refers to any circumstance where the odds of possible outcomes are unknown and hence it is impossible to make precise forecasts about the likelihood of events happening. Importantly, it does not coincide with risk that, instead, denotes situations

where estimating the likelihood of future realizations is possible. Therefore, both uncertainty and risk share randomness, but only risk entails quantifiable randomness (Knight, 1921).

However, despite this difference, we will use the term "uncertainty" to indicate a mixture of both concepts, hereafter. In addition, we define uncertainty shocks as sudden events that raise the number of possible future scenarios, generating more heterogenous forecasts. Uncertainty shocks make forecasting more complicated.

Uncertainty can be measured in many ways, but this dissertation will consider only two kinds of measures: the text-based measures and the implied volatility measures.

Implied volatility measures rely on the assumption that the volatility of a data series is a good proxy for the related uncertainty since the higher the volatility is, the harder it is to forecast the series. Relevant examples of such measures are the VIX and GFU indexes (Bloom, 2014).

Text-based measures of uncertainty, instead, estimate the quantity of uncertainty as the frequency of newspaper articles containing words that are usually related to uncertainty. The GEPU and GPR indexes are both text-based measures (Bloom, 2014).

### *1.2.1 The interconnection between economic growth and uncertainty*

Uncertainty seems to be countercyclical, in the sense that it spikes during recessions, regardless of whether it concerns macroeconomic aggregates or microeconomic ones. As a matter of fact, theory literature provides evidence that surges in uncertainty might be led by bad economic conditions. In addition, some exogenous shocks that typically cause recessions, such as oil price shocks, terrorist acts, financial panics, and wars, might increase uncertainty. Indeed, these dramatic events reduce people's confidence in their forecasts on future economic growth. Lastly, uncertainty shocks seem to negatively impact on business cycle (Bloom, 2014).

There are multiple reasons why recessions might trigger higher macroeconomic uncertainty. First, a deteriorated business induces firms to trade less actively and thereby to spread less public information, which increases uncertainty. Furtherly, there is evidence that firms are more willing to innovate in distressed times, destinating more resources to research and development. This generates heightened microeconomic uncertainty, which could induce potentially higher macroeconomic one. In addition, people are less confident during recessions, since they are unfamiliar with such rare events. A lower level of confidence makes forecasting harder. Lastly,

economic policies tend to be more unclear and experimental during recessions, raising uncertainty (Bloom, 2014).

As well as macroeconomic uncertainty, financial uncertainty rises in correspondence of recessions too. As a matter of fact, several financial prices, such as stock market returns, exchange rates and bond yields, experience a surge in volatility during recessions. For example, the VIX index, which measures stock market volatility, increases by 58 percent on average. This could be due mainly to two reasons. First, firms tend to increase their level of indebtedness during recessions and, as a result, their stock-returns volatility rises. Second, recessions trigger higher risk aversion, which in turn causes higher option prices and thereby higher levels of the VIX index (Bloom, 2014).

As previously mentioned, economic literature provides evidence that a rise in uncertainty leads to lower levels of economic growth in the short run. In fact, it reduces investment, consumption and hiring through several mechanisms and raises the borrowing costs for every kind of financial player (Bloom, 2014).

An important channel through which uncertainty affects consumption, investment, and hiring is represented by the positive effect of heightened uncertainty on the value of real options which consumers and firms are provided with. More specifically, an uncertainty shock raises the option value of waiting related to investment and hiring decisions of firms and to the decisions of purchasing durable goods. In fact, such choices cannot be reverted without bearing an irreversible capital cost and, hence, when uncertainty is high, people find more convenient to postpone them. Summing up, an uncertainty shock causes a drop in consumption, investment and hiring by making economic players more cautious. Secondly, a higher level of uncertainty leads consumers to increase their precautionary savings, which reduces consumption and is likely to negatively impact on economic growth in the short run. Finally, a rise in uncertainty causes a drop in investment due to the lack of diversification usually observed in top managers. Indeed, an executive whose financial assets and human capital are disproportionately tied up in their firm is likely to delay long-term investment decisions, when uncertainty is high (Bloom, 2014).

Heightened uncertainty raises the cost of finance since it mainly increases risk premia (Bloom, 2014). As a matter of fact, when uncertainty grows, investors want to be compensated for the higher levels of risk in their investments and will demand a higher excess return, since they are risk averse. In order to achieve this objective, they will be less willing to pay every kind of risky

financial asset and, as a consequence, the prices of risky financial assets fall, which makes it harder to raise funds for firms and financial institutions.

In conclusion, uncertainty and the business cycle are deeply interconnected and influence each other. It is useful for our empirical research to identify the channels through which uncertainty affects economic growth since it allows us to elaborate a hypothesis as to how a global uncertainty shock may impact on macroeconomic aggregates and especially on the global factor of worldwide risky assets prices. In fact, following these arguments, the world economic growth and GFC should drop in response to a rise in worldwide uncertainty. More specifically, due to the overmentioned irreversible capital adjustment costs, firms tend to postpone important investment decisions in periods of elevated uncertainty, which negatively impacts on their financial assets value. In fact, in response to a reduced volume of financial assets in firms' balance sheets, investors expect lower future profits from firms, leading to lower returns for firms' financial assets, for example. Hence, the GFC, which is based on the returns of worldwide financial assets, experiences a low phase.

### *1.3 Uncertainty measures and their economic and financial impacts*

This paragraph will briefly present the measures of uncertainty which will be used for the empirical research. In addition, some of their documented effects on macroeconomic and financial aggregates will be illustrated.

#### *1.3.1 GFU*

The Global Financial Uncertainty index is a measure of global financial uncertainty, elaborated by Castelnuovo and Caggiano in 2022. They computed the GFU index by estimating a dynamic hierarchical factor model a la Moench, Ng, and Potter (see Caggiano and Castelnuovo, 2023). It is based on about 38,000 financial volatility observations covering the period from 1992 to 2020 and including 42 countries from all over the world, which account for about 83% of global industrial production (Caggiano and Castelnuovo, 2023).

By estimating several SVAR models, they concluded that GFU shocks negatively impacts on GFC and World Industrial Production (WIP), a measure of global output that will be explained in detail afterwards. The median contribution of such shocks to GFC variance and to that of global output is about 30% and 9%, respectively. Besides, they showed that GFU shocks were

relevant in determining the loss in WIP observed during the Great Recession: in absence of GFU shocks, loss would have been 13% lower in magnitude (Caggiano and Castelnuovo, 2023).

GFU index turns out to be a reliable measure of global financial uncertainty for many reasons. First of all, it spikes in association with well-known historical episodes of global financial volatility, e.g., the Great Recession, and it is highly and positively correlated with proxies for global financial uncertainty, such as VIX and the financial uncertainty index recently proposed by Ludvigson, Ma, and Ng (Caggiano and Castelnuovo, 2023).

Secondly, it shows a strong positive correlation with uncertainty specific to "hegemon" areas, such as Europe and North America. On the other hand, GFU is correlated with uncertainty in small-open economies, e.g., Australia, and it is poorly correlated with uncertainty specific to areas and countries that typically follow idiosyncratic dynamics, such as Italy and China (Caggiano and Castelnuovo, 2023).

Besides, the authors found, through a SVAR analysis, that GFU outperforms VIX in impacting GFC, even though it displays a lower correlation with GFC than VIX. Their interpretation, indeed, is that GFU is a more proper measure for global financial volatility, given that it is based on volatilities coming from all around the world and not only from the US market, as instead VIX does. Hence, VIX is not a perfect substitute for GFU, as illustrated by *Figure 3*, and it can function just as a mere proxy for GFU. As a matter of fact, GFU seems to react more to the Great recession compared to VIX. In that period, GFU peaks with a value that is 5,5 times higher than the value that it records in the first month of 2008, while the maximum associated to VIX is just 2,5 times bigger than its own value in the first month of 2008 (Caggiano and Castelnuovo, 2023).

### *1.3.2 GEPU*

The Global Economic Policy Uncertainty (GEPU) index is a measure of global uncertainty regarding economic policies, ideated by Baker, Bloom and Davis in 2016. It is the GDP-weighted average of the country-specific Economic Policy Uncertainty (EPU) index of 21 countries from all around the world, that cover two-thirds of global output (Baker, Bloom, and Davis, 2016).

The EPU index quantifies the policy-related economic uncertainty of a given country and was computed by Baker, Bloom and Davis as well. It is based on the share of newspaper articles related to economic policy uncertainty published in a given month. More specifically, this index

is constructed on an algorithm that selects the newspaper articles containing at least a term for each of the following three categories: uncertainty, economy, and policy. The aim of EPU is to capture uncertainty about the contents of economic policies, their economic implications and the subjects that eventually will make such decisions (Baker, Bloom, and Davis, 2016).

The EPU index turns out to be a reliable measure of economic policy uncertainty, being strongly correlated with other text-based measures of policy uncertainty, e.g., the frequency with which the Federal Reserve System's Beige Books mention policy uncertainty. Notably, the US EPU spikes around 9/11, COVID-19 pandemics, the Lehman Brothers bankruptcy, and other well-known episodes of elevated economic policy uncertainty for US. In addition, it received significant market validation, since it is used by important commercial data providers, including Bloomberg and FRED. Lastly, a human audit on 12,000 articles drawn randomly from U.S. newspapers was carried out in order to provide a further robustness check. The human- and computer-generated indices turn out to be highly correlated (Baker, Bloom, and Davis, 2016).

As regards the macroeconomic effects of EPU, its shocks are found to foreshadow declines in investment, output, and employment in the United States and in 12 relevant economies (Baker, Bloom, and Davis, 2016).).

The authors realized two versions of GEPU, both starting in 1997 and being updated approximately every month. This research will focus just on the one based on PPP-adjusted GDP. This kind of GEPU Index clearly peaks in reaction to historical events characterized by heightened worldwide economic policy uncertainty, chiefly the Asian and Russian Financial Crises, 9/11, the Great Recession in 2008- 09 and, the burst of COVID-19 pandemics in 2020. This pattern, which is extremely consistent with the theoretical time path of global uncertainty surrounding economic policies, confirms the plausibility of the GEPU index (Baker, Bloom, and Davis, 2016).

*Figure 4* plots GEPU time series in subsample which goes from January 1997 and April 2019.

Finally, GEPU was found to affect crude oil volatility (Yongjian Lyu et al., 2021) and stock volatility in nine emerging economies (Yu, Huang, and Xiao, 2021). Besides, Ozcelebi (2021) showed that GEPU has an impact on the global economic activity and hence on oil prices.

### *1.3.3 GPR*

The geopolitical risk index captures the uncertainty concerning geopolitics or better still the circumstance that international actors will continue to have peaceful relationships with each other. It was elaborated by Caldara and Iacoviello (2022) and it aims at measuring the geopolitical risk as perceived by newspapers, investors, and people in general. The authors define geopolitical risk as "the threat, realization, and escalation of adverse events associated with wars, terrorism, and any tensions among states and political actors that affect the peaceful course of international relations" (Caldara and Iacoviello, 2022, p.1197).

The time series has a monthly frequency, starting in 1985, and it is updated on a monthly basis. The GPR is equal to the number of newspapers articles which discuss adverse geopolitical events and threats, in a given month, divided by the total number of published articles in the same month. This share was computed by applying a specific algorithm. The selected newspapers are six leading newspapers from US, United Kingdom, and Canada, which means that GPR reflects the perspective of just a few countries. The articles contributing to GPR mention words that align with the definition of geopolitical risk given by the authors or that in general have a high probability to be associated with adverse geopolitical events (Caldara and Iacoviello, 2022).

GPR index turns out to be a plausible measure of geopolitical risk for a variety of motives. First of all, it peaks during well-known historical episodes of war and international crises, such as the Gulf War, the 2003 invasion of Iraq, and the North Korea crisis in 2017-2018, as showed by *Figure 2*. Additionally, relevant spikes are reached after notorious terrorism acts, such as 9/11 and Paris terrorist attack. Importantly, differently from GEPU and GFU, it does not react at all to the Great financial crisis, highlighting the fact that it captures just geopolitical risk fluctuations. Another key feature of GPR time series is its high volatility compared to GFU and GEPU (Caldara and Iacoviello, 2022).

Besides, the authors carried out a formal audit of a sample of 7,000 newspaper articles, found GPR being highly correlated with a narrative counterpart and performed other robustness checks that furtherly testify that GPR is an accurate and meaningful index (Caldara and Iacoviello, 2022).

GPR has important macroeconomic effects. As a matter of fact, shocks to geopolitical risk have been found to lead a reduction in stock prices, investment, and employment. In addition, there

is a link between higher values of the GPR index and higher probability of economic disasters, lower expected GDP growth, and higher downside risks to GDP growth (Caldara and Iacoviello, 2022).

# 2. STATE OF THE ART

This chapter will provide an introductory illustration of the state of the art of structural and reduced form Vectorial Autoregressive (VAR) models, detailing the tools, the identification methods, and the estimation techniques that will be employed for carrying out the empirical research of Chapters 4 and 5. The same notation will be used for denoting variables along the entire chapter, exception made for the cases where variables are explicitly specified in different manners.

## *2.1 VAR models*

Vector Autoregressive (VAR) models are one of the most widely used tools for carrying out empirical researches concerning multivariate time series, in particular when referring to the fields of macroeconomics and finance (Kilian and Lütkepohl, 2017). In fact, since the seminal work of Sims (1980), they have proved to be extremely useful and reliable instruments for forecasting and for describing economic and financial time series (Stock and Watson, 2001).

VAR models are the vector generalization of univariate autoregressive processes. They assume that each variable is a linear function of at least its own past and of the past of the other model variables. More specifically, given a number k of variables, VAR models consist of a system of k linear regression equations, each one regressing a specific model variable on its own lagged values and on the lagged values of the remaining k-1 variables. The maximum number of lags considered takes the name of "lag-order" or simply "order" of the VAR model. A VAR model of order p, commonly referred to as VAR(p), is indeed a model that takes account of the lagged observations of the data series up to the p-th lag. The data frequency is usually monthly or quarterly (Kilian and Lütkepohl, 2017).

There are two main versions of VAR models: reduced form VAR models and structural VAR models. Reduced form VAR models assume that all the actual values of the k time series are explained by just their own lagged values, the lagged values of the other model variables, a constant, and an error term. Therefore, the contribution of contemporaneous relationships between the variables is excluded in a reduced form VAR model. The observed time path of a set of macroeconomic aggregates is generally approximated by reduced form VAR models, since they provide a reliable finite-order approximation for general linear processes (Kilian and Lütkepohl, 2017).

If we suppose p being equal to two and the number of model variables equal to 3, we get the following reduced form VAR model:

$$\begin{cases} x_t = c_1 + a_{11,1}x_{t-1} + a_{12,1}\, z_{t-1} + a_{13,1}g_{t-1} + a_{11,2}x_{t-2} + a_{12,2}\, z_{t-2} + a_{13,2}g_{t-2} + u_{1t} \\ z_t = c_2 + a_{21,2}x_{t-1} + a_{22,1}\, z_{t-1} + a_{23,1}g_{t-1} + a_{21,2}x_{t-2} + a_{22,2}\, z_{t-2} + a_{23,2}g_{t-2} + u_{2t} \\ g_t = c_3 + a_{31,2}x_{t-1} + a_{32,1}\, z_{t-1} + a_{33,1}g_{t-1} + a_{31,2}x_{t-2} + a_{32,2}\, z_{t-2} + a_{33,2}g_{t-2} + u_{3t} \end{cases}$$

*(2.1)*

Its vector representation is:

$$\boldsymbol{y_t = c + A_1 y_{t-1} + A_2 y_{t-2} + u_t},$$

*(2.2)*

where $\boldsymbol{y_t}$, $\boldsymbol{y_{t-1}}$, and $\boldsymbol{y_{t-2}}$ are the vectors collecting, respectively, the actual values of model variables, the values at lag 1, and the values at lag 2. The vector of error terms -also referred to as residuals or innovations- denoted by $\boldsymbol{u_t}$, represent the unpredictable component of each equation, given the past observations of model variables. It is supposed to be a zero mean white noise process with covariance matrix $\boldsymbol{\Sigma_u}$, in order to allow for serially uncorrelated error terms. However, notice that this hypothesis does not rule out mutual correlation of residuals. In addition, $\boldsymbol{A_1}$, and $\boldsymbol{A_2}$ are the matrix containing the coefficients associated to first lags and second lags variables, respectively. Lastly, $\boldsymbol{c}$ denotes the vector of constants, as follows:

$$\boldsymbol{y_t} = \begin{pmatrix} x_t \\ z_t \\ w_t \end{pmatrix},\ \boldsymbol{c} = \begin{pmatrix} c_1 \\ c_2 \\ c_3 \end{pmatrix},\ \boldsymbol{A_i} = \begin{pmatrix} a_{11,i} & a_{12,i} & a_{13,i} \\ a_{21,i} & a_{22,i} & a_{23,i} \\ a_{31,i} & a_{32,i} & a_{33,i} \end{pmatrix}, i = 1,2,\ and\ \boldsymbol{u_t} = \begin{pmatrix} u_{1t} \\ u_{2t} \\ u_{3t} \end{pmatrix}$$

However, a more compact way to write reduced form VARs is the so-called "companion form". It allows to represent a generic k-dimensional VAR(p) process as the following pk-dimensional VAR (1) process:

$$\boldsymbol{Y_t = c + AY_{t-1} + U_t},$$

*(2.3)*

where

$$\underset{kp \times 1}{\boldsymbol{c} \equiv \begin{bmatrix} c \\ 0 \\ \vdots \\ 0 \end{bmatrix}}, \qquad \underset{kp \times kp}{\boldsymbol{A} \equiv \begin{bmatrix} \boldsymbol{A_1} & \boldsymbol{A_2} & \dots & \boldsymbol{A_{p-1}} & \boldsymbol{A_p} \\ \boldsymbol{I_k} & \boldsymbol{0} & \dots & \boldsymbol{0} & \boldsymbol{0} \\ \boldsymbol{0} & \boldsymbol{I_k} & & \boldsymbol{0} & \boldsymbol{0} \\ \vdots & & \ddots & \vdots & \vdots \\ \boldsymbol{0} & \boldsymbol{0} & \dots & \boldsymbol{I_k} & \boldsymbol{0} \end{bmatrix}}, \qquad \text{and } \underset{kp \times 1}{\boldsymbol{U_t} \equiv \begin{bmatrix} u_t \\ 0 \\ \vdots \\ 0 \end{bmatrix}}$$

The matrix **A** is referred to as the companion matrix of the process. The matrixes **A** and $\boldsymbol{\Sigma_u}$ and the vector $\boldsymbol{c}$ are defined as the reduced form parameters of the VAR model. $\boldsymbol{Y_t}$ equals to $\left(\boldsymbol{y_t'}, \dots, \boldsymbol{y_{t-p+1}'}\right)'$ and $\boldsymbol{I_k}$ corresponds to the k-dimensional identity matrix (Kilian and Lütkepohl, 2017).

An important property of VAR models is stability since, if present, it allows to express key features of the time series into an easy form and to deduce stationarity. Relatively to linear difference equations, a stable model is such that a shock to one of the model variables does not lead to persistent variations in model variables (Hamilton, 1994). Formally, a VAR process is stable if all the roots of its own characteristic lag polynomial lie outside the unit circle or, equivalently, if all the eigen values of the related companion matrix **A** lie inside the unit circle (Kilian and Lütkepohl, 2017).

Stability is useful since it implies weakly stationarity of the VAR process under the common assumptions that the mean is a constant term, and the residuals are white noises. In contrast, weakly stationarity always entails stability, but it is difficult to be assessed directly. A weakly stationary or covariance stationary process is such that its first and second moments exist and are time invariant. As regards VARs, they are stationary if all the model variables are stable. Weakly stationarity in VARs is extremely important, since it primarily allows the computation of FEVD and IRF and the existence of a unique companion matrix **A** (Kilian and Lütkepohl, 2017).

In this dissertation the hypothesis according to which the reduced form residuals follow a white noise process will be assessed graphically by means of the charts of the Sample Auto Correlation Function (SACF) and the overall time path of such errors. Indeed, if these two charts show specific characteristics, the process of the reduced form residuals can be reasonably approximated by a white noise one. More precisely, the sample autocorrelations must quickly die out, loosing almost completely significance after the first or second lag on the one hand, and the time series of residuals must not exhibit clear trends, on the other one.

Weakly stationarity allows to write the VAR process as the sum of its present and past innovations, using the so- called Wold Moving Average (MA) form:

$$\boldsymbol{y_t} = \boldsymbol{c} + \sum_{i=0}^{\infty} \boldsymbol{\Phi_i u_{t-i}} \,,$$

*(2.4)*

where $\boldsymbol{\Phi_0} = \boldsymbol{I_k}$, $\boldsymbol{\Phi_i} = \sum_{j=1}^{i} \boldsymbol{\Phi_{i-j} A_j}$, $\boldsymbol{i} = \boldsymbol{1, 2}$, ..., and $\boldsymbol{A_j} = \boldsymbol{0}$ for $j > p$.

This representation of a VAR process as a weighted average of its current and past shocks is extremely useful for expressing the structural IRF and FEVD into handy formats, as it will be better explained in the next paragraphs (Kilian and Lütkepohl, 2017).

In addition, weakly stationarity permits consistent estimates through classical methods, i.e., ML and OLS. However, it is not strictly required to get such a result. In fact, even in presence of unit rooted variables, standard estimation techniques can retrieve consistent estimates. As suggested by Canova (see Caggiano and Castelnuovo, 2023), it is enough to model possible unit-rooted variables in log-levels and to assess that estimated residuals are indeed white noises. If they are, then OLS or ML leads to consistent estimates; if they are not, instead, the order of the VAR model has to be increased.

### *2.1.1 Structural VAR models and the identification problem*

A structural VAR(p) model, often referred to as SVAR, is such that:

$$\boldsymbol{B_0 y_t} = \boldsymbol{B_1 y_{t-1}} + \cdots + \boldsymbol{B_p y_{t-p}} + \boldsymbol{w_t},$$

*(2.5)*

where $\boldsymbol{y_t}$ is the vector of the time series of interest as in equation *2.2*, $\boldsymbol{B_i}$ collects the slope coefficients at the i-th lag, analogously to $\boldsymbol{A_i}$ in equation *2.2*, $\boldsymbol{w_t}$ is the vector of the so-called structural residuals or shocks, and $\boldsymbol{B_0}$ is the matrix whose elements capture the contemporaneous relationship between model variables (Kilian and Lütkepohl, 2017)..

SVARs allow for instantaneous relations among model variables, differently from reduced form VARs. In addition, they assume that the structural shocks are zero mean white noises which are both serially and mutually uncorrelated. This implies that the covariance matrix of the structural

shocks $\boldsymbol{\Sigma_w}$ is a diagonal matrix of full rank, such that the number of variables coincides with the number of shocks. In other words, mutual uncorrelation allows to attribute a distinct kind of economic interpretation to each shock and, in this sense, these shocks are "structural". Besides, uncorrelation leads to the possibility of computing the IRFs of SVARs as simple functions of the structural shocks. Consequently, every fluctuation in the data series of a stable VAR could be viewed as generated by the structural innovations (Kilian and Lütkepohl, 2017)..

SVARs and reduced form VARs share an important link with each other: reduced form VARs indeed can be interpreted as the data created by an underlying SVAR. A SVAR model can be easily converted into the related VAR representation by multiplying both sides of equation *2.5* by $\boldsymbol{B_0^{-1}}$. Hence, $\boldsymbol{A_i = B_0^{-1} B_i}$ and $\boldsymbol{u_t = B_0^{-1} w_t}$. The reduced form innovations can be represented as linear combinations of the structural ones. On the other hand, knowing the matrix $\boldsymbol{B_0}$ or its inverse is all what we need to retrieve the SVAR process underlying an estimated VAR model. By normalizing $\boldsymbol{\Sigma_w}$ to the identity matrix $\boldsymbol{I_k}$ without any loss of generality, it is possible to use this equation to recover $\boldsymbol{B_0^{-1}}$:

$$\boldsymbol{\Sigma_u = B_0^{-1} B_0^{-1'}}$$

*2.6)*

This is a system of nonlinear equations, whose unknown parameters are the elements of $\boldsymbol{B_0^{-1}}$. It can be solved, only if the number of unknown parameters does not exceed the number of independent equations provided by $\boldsymbol{\Sigma_u}$. This is the so-called order condition, which is a necessary condition for the exact identification of structural shocks and it is not met in the equation. In fact, there are $k^2$ unknown parameter and only $k(k+1)/2$ independent equations. Consequently, it is necessary to impose some restrictions on the elements of $\boldsymbol{B_0^{-1}}$ to satisfy the order condition. Choosing the suitable economic restrictions in order to uniquely identify $\boldsymbol{B_0^{-1}}$, and hence the other structural parameters, represents the so-called identification problem in structural autoregressions. A variety of strategies has been implemented over the years to address this problem (Kilian and Lütkepohl, 2017).

However, this dissertation will present just those that will be employed in the empirical research of the next chapters, i.e., the widely used Cholesky decomposition, which leads to the recursively identified models, and the Penalty Function Approach (PFA). Before illustrating them, this chapter will be devoted to explaining IRF, FEVD, Granger causality, and Bayesian estimation.

### *2.2 Granger causality*

Granger proposed a way to assess the theoretic dynamic relationships between economic variables in a VAR framework, which nowadays takes the name of Granger causality (see Kilian and Lütkepohl, 2017). Let suppose a bivariate reduced form VAR (p) model with variables g and x:

$$\begin{cases} g_t = c_1 + a_{11,1} g_{t-1} + a_{12,1}\, x_{t-1} + a_{11,2} g_{t-2} + a_{12,2}\, x_{t-2} + u_{1t} \\ x_t = c_2 + a_{21,2} g_{t-1} + a_{22,1}\, x_{t-1} + a_{21,2} g_{t-2} + a_{22,2}\, x_{t-2} + u_{2t} \end{cases}$$

*(2.7)*

The variable x is said to Granger cause g, if x is helpful for predicting g, reducing the mean squared error for g. This happens if at least one of the lags associated with x displays a slope coefficient different from zero in the equation whose dependent variable is $g_t$. Therefore, a common way to assess whether x Granger causes g is to the test the null hypothesis that imposes joint zero restrictions on all the slope coefficients related to the lags of x in the overmentioned equation. This is typically done by conducting a standard Wald test, if the VAR model is weakly stationary. On the contrary, if we are not sure about the stationarity, it is recommended to add a number of lags to the VAR process equal to the suspicious integration order of the process. In Chapter 4, Granger causality analysis will be carried out only in bivariate VARs.

It is important to stress that Granger causality is not a bidirectional concept: if x is found to Granger cause g, g might not Granger cause x. Hence, it is required to run another test to evaluate if g Granger causes x. If both tests lead to the rejection of the null, x and g are said to be in a bidirectional Granger causality relationship.

Despite what its name might suggest, nowadays Granger causality is not used for establishing causal relationships among the variables of a VAR model. As a matter of fact, both Granger causality and Granger non causality between two variables can be justified by the omission of a third one or by other factors. Granger causality just reflects the dynamic correlations between variables and can be useful only for rejecting strict exogeneity of a variable with respect to another one. It does not entail causality but precedence. In fact, if x Granger causes g, x leads or predate movements in g and it is said to lead g. On the other hand, if there is a bidirectional

Granger causality between g and x, g and x are said to be in a feedback relationship (Kilian and Lütkepohl, 2017).

### *2.3 The structural Impulse Response Functions*

One of the main research questions investigated by economists concerns how economic aggregates react to unanticipated changes in another economic variable. With reference to equation *2.5*, this maps into assessing the effects of a one-time variation or impulse in the structural shocks $\boldsymbol{w_t}$ on the model variables $\boldsymbol{y_t}$, after having identified $\boldsymbol{w_t}$. Formally, given a number of periods h after the impulse to structural shock $q = 0,1,2,\dots,k$ occurred at time t (h is the so-called horizon), the marginal effect of the impulse of $w_{qt}$ on the model variable $y_{jt}$ is the partial derivative of $y_{jt}$ with respect to $w_{qt}$ at horizon h. This is the so-called structural impulse response of $y_{jt}$ to $w_{qt}$ at horizon h, denoted by $\theta_{jq,h}$ hereafter:

$$\theta_{jq,h} = \frac{\partial y_{j,t+h}}{\partial w_{qt}}, \qquad h = 0,1,2,\dots,H.$$

*(2.8)*

H is the maximum propagation horizon of the shock. The matrix whose elements are the structural impulse responses of $\boldsymbol{y_t}$ at a given horizon h for every different shock is the structural impulse response matrix at horizon h, which is equal to:

$$\boldsymbol{\Theta_h} = \frac{\partial \boldsymbol{y_{t+h}}}{\partial \boldsymbol{w_t'}}.$$

*(2.9)*

One of the main goals of economic SVAR analyses is typically to plot the impulse responses of each variable to a specific shock j over time, i.e., over different horizons, up to H. This gives place to k squared charts, defined as the structural impulse response functions. IRFs provide a useful representation of how much and in which direction the model variables react after an economically interpretable shock has occurred.

As previously mentioned, if a VAR (p) process is weakly stationary, a handy expression for the structural impulse responses can be recovered. In fact, by exploiting the MA form and the

relation between the structural and the reduced form errors outlined in the paragraph *2.1.1*, every weakly stationary VAR (p) model can be written as the following weighted average of past structural shocks:

$$y_t = \sum_{h=0}^{\infty} \boldsymbol{\Phi_h B_0^{-1} w_{t-h}}$$

*(2.10)*

where $\boldsymbol{\Phi_h}$ denotes the matrix of reduced form impulse responses of the VAR (p) model in question at horizon h, i.e., $\boldsymbol{\Phi_h} = \frac{\partial \boldsymbol{y_{t+h}}}{\partial \boldsymbol{u_t'}}$ with $\boldsymbol{u_t}$ representing the vector of reduced form errors. In addition, covariance-stationarity implies that:

$$\boldsymbol{\Theta_h} = \frac{\partial \boldsymbol{y_{t+h}}}{\partial \boldsymbol{w_t'}} = \frac{\partial \boldsymbol{y_t}}{\partial \boldsymbol{w_{t-h}'}}$$

*(2.11)*

Thus, combining equation *2.10* with equation *2.11*, the structural responses can be expressed as follows:

$$\boldsymbol{\Theta_0 = B_0^{-1}}$$

$$\boldsymbol{\Theta_1 = \Phi_1 B_0^{-1}}$$

$$\boldsymbol{\Theta_2 = \Phi_2 B_0^{-1}}$$

$$\vdots$$

By definition, stability ensures that all the structural and reduced form impulse responses will die out after some horizons, totally reverting to zero. However, the structural impulse responses can be derived from the related reduced form ones by using the same equations, even if the model is not stable.

Since $\boldsymbol{\Theta_0}$ is equivalent to $\boldsymbol{B_0^{-1}}$, $\boldsymbol{B_0^{-1}}$ is often referred to as the structural impact multiplier matrix. In fact, $\boldsymbol{\Theta_0}$ represents the responses of model variables to the structural shocks at horizon 0, that is upon impact. This matrix $\boldsymbol{B_0^{-1}}$ is commonly chosen such that each structural shock represents a one standard deviation of the time series of structural shocks.

Operationally, the estimates of the structural IRFs are typically computed through OLS estimates of $\mathbf{A}$ and $\boldsymbol{\Sigma_u}$ and the chosen identification restrictions. The uncertainty of these estimates is often replicated by applying bootstrap algorithms, which simulate a sample of data of the actual data sample n-times and compute the structural IRF for each simulated sample. From these n- structural IRFs values, the researcher typically picks two percentiles as upper and lower bounds of the uncertainty point estimates e.g., [$5^{th}$, $95^{th}$] and [$16^{th}$, $84^{th}$ ], also known as the confidence bands, per each horizon. In addition, a researcher usually uses the median or the mean of the density of simulated IRFs as main point estimate of the structural IRFs (Kilian and Lütkepohl, 2017).

### *2.4. Forward error variance decomposition*

Structural VAR analysis is able to estimate the relevance of each identified structural shock in explaining the average deviation of each variable from its own prediction at a certain horizon, or, in other terms, the importance of each structural shock in determining the unexpected fluctuations of each model variable by means of the so-called Forward Error Variance Decomposition. Indeed, with respect to equation *2.5*, the FEVD describes how much of the forecast error variance or prediction mean squared error (MSPE) of $\boldsymbol{y_{t+h}}$ at horizon $h = 0,1,2,\dots,H$ is explained by each structural shock $w_{qt}$ , with $q = 0,1,2,\dots,k$.

Firstly, let us define the mean squared prediction error at horizon h for a VAR model as:

$$MSPE(h) = \sum_{i=0}^{h-1} \boldsymbol{\Theta_i \Theta_i'}$$

*(2.12)*

where $\Theta_i$ represents the structural impulse matrix at horizon i as in the previous paragraph. Hence, using the same notation as in paragraph 2.3, the contribution of shock q to the MSPE of $y_{jt}$ at horizon h corresponds to:

$$MSPE_q^j(h) = \theta_{jq,0}^2 + \cdots + \theta_{jq,h-1}^2$$

*(2.13)*

As a consequence, the total MSPE of $y_{jt}$ at horizon h can be written as:

$$MSPE^j(h) = \sum_{i=1}^{k} MSPE_i^j(h)$$

*(2.14)*

Therefore, the MSPE of $y_{jt}$ can be decomposed as follows:

$$1 = \frac{MSPE_1^j(h)}{MSPE^j(h)} + \frac{MSPE_2^j(h)}{MSPE^j(h)} + \cdots + \frac{MSPE_k^j(h)}{MSPE^j(h)}$$

*(2.15)*

where $\frac{MSPE_i^j(h)}{MSPE^j(h)}$ represents the fraction of the contribution of shock q to the forecast error variance of variable j.

Operationally, FEVDs estimates are computed similarly to IRFs, using bootstrap algorithms in order to infer the confidence bands and the mean or median values (Kilian and Lütkepohl, 2017).

### *2.5 Bayesian estimation: prior, likelihood and posterior distributions*

As previously mentioned, VAR models are traditionally estimated through Maximum Likelihood and OLS methodologies, which are based on the so-called "frequentist approach". Given a parameter vector of interest, say $\boldsymbol{\theta}$, which governs the process generating the sample of data under observation, frequentists assume $\boldsymbol{\theta}$ to be deterministic and the samples of data to be stochastic. They aim at inferring $\boldsymbol{\theta}$ from the available sample, by exploiting the properties of the estimator $\boldsymbol{\theta}$ in repeated sampling. In contrast, Bayesians consider data non-stochastic, whereas $\boldsymbol{\theta}$ is treated as stochastic. In fact, they estimate $\boldsymbol{\theta}$ by using the researchers' beliefs about this parameter, expressed in the form of subjective probability distributions. The assumed distribution of $\boldsymbol{\theta}$ before observing the sample takes the name of prior distribution (or simply prior), denoted by $g(\boldsymbol{\theta})$. The subjective distribution of $\boldsymbol{\theta}$ after having observed the data is called posterior distribution or posterior, indexed by $g(\boldsymbol{\theta}|\boldsymbol{y})$, where $\boldsymbol{y}$ is a vector of data. The link between the prior and the posterior distributions is given by the Bayes' theorem:

$$g(\boldsymbol{\theta}|\boldsymbol{y}) = \frac{f(\boldsymbol{y}|\boldsymbol{\theta})g(\boldsymbol{\theta})}{f(\boldsymbol{y})}$$

*(2.16)*

where $f(\boldsymbol{y}|\boldsymbol{\theta})$ is the sample probability distribution function conditional on a given value of $\boldsymbol{\theta}$ and $f(\boldsymbol{y})$ indicates the unconditional sample density. The former function is identical to the likelihood function and represents the amount of information conveyed by the data. Hence, Bayesians start by assuming a specific prior and a likelihood function for $\boldsymbol{\theta}$ and then, after the observation of the sample of data, update their beliefs in the form of the posterior. Finally, they infer and estimate $\boldsymbol{\theta}$, by exploiting the posterior. If the prior results in a posterior that has the same functional form, it is said to be a conjugate prior. Additionally, if a conjugate prior shares its distribution family with the likelihood, it is called a natural conjugate prior.

More specifically, the objective of Bayesian inference is to randomly draw n-times from the posterior distribution of $\boldsymbol{\theta}$ or from a function of it, such as the structural IRF of a VAR model. Random samples are easy to draw if the posterior is from a known distribution family, by using the random number generator, a tool commonly available in modern software packages, which generates automatically a prespecified number of random samples from a known distribution. However, this is rare in practice and hence it is necessary to employ more sophisticated sampling techniques, such as the Markov Chain Monte Carlo methods, which will be used for the empirical research. They exploit a Markov Chain algorithm to generate a large number of serially dependent random draws of the parameter vector. Creating a high number of random draws and discarding a large number of initial sample values, also known as the burn-in sample, are usually necessary conditions to ensure that the posterior can be well approximated by the distribution of the random sample.

The main advantages of the Bayesian approach are to reduce the uncertainty surrounding the unrestricted LS estimates of $\boldsymbol{\theta}$ and to incorporate extraneous information. On the contrary, the main issue linked to Bayesian analysis is represented by the often-required extensive computations. Recently, it has become a quite popular estimation method, since modern computers have allowed to reduce the cost of making calculations, regardless of their complexity.

The next subsections will illustrate the priors and the respective posteriors used for the empirical research (Kilian and Lütkepohl, 2017).

### *2.5.1 The Minnesota prior*

The prior is usually specified in a way that the posterior is from a known distribution family, or the posterior analysis is at least simplified. A common practice to get such a result is to use priors from a known distribution family. In addition, priors are usually provided with an additional structure in order to reduce the number of parameters required for a full specification of the prior to a small number of parameters, known as hyperparameters. The hyperparameters can be selected following different criteria. An important example is choosing the values of the hyperparameters that maximize the marginal likelihood function, i.e., the sample density function conditional on the hyperparameters (Kilian and Lütkepohl, 2017).

Before defining the Minnesota prior, it is useful to notice that, for $t = 1, \dots, T$, where T denotes the size of the sample, a generic reduced-form VAR(p) model can be rewritten as follows:

$$\boldsymbol{Y} = \boldsymbol{AX} + \boldsymbol{U},$$

*(2.17)*

where $\boldsymbol{Y} \equiv [\boldsymbol{y_1}, \dots, \boldsymbol{y_T}]$, $\boldsymbol{A} \equiv [\boldsymbol{c}, \boldsymbol{A_1}, \dots, \boldsymbol{A_p}]$, $\boldsymbol{X} \equiv [\boldsymbol{X_0}, \dots, \boldsymbol{X_{T-1}}]$ with $\boldsymbol{X_{t-1}} \equiv \left(\boldsymbol{1}, \boldsymbol{y'}_{\boldsymbol{t-1}}, \dots, \boldsymbol{y'}_{\boldsymbol{t-p}}\right)'$ (Kilian and Lütkepohl, 2017).All the priors which will be treated are imposed on the reduced-form parameters, i.e., the matrixes $\boldsymbol{\Sigma_u}$ and **A**.

One of the most notorious priors in VAR literature is the so-called Minnesota prior, which dates back to Doan, Litterman, and Sims (1984). The Minnesota prior assumes that the distribution of the coefficient matrix **A** is centred at a value which implies a random-walk dynamics for the VAR variables. In other words, each model variable is supposed to depend just on its own value at lag 1 and on the error term. There exist two alternatives to implement the Minnesota prior: the first one is to specify a distribution for **A**, whereas the second one consists of using the so-called dummy observations. Dummy observations are fictitious observations of the model variables which might be actual observations from other countries or observations generated by simulations or by introspections. They are plugged in matrixes **Y** and **X** in order to create priors for VARs parameters. The main advantage of using dummy observations for implementing the Minnesota prior is the fact that it allows to introduce plausible correlations between VARs parameters in a parsimonious way (Del Negro and Schorfheide, 2011).

The Minnesota prior is usually specified by employing several hyperparameters and in the empirical research they will be used to create the dummy observations as in Del Negro and Schorfheide (2011). The overmentioned authors exploit seven hyperparameters. Two hyperparameters are the vectors of the means and of the standard deviations of a given pre-sample. Each one of the remaining hyperparameters is stacked in the vector $\boldsymbol{\lambda}$ and governs a specific characteristic of the priors of the VARs parameters, by interacting with the vectors of the pre-sample means and standard deviations. The hyperparameter $\boldsymbol{\lambda_1}$controls the tightness of the prior for the matrix of the coefficients associated to the variables at lag 1, i.e., the inverse of the standard deviations of the priors for the elements of matrix $\boldsymbol{A_1}$. The hyperparameter $\boldsymbol{\lambda_2}$ controls the tightness of the priors for the coefficient matrixes of the remaining lagged variables, namely the matrixes from $\boldsymbol{A_2}$ to $\boldsymbol{A_p}$. The hyperparameter $\boldsymbol{\lambda_3}$ regulates the prior for the covariance matrix Sigma, centred at a matrix that is diagonal with elements equal to the pre-sample variance of model variables. Finally, the hyperparameters $\boldsymbol{\lambda_4}$ and $\boldsymbol{\lambda_5}$ govern the strength of two different beliefs about VARs parameters. More specifically, $\boldsymbol{\lambda_4}$ refers to the belief that the pre-sample mean of a variable is likely to be a good forecast for its own actual value, if its lagged values are at the pre-sample mean level, regardless of the value of other variables; whereas $\boldsymbol{\lambda_5}$ is related to the belief that the actual values of the model variables tend to persist at their own pre-sample means, if all their lagged values are at this level (Del Negro and Schorfheide, 2011).

A crucial advantage of using the Minnesota prior is the fact that it implies Normal posteriors, which are simple and analytically tractable. Lastly, it is important to notice that the Minnesota prior is reasonable only for non-stationary economic time series, since it implies a random walk behaviour for the model variables, as previously explained (Kilian and Lütkepohl, 2017).

### *2.5.2 The natural conjugate gaussian – inverse wishart prior*

The natural conjugate gaussian – inverse Wishart prior assumes that the covariance matrix of the error term, Sigma, follows an inverse Wishart prior distribution and the coefficient matrix A in its columnwise vectorized form, i.e., vec(B), follows a Normal prior distribution, conditionally on Sigma (Uhlig, 2005). More formally, the following priors are specified:

$$\mathrm{vec}(\boldsymbol{A})|\boldsymbol{\Sigma_u} \sim N\left(\mathrm{vec}(\overline{\boldsymbol{A_0}}), \boldsymbol{\Sigma_u} \otimes \boldsymbol{N_0^{-1}}\right),$$

$$\boldsymbol{\Sigma_u} \sim IW_k\left(\frac{\boldsymbol{S_0^{-1}}}{v_0}, v_0\right).$$

As we can see from this equation, four parameters define the priors: a positive definite mean covariance *k x k* matrix $\boldsymbol{S_0}$, a mean coefficient matrix *kp x p* $\overline{\boldsymbol{A_0}}$, a positive definite matrix $\boldsymbol{N_0}$ of size *kp x kp* and the real number of degrees of freedom, $v_0$, that is non-negative and indicates the uncertainty of **A** and $\boldsymbol{\Sigma_u}$ around $\overline{\boldsymbol{A_0}}$ and $\boldsymbol{S_0}$, respectively. These four parameters are freely chosen by the researcher (Uhlig, 2005). The operator "vec" denotes the so-called vectorization, a linear transformation which converts a generic matrix **C** of size m x n into a column vector of size *mn x 1*. The symbol "⊗ " stands for the Kronecker product. If **C** is an $m \times n$ matrix and **D** is a generic $p \times q$ matrix, then the Kronecker product **C** ⊗ **D** is the following $pm \times qn$ matrix:

$$\begin{bmatrix} c_{11}\boldsymbol{D} & \cdots & c_{1n}\boldsymbol{D} \\ \vdots & \ddots & \vdots \\ c_{m1}\boldsymbol{D} & \cdots & c_{mn}\boldsymbol{D} \end{bmatrix}$$

The Wishart distribution can be deemed as the multivariate generalization of a $\chi^2(n)$ distribution and derives from the interaction of a number n of k-dimensional, independent, and identically distributed Normal random vectors (Kilian and Lütkepohl, 2017).

The previously specified priors for **A** and $\boldsymbol{\Sigma_u}$ are such that they imply the same distribution family for the respective posteriors and, hence, they are conjugate priors. More precisely, it is a natural conjugate prior, since the posterior has the same functional form as the likelihood. In fact, given the matrix **Y** of the actual T-periods- observations of equation *2.17*, the posteriors are the following:

$$\mathrm{vec}(\boldsymbol{A})|\boldsymbol{\Sigma_u}, vec(\boldsymbol{Y}) \sim N\left(\mathrm{vec}(\overline{\boldsymbol{A_T}}), \boldsymbol{\Sigma_u} \otimes \boldsymbol{N_T^{-1}}\right),$$

$$\boldsymbol{\Sigma_u}|vec(\boldsymbol{Y}) \sim IW_k(\boldsymbol{S_T^{-1}}/v_T, v_T),$$

where $v_T = v_0 + T$, $\boldsymbol{N_T} = \boldsymbol{N_0} + \boldsymbol{XX'}$, $\overline{\boldsymbol{A_T}} = \boldsymbol{N_T^{-1}}\left(\boldsymbol{N_0}\overline{\boldsymbol{A_0}} + \boldsymbol{XX'}\widehat{\boldsymbol{A}}\right)$, $\boldsymbol{S_T} = \frac{v_0}{v_T}\boldsymbol{S_0} + \frac{T}{v_T}\widehat{\boldsymbol{\Sigma_u}} + \frac{1}{v_T}\left(\widehat{\boldsymbol{A}} - \overline{\boldsymbol{A_0}}\right)'\boldsymbol{N_0}\boldsymbol{N_T^{-1}}\boldsymbol{XX'}^{\left(\widehat{\boldsymbol{A}}-\overline{\boldsymbol{A_0}}\right)}$. $\widehat{\boldsymbol{A}}$ and $\widehat{\boldsymbol{\Sigma_u}}$ denote the OLS estimates for **A** and $\boldsymbol{\Sigma_u}$, respectively (Uhlig, 2005).

One of the main advantages of using the natural conjugate gaussian – inverse Wishart prior is the fact that, if the structural VAR model is just identified, the posterior distributions of the structural impulse response functions can be easily simulated by drawing from the joint posterior distribution of the reduced form parameters **A** and $\boldsymbol{\Sigma_u}$ (Kilian and Lütkepohl, 2017).

Drawing from the inverse Wishart distribution $IW_k\left(\frac{\boldsymbol{S_T^{-1}}}{v_T}, v_T\right)$ is pretty straightforward. Indeed, a draw for $\boldsymbol{\Sigma_u}$ is equal to $(\boldsymbol{RR'})^{\boldsymbol{-1}}$, where **R** is a *k x v* matrix whose columns are independent draws from the Normal distribution $N\left(0, \frac{\boldsymbol{S_T^{-1}}}{v_T}\right)$ (Uhlig, 2005).

### *2.6 Recursively identified models and the Cholesky decomposition*

A common way of uniquely identifying the structural shocks is to exploit the so-called lower-triangular Cholesky decomposition of $\boldsymbol{\Sigma_u}^{\boldsymbol{2}}$, which is a *k x k* lower triangular matrix P with specific characteristics (Kilian and Lütkepohl, 2017). It is provided with a positive main diagonal such that $\boldsymbol{\Sigma_u = PP'}$(Kilian and Lütkepohl, 2017). Thus, using the Cholesky decomposition to address the identification problem previously mentioned means imposing $\boldsymbol{B_0^{-1} = P}$, since it allows to satisfy the order condition (Kilian and Lütkepohl, 2017). In fact, $\boldsymbol{P}$ has $\frac{k(k-1)}{2}$ zero parameters, given that it is a lower-triangular matrix. In other words, this identification strategy imposes $\frac{k(k-1)}{2}$ zero restrictions on the elements of $\boldsymbol{B_0^{-1}}$ as well as of $\boldsymbol{B_0}$. It makes the reduced form errors mutually uncorrelated, on one hand, and introduces a particular recursive order or causal chain between the structural shocks and between the model variables, on the other one (Kilian and Lütkepohl, 2017). Using the same notation as equations *2.5* and *2.2*, an example of a trivariate SVAR identified through the Cholesky decomposition will clarify this:

$$\begin{pmatrix} u_{1t} \\ u_{2t} \\ u_{3t} \end{pmatrix} = \begin{pmatrix} b_{11} & 0 & 0 \\ b_{21} & b_{22} & 0 \\ b_{31} & b_{32} & b_{33} \end{pmatrix} \begin{pmatrix} w_{1t} \\ w_{2t} \\ w_{3t} \end{pmatrix}$$

*(2.18)*

In this example, the structure of matrix $\boldsymbol{B_0^{-1}}$ implies the following assumptions: the structural shock $w_{3t}$ has not any contemporaneous impact on the other shocks, $w_{2t}$ does not affect $w_{1t}$, and $w_{1t}$ influences all the other variables contemporaneously. An analogous recursive order can be easily proved to exist for the related variables. This means that it is supposed that x causes or predates z and z causes or predates g in the system of three equations *2.1*. Therefore, the use of the Cholesky decomposition is reasonable only if the implied causal chain between the model variables is somehow justified from an economic point of view (Kilian and

Lütkepohl, 2017). In the literature, there exist many different sources of this economic rationale, but the most common is surely the use of economic theory or of an underlying economic model (Kilian and Lütkepohl, 2017). However, in practice, it is important to underline that economic aggregates are rarely found to be in a recursive relationship with each other and hence the use of Cholesky decomposition as identification strategy could give place to imprecise or even incorrect estimates of IRFs and FEVDs. Consequently, researchers tend to rely more often on other identification strategies, which are usually more complicated but imply more realistic restrictions on VARs coefficients, such as the Penalty Function approach, that will be illustrated in the next subsection. Nevertheless, the Cholesky decomposition turns out to be a useful strategy, since it provides a reliable lower bound of the effects of the last-placed variable on the other ones.

### *2.7 The Penalty Function Approach*

The Penalty Function Approach was introduced by Faust (1998) and Uhlig (2005). Over the years, many authors have employed it, by providing some variations to suit their research questions. Hereafter, the version of the PFA elaborated by Caldara et al. (2016) will be followed. First of all, let rewrite the structural VAR model in equation *2.5* as:

$$\boldsymbol{y'}_{\boldsymbol{t}}\boldsymbol{B_0} = \boldsymbol{X'}_{\boldsymbol{t}}\boldsymbol{B_+} + \boldsymbol{\omega'}_{\boldsymbol{t}},$$

*(2.19)*

where $\boldsymbol{B_+} = \left[\boldsymbol{B'}_{\boldsymbol{1}} \dots \boldsymbol{B'}_{\boldsymbol{p}}\ \boldsymbol{c'}\right]$ and $\boldsymbol{X'}_{\boldsymbol{t}} = \left[\boldsymbol{y'}_{\boldsymbol{t-1}} \dots \boldsymbol{y'}_{\boldsymbol{t-p}}\ \boldsymbol{1}\right]$ . $\boldsymbol{B_0}$ and $\boldsymbol{B_+}$ are the so-called structural parameters. The structural IRF of the i-th variable to the j-th structural shock at the finite horizon h is equal to the element in the i-th row and the j-th column of the matrix $\left[\boldsymbol{B_0^{-1}}\boldsymbol{J'}^{\boldsymbol{F^h}}\boldsymbol{J}\right]$, where

$$\boldsymbol{F} = \begin{bmatrix} \boldsymbol{B_1B_0^{-1}} & \boldsymbol{I_n} & \cdots & \boldsymbol{0} \\ \vdots & \vdots & \ddots & \vdots \\ \boldsymbol{B_{p-1}B_0^{-1}} & \boldsymbol{0} & \cdots & \boldsymbol{I_n} \\ \boldsymbol{B_pB_0^{-1}} & \boldsymbol{0} & \cdots & \boldsymbol{0} \end{bmatrix} \quad \text{and} \quad \boldsymbol{J} = \begin{bmatrix} \boldsymbol{I_k} \\ \boldsymbol{0} \\ \vdots \\ \boldsymbol{0} \end{bmatrix}.$$

Let this structural IRF be denoted by $\boldsymbol{L_h}(\boldsymbol{B_0}, \boldsymbol{B_+})_{ij}$. Defining $\mathcal{O}(k)$ as the set of all orthonormal *k x k* matrixes $\boldsymbol{Q}$, $\boldsymbol{B_0^{-1}}$ can be set equal to the product $\boldsymbol{PQ}$, where $\boldsymbol{P}$ is the Cholesky

decomposition of $\boldsymbol{\Sigma_u}^{\boldsymbol{2}}$, which satisfies the equation *2.6*. So, the identification problem can be solved by adding restrictions on $\boldsymbol{Q}$. In fact, for instance, imposing $\boldsymbol{Q} = \boldsymbol{I_k}$ means using the identification strategy based on the Cholesky decomposition. On the other hand, this kind of expression for $\boldsymbol{B_0^{-1}}$ returns $(\boldsymbol{P^{-1}}, \boldsymbol{AP^{-1}})$ as structural parameters, where **A** is the matrixes of the reduced-form coefficients as in equation *2.17* (Caldara et al., 2016).

The PFA consists of identifying just a subset n of the k- structural shocks. Any identified shock $\boldsymbol{q_j}$ corresponds to $\boldsymbol{Qe_j}$, where $j = 1, \dots, n$ and $\boldsymbol{e_j}$ is the j-th column of $\boldsymbol{I_k}$. This approach identifies each structural shock j as the value $\boldsymbol{q_j}^*$ that minimizes a penalty function $\Psi(\boldsymbol{q_j})$ subject to three constraints on the structural IRFs. More specifically, it assumes that the sign of the structural IRF of some variables is restricted to be negative or positive for $H \geq 0$ periods. The set of variables whose IRF is restricted to be positive is denoted by $I_j^+$, whereas the set of variables whose IRF is required to be negative is indexed by $I_j^-$. Both sets are subsets of $\{0,1, \dots, k\}$. The third constraint requires that the shock j is orthogonal to shocks $1, \dots, j-1$ (Caldara et al., 2016).

As regards the penalty function, it is made of the sum of the tightness - weighted IRFs of the model variables. Indeed, the IRF of a variable is divided by the standard deviation of that variable. In addition, the IRFs restricted to be positive are flipped by sign. More precisely, the penalty function $\Psi(\boldsymbol{q_j})$ is equal to:

$$\sum_{i \in I_j^+} \sum_{h=0}^{H} \left( - \frac{\boldsymbol{e_i}' \boldsymbol{L_h}(\boldsymbol{P^{-1}}, \boldsymbol{AP^{-1}}) \boldsymbol{q_j}}{\omega_i} \right) + \sum_{i \in I_j^-} \sum_{h=0}^{H} \left( \frac{\boldsymbol{e_i}' \boldsymbol{L_h}(\boldsymbol{P^{-1}}, \boldsymbol{AP^{-1}}) \boldsymbol{q_j}}{\omega_i} \right),$$

where $\omega_i$ denotes the standard deviation of variable i and can be estimated by the OLS residuals associated to variable i and $\boldsymbol{e_i}' \boldsymbol{L_h}(\boldsymbol{P^{-1}}, \boldsymbol{AP^{-1}}) \boldsymbol{q_j}$ corresponds to the IRF of variable i to the structural shock $\boldsymbol{q_j}$. Thus, the PFA identifies the structural shocks as those that provide the largest sum of tightness - weighted IRFs, satisfying the three previously mentioned constraints (Caldara et al., 2016).

More formally, the PFA solves the following optimization problem:

$$\boldsymbol{q_j}^* = \min_{\boldsymbol{q_j}} \Psi(\boldsymbol{q_j})$$

$$subject\ to$$

$$\boldsymbol{e_i}'\boldsymbol{L_h}(\boldsymbol{P^{-1}}, \boldsymbol{AP^{-1}})\boldsymbol{q_j} > 0, \qquad i \in I_j^+ \; and \; h = 0, \dots, H;$$

$$\boldsymbol{e_i}'\boldsymbol{L_h}(\boldsymbol{P^{-1}}, \boldsymbol{AP^{-1}})\boldsymbol{q_j} < 0, \qquad i \in I_j^- \; and \; h = 0, \dots, H;$$

$$\boldsymbol{Q_{j-1}^{*'}}\boldsymbol{q_j} = 0,$$

where $\boldsymbol{Q_{j-1}^{*'}} = [\boldsymbol{q_j}^* \dots \boldsymbol{q_{j-1}}^*]$.

It is important to stress that the third constraint implies a sort of recursive ordering to model variables, if each structural shock is identified sequentially through the PFA. In fact, the sequential identification through PFA is not invariant to the ordering of the shocks and, if the penalty function of each variable j consists only of the response upon impact of variable j, it coincides with a Cholesky decomposition identification strategy. However, except for this case, this sequential approach does not imply any zero restrictions on the structural parameters or on the IRFs for any horizon *h*, allowing structural innovations to influence each other. In addition, note that the original specifications of Uhlig (2005) and Faust (1998) employed a penalty function based on FEVDs rather than on IRFs, as the version elaborated by Caldara et al. (2016) does. This difference is due to the fact that maximizing IRFs is a more suitable criterion for the types of shocks that Caldara et al. (2016) identified.

## 3. DATA AND ECONOMETRIC SPECIFICATIONS

This chapter briefly illustrates the data series and the three econometric specifications that will be employed for the SVAR models. Every econometric specification denotes a different combination of assumptions, estimation techniques and identification strategies used to retrieve the FEVDs and the IRFs of the model variables to each uncertainty shock.

### *3.1 Data*

All the econometric specifications are based on the same dataset, consisting of the monthly time series of the World Industrial Production (WIP), the Consumer Price Index (CPI), the shadow rate, the Global factor for risky financial assets returns (GFC) - that is the global financial cycle measured by Miranda - Agrippino and Rey (2021) - GPR, GFU, and GEPU. More specifically, three econometric specifications will be used, each one estimating three SVAR models. Each one of the three SVAR models considers a specific uncertainty measure, six lags, and monthly frequency. The number of lags of the models has been chosen by taking inspiration from Caldara et al. (2016). The estimated reduced form VAR models will have the same form as eq. 2.2, whereas the estimated SVAR will be in the form of eq. *2.5*, since the constant will be always included. However, all of these 9 models consider the following vector of variables:

$$[UNC_t, GFC_t, shadowrate_t, \log(WIP_t) * 100, CPI_t]'$$

where $UNC_t$ stands for one of the three measures of uncertainty.

The choice of including shadow rate, the WIP growth rate and CPI in the models takes inspiration from Caggiano and Castelnuovo (2023), who achieved very striking results on the effects of GFU shocks in estimated SVAR models comprehensive of these three variables and GFC.

The order in which the time series appear in this vector is not random, but it aims mostly at imposing a plausible recursive order between the model variables, when identifying the structural shocks by means of the Cholesky decomposition, used only in the first econometric specification. Indeed, this identification strategy specifies a causal chain between the variables and between the related structural shocks according to their ordering in the vector, as mentioned in Chapter 2. More specifically, starting from the right-hand-side of the vector, the first variable is supposed to be not contemporaneously determined by the others, i.e., to happen independently from the other series' contemporaneous levels, and hence could be deemed as

the first variable to be observed in a month. On the other hand, the first variable influences all the remaining ones contemporaneously. The second one is assumed to be contemporaneously led only by the values of the first variable and to impact on all the others. Following this reasoning, the latest should be determined by all the other series contemporaneous levels and should not impact on any of them. Even if this order is mainly useful for the first econometric specification, it will remain the same across all the specifications and VAR models.

Importantly, notice that PFA, that is employed for the rest of the econometric specifications, imposes a sort of causal chain between model variables and between structural shocks as well, which depends, however, on the order followed to optimize the penalty function and hence to identify the structural shocks. Indeed, the sequential identification of the structural shocks is conditional on their sequential orthogonalization.

Going back to the reasons which underline the order of the model variables in the vector, the uncertainty measure is always ordered as the latest variable in order to minimize its impacts on the other ones, when using the Cholesky decomposition. In other terms, this means that the estimated effects of uncertainty shocks will be just a lower bound of what they could be. In fact, as previously explained, the last variable is supposed to occur chronologically after every other one, which implies that every related shock cannot affect the other time series contemporaneously and that its effects should be the least of what they could be in a recursive model.

GFC is the fourth variable in the vector, following Caldara et al. (2016), that placed the proxy for the financial conditions in the same position. The shadow rate, instead, is in the central position because of the following standard macroeconomic assumption: policy rate is supposed to be set by central banks after having observed the actual levels of unemployment and GDP. In fact, the policy rate is an important instrument in the hands of central banks to offset unpleasant economic conditions. Besides, shadow rate, which is a measure of US conventional and unconventional monetary policies, should impact on the Global financial cycle, as documented by Miranda - Agrippino and Rey (2020).

The log of WIP multiplied by one hundred is the second variable since it is typically driven by oil price shocks and other inflation shocks. Consequently, CPI occupies the last position, being not theoretically affected by any other time series of the model by assumption.

It is worth underlying that the uncertainty measure have no economic reason to be placed after GFC. Indeed, as showed in Chapter 1, GFC should be highly correlated with measures of uncertainty and, more generally, fluctuations in financial aggregates and in uncertainty often happen at the same time. Due to this motive, whatever the sequential ordering and the identification strategy are, it is usually difficult to identify financial and GFC shocks separately from the uncertainty shocks. Hence, the recursiveness implied by the Cholesky decomposition is unrealistic for these shocks, since it introduces unplausible dynamics between uncertainty and GFC.

As the vector clearly points out, all the time series are taken in levels, with the exception of WIP, that is modelled in natural logarithms and multiplied by one hundred. Log-levels transformation allows to make a clearly trending and highly skewed time series, such as WIP, more stationary and more normalized. As opposed to using growth rates, log-levels transformation is useful to minimize the problems due to over differencing. In addition, as suggested by Canova, modelling the variables of a reduced form VAR in log-levels leads to consistent estimates with classical methods if the residuals are stationary. This holds even in presence of unit-rooted time series (see Caggiano and Castelnuovo, 2023).

The sample used to perform the SVAR analyses ends in April 2019, regardless of the model, due to the limitation given by the Global factor time series. On the contrary, the starting month of the sample varies according to data availability specific to every SVAR model. In fact, the GPR-related SVAR models cover the sample from January 1990, the initial month of the shadow rate series; the period underlying the GFU- related SVAR models begin in July 1992, the first available observation of GFU; lastly, the SVAR models specific to GEPU focus on a period starting in January 1997, the first month associated to the GEPU series. These considerations hold for all the econometric specifications.

In what follows, this section will briefly present WIP, CPI, and shadow rate.

### *3.1.1 Shadow rate*

The shadow rate variable was elaborated by Wu and Xia (2016), with the goal of better describing US monetary policies' time path compared to the traditional effective federal fund rate. In fact, it has one main advantage with respect to the effective federal fund rate. It is structured to capture not only the movements in the federal fund rate but also the changes in the unconventional monetary policy tools, such as forward guidance and quantitative easing. These

are important instruments for the FED and the ECB nowadays and were crucial for raising inflation during the Great Financial crisis of 2008. In that period, indeed, the nominal interest rates reached the zero lower bound and thereby it was impossible for central banks to stimulate the economic system through traditional monetary policies.

Therefore, in contrast with the effective federal fund rate, the shadow rate can be negative and hence it can convey information about the monetary policies adopted, even in times where the federal fund rate reaches the zero lower bound, as it can be noticed in *Figure 5*.

We consider the subsample of the monthly time series, which starts in January 1990 and ending in April 2019.

### *3.1.2 WIP*

The WIP index works as a measure of the global industrial production and was developed by Baumeister and Hamilton (2019). It is based on the national industrial productions from countries all around the world, which account, all together, for 79% of worldwide petroleum consumption and 75% of global GDP. It includes all OECD nations and other six important developing economies. The data series is downloaded by Baumeister's web site, and it covers a period spanning from January 1950 to July 2022. However, the time series represented in *Figure 6* covers a time window that starts in January 1990 and ends in April 2019, which is the most extended common subsample for SVAR models, as previously explained. As we can notice from *Figure 6*, WIP growth rate exhibits an increasing pattern over time, despite the log – transformation.

### *3.1.3 CPI*

CPI is a measure of US inflation as experienced by consumers in their day-to-day living expenses and is computed by the U.S. bureau of labour statistics. More specifically, "the CPI index is a measure of the average change over time in the prices paid by urban consumers for a representative basket of consumer goods and services" (U.S. Bureau of Labor Statistics). The series has a monthly frequency, and it is plotted in *Figure 7*. We employ the subsample which starts in January 1990 and ends in April 2019.

### *3.2 The econometric specifications*

As previously anticipated, there are three econometric specifications used to carry out the empirical research. The first one is based on the Cholesky decomposition and on the OLS estimation of the reduced form VAR models. As underlined in paragraph 3.1.1, the recursive ordering, which is implied by the Cholesky decomposition, is unrealistic in order to identify uncertainty shocks and hence the IRFs and FEVDs computed with this first specification are not that reliable. It is useful only to get a lower bound of the effects and of the contributions of uncertainty shocks on the GFC. This first specification will be referred to as the "Chol" specification hereafter.

The other two specifications follow the same econometric approach used by Caldara et al. (2016), which exploits economically meaningful assumptions and sophisticated econometric techniques resulting in suggestive and economically consistent findings related to uncertainty and financial shocks. Thus, such a methodology should suit the empirical research, leading to more reliable results compared to those coming from the Cholesky decomposition. This approach is characterized by the use of a specific PFA and the Bayesian estimation, where the posterior distributions of the IRFs and of the FEVDs are simulated through a Markov Monte Carlo Chain with 1000 draws and burn-in sample equal to 200 observations. However, differently from Caldara et al. (2016), the number of lags is not determined by using the overmentioned algorithm, but it is fixed to six, as previously mentioned.

By construction of the PFA à la Caldara et al. (2016) that will be explained better in the next paragraph, these two specifications estimate the effects and the contributions of uncertainty shocks at their maximums, retrieving a useful upper bound. Therefore, the use of the three econometric specifications aims at providing the lowest and the highest values that can be taken by the IRFs and the FEVDs associated to the uncertainty shocks. This allows to identify a reliable interval of values within which the "true" effects of the uncertainty shocks are situated.

The only difference between the two last specifications is represented by the prior. In fact, the second specification employs the Minnesota prior, whereas the third one is based on the Conjugate Gaussian Inverse Wishart prior. More specifically, the second specification, which will be denoted by "PFA - Min" specification, imposes the Minnesota prior for the reduced form parameters, as defined in Chapter 2, by means of dummy observations. The random walk dynamic imposed by the Minnesota prior is consistent with the fact that the model variables are typically unit rooted. Besides, following the approach of Caldara et al. (2016), the five

hyperparameters are selected by maximizing the marginal data density through the CMA-ES algorithm elaborated by Hansen et al. (2003), with the exception of the third one, which is set to 1 by hypothesis.

On the other hand, the last specification employs the conjugate natural Normal inverse Wishart prior such that $v_0$ and $N_0$ are both set to 0, as in Uhlig (2005). The objective of the third specification, indeed, is to assess that the relevance of each uncertainty measure in affecting GFC is invariant to changing prior for the reduced form parameters. Due to the specific kind of prior imposed, the third strategy will be referred to as the "PFA - Conj" specification hereafter.

### *3.2.1 The Penalty Function Approach used to identify the structural shocks*

Except for the Chol specification, all the econometric specifications employ the PFA elaborated by Caldara et al. (2016) to identify the structural shocks. Specifically, this empirical research identifies only the uncertainty and GFC shocks. Following the PFA ideated by Caldara et al. (2016), uncertainty shocks are identified as those innovations that trigger the greatest surge in uncertainty for the first six months. More specifically, they are the shocks that maximize the sum of the tightness - weighted IRFs of the related uncertainty measure until the fifth month after the impact, where each IRF is restricted to be positive. The maximization covers until the fifth month, because in our notation, which is the one used by Caldara et al. (2016), the impact response happens in month 0. Hence, with reference to the general form presented in section 2.17.1, the penalty function that has to be minimized for the uncertainty shock $\boldsymbol{q_j}$ is the following:

$$\sum_{h=0}^{5}\left(-\frac{\boldsymbol{e_1}'\boldsymbol{L_h}(\boldsymbol{P^{-1}},\boldsymbol{AP^{-1}})\boldsymbol{q_j}}{\omega_1}\right),$$

where

$$\boldsymbol{e_1}'\boldsymbol{L_h}(\boldsymbol{P^{-1}},\boldsymbol{AP^{-1}})\boldsymbol{q_j} > \boldsymbol{0}, \qquad h = 0,\dots,5;$$

$$\boldsymbol{Q_{j-1}^{*'}}\boldsymbol{q_j} = 0.$$

Notice that i = 1, because the uncertainty shock is the first variable in the VAR models and j = 1, since the uncertainty shock is the first one to be identified. As a consequence, the

orthogonality condition, i.e., the equation $\boldsymbol{Q}_{\boldsymbol{j-1}}^{*'}\boldsymbol{q}_{\boldsymbol{j}} = 0$, is ruled out, when identifying the uncertainty shocks.

Analogously to uncertainty shocks, the GFC shock is identified as the one that generates the most relevant increase in GFC for the first six months. Therefore, the penalty function that has to be minimized to identify GFC innovation is identical to that used to identify the uncertainty shocks, with the only difference that i = 2, because the GFC shock is identified after the uncertainty one.

These specific penalty functions used to identify uncertainty and GFC shocks derive from one fundamental assumption: perturbances in uncertainty measures and fluctuations in GFC are explained mainly by uncertainty shocks and GFC shocks, respectively. In addition, both these shocks lead their corresponding variable to rise persistently in the short-term. However, it is important to stress that, differently from the identification through the Cholesky decomposition, both variables are allowed to react contemporaneously to the other variable's shocks (Caldara et al., 2016).

# 4. A PRELIMINARY ANALYSIS OF THE UNCERTAINTY MEASURES

This chapter performs an analysis of the relationships that GPR, GFU and GEPU have with each other, with the Global financial cycle, and with the WIP index. Every relation will be examined by just considering correlations and Granger causalities between the overmentioned variables. This kind of analysis is useful to assess whether the chosen measures of uncertainty are indeed countercyclical and able to predate future perturbances in the global financial cycle. In addition, it allows to check whether each measure of uncertainty conveys an independent and peculiar type of information compared to the others and if the measures of uncertainty are somehow linked to each other. For the sake of simplicity, the term "causality" will denote any "Granger causality" relationship between two variables.

## *4.1 How the measures of uncertainty relate to each other*

In this section the relationships between GEPU, GFU, and GPR will be investigated, by analysing their time series' charts, their pairwise correlations, and their bidirectional Granger causalities. Each series will be standardized and then summed to one hundred to facilitate comparisons. For each relationship a different sample will be used, in order to exploit all the available data and hence to achieve the most reliable results as possible. In fact, for each of them, the most extended common sample will be taken into account.

Every plot chart represents a couple of series over the overmentioned sample and displays their Pearson correlation index, denoted by "$\rho_{XY}$''.

Two Granger causality tests have been run for each possible couple of uncertainty measures, in order to assess whether one of the two variables Granger causes the other one at the 95% significance level. The test assumes that each couple of time series is described by a bivariate VAR model with 6 lags; consequently, the underlying null hypothesis to be tested is that none of the 6 lags is different from zero with a level of significance equal to 95%. The choice of 6 lags descends from the fact that the SVAR analysis is based on VAR models with the same number of lags.

Additional Granger causality tests on 12 and 24 lags VAR models have been conducted to assess possible longer term causal relationships, even though they are not the focus of the

empirical research. The Granger causality test on 7 lags VAR models has been run as well, since the model variables are potentially unit rooted.

Lastly, a specific causality test with a significance level of 97.5% has been carried out for those couples of variables with a feedback relationship documented by the overmentioned Granger causality tests.

### *4.1.1 A preliminary overview*

As a preliminary step, we analyse the chart of the time series of the standardized uncertainty measures, plotted together in their common sample, covering the period from January 1997 to May 2020.

Two main remarks can be made, by looking at *Figure 8*. First, all the measures spike in correspondence of famous geopolitical adverse events, such as invasion of Iraq in 2003 and the 9/11, with GPR displaying the highest peak. Secondly, as previously stated, GPR does not react to very well-known episodes denoted by high levels of global uncertainty, primarily the begin of Covid 19 pandemics and the Great financial crisis, showing an opposite pattern with respect to GEPU and GFU. Consequently, GPR might be a driver of GEPU and GFU, while GFU and GEPU should not lead GPR. This could make sense, since heightened geopolitical uncertainty could make the forecasts on future financial returns more volatile, as well as it could make economic policies more unpredictable. These circumstances raise GFU and GEPU, respectively. However, there could be just the fact that adverse geopolitical acts impact on all the three variables.

In addition, the common responses of GEPU and GFU to many globally relevant events do not exclude the possibility that the two measures share some link with each other. In fact, higher uncertainty regarding economic policies could lead to higher future levels of financial uncertainty. Actually, even past values of financial uncertainty could determine actual economic policy uncertainty. These hypotheses will be evaluated in the following subsections, by means of the Granger causality analysis.

### *4.1.2 GPR vs GEPU*

*Figure 9* shows the time series of standardized GPR and GEPU in the period from January 1997 to July 2022. The extended sample allows to monitor the variables' reactions to the Russian invasion of Ukraine, occurred in March 2022, and to COVID-19 pandemics. Both series

increase dramatically in response to these events, confirming the pattern pointed out in the previous subsection.

The correlation computed in the overmentioned common sample is statistically insignificant, being the related p-value equal to 0,452, and poorly positive (0,0704). This weak association confirms the fact that both measures are sources of distinct uncertainties.

The null hypotheses that one of the two variables Granger causes the other one are both rejected at the 95% level, in a VAR setting with 6 lags. This means that there should not be lagged values of GEPU, up to lag 6, that help in predicting actual GPR or vice versa. The same holds with 7, 12 and 24 lags. Hence, GPR and GEPU carry on different types of information, that do not share any causal link with each other.

### *4.1.3 GFU vs GPR*

The sample common to both variables coincides with the overall available sample for GFU, as we can see from *Figure 10*. Relatively to this time span, they appear to be uncorrelated, confirming that the two data series are independent sources of information. The correlation index is equal to 0,0526 and is not significant at the 90% confidence level. In addition, Granger causality hypotheses are always rejected at any number of lags, suggesting the absence of causal relationships.

### *4.1.4 GEPU vs GFU*

*Figure 11* shows GFU and GEPU over the period spanning from January 1997 to May 2020, that is the same used in *Figure 11*. As for the previous couples, their correlation index, equal to -0,1779, is insignificant at the 95% level. However, differently from the other relationships, GEPU and GFU seem to Granger cause each other at any number of lags. As a matter of fact, the null hypothesis that none of the lags of GEPU helps in predicting GFU can be rejected in any VAR setting at a level of significance of 97.5%. The same holds for the lags of GFU. In other words, the two series appear to be in a strong feedback relationship, even though they are uncorrelated.

### *4.1.5 Concluding remarks*

To sum up, each uncertainty measure conveys information specific to a peculiar kind of uncertainty, which differs from the others' ones, since the correlation index turns out to be

always insignificant at 10% level. In other terms, this implies that it is reasonable to perform a separate SVAR analysis for each of them, as it will be done in the following chapter. Secondly, they seem to not share any causal link, with the exception of GFU and GEPU, which, instead, preliminarily share a feedback relationship hard to be rejected.

### *4.2 Are uncertainty measures indeed countercyclical?*

The countercyclicality of each measure of uncertainty has been assessed by comparing each standardized time series with that of WIP growth rate, computed as the first difference of log WIP * 100. Both series are scaled by one hundred. Thereby, three figures have been generated, each one representing the time series of an uncertainty measure and WIP growth rate in their largest common sample and displaying the related correlation index. They are *Figure 12, Figure 13*, and *Figure 14.*

The period of analysis for GPR is the largest among the three measures. In fact, it spans from January 1980 to July 2022, while for GFU and GEPU it goes from July 1992 to May 2020 and from January 1997 to July 2022, respectively.

Each time series turns out be countercyclical, since all the three correlation indexes are negative and statistically significant. Hence, the considerations made in the first chapter are empirically confirmed. However, GPR and GEPU display poorly significant and weakly negative correlations, equal to -0,085 and -0,109, respectively. The significance is at 5% for both the measures. On the contrary, GFU's correlation index with WIP growth rate is strongly significant and much more negative (-0,312). In fact, the associated p-value is below the 1% threshold.

In addition, as previously underlined and pointed out by *Figures 13* and *14*, GEPU and GFU spike in correspondence of the Great Recession and Covid 19 pandemics, which record dramatic reductions in WIP growth rate. In fact, the three lowest values of WIP growth rate are reached during the overmentioned negative events and the Russian invasion of Ukraine in 2022, that triggered heightened levels of GEPU and GPR.

### *4.3 The relationships between the uncertainty measures and the Global financial cycle*

In this section we will investigate how the uncertainty measures relate to the Global Financial Cycle in their longest common sample. Both the uncertainty measures and the Global Financial Cycle will be standardized and summed to one hundred to make easier and more immediate graphical comparisons. In fact, as a first step, the time series of each uncertainty variable will be represented together with the time series of the Global Financial Cycle. The time series are plotted in *Figures 15, 16*, and *17*, specifically. Consequently, as for the previous analyses, three charts will be created, one for each uncertainty measure. Every chart displays the correlation between the represented time series.

Secondly, nine Granger causality tests will be carried out to assess whether the uncertainty measures could be deemed as determinants of the global financial cycle. Each Granger causality test assumes a bivariate VAR setting for standardized GFC and the standardized uncertainty measure. Six, seven, twelve, and twenty-four lags will be considered. The confidence level is always at the 95% threshold.

Other nine Granger causality tests will be run to evaluate the possibility that the Global Financial Cycle may Granger cause the uncertainty data series. They employ the same hypotheses that have been outlined in the previous paragraph.

Additional Granger causality tests have been performed to assess possible feedback relationships with a confidence level of 97,5%.

As robustness checks, the same overmentioned Granger causality tests have been carried out in the period in which the SVAR analyses will be indeed conducted. Hence, the Granger causality tests have been made in the time spans from January 1990 to April 2019 for GPR, from January 1997 to April 2019 for GEPU, and from July 1992 to April 2019 for GFU.

#### *4.3.1 GPR vs GFC*

The comparison has been made in the period from January 1985 to April 2019. The related correlation index turns out to be negative (-0,1779) and statistically significant, displaying a p-value lower than 0,01. Their time series are showed by *Figure 15*. However, despite the significance, this is a barely negative value, which indicates a weak negative relation between GPR and GFC. This is furtherly confirmed by the fact that the two variables do not share important historical peaks.

The Granger causality tests lead always to not reject the null, suggesting the absence of causality between GPR and GFC, regardless of the direction. This means that, even if the underlying VAR model should account for lower frequency data, GPR would still not causally relate to GFC. These results hold in the subsample going from January 1990 to April 2019.

### *4.3.2 GFU vs GFC*

Their relationship has been analysed in the time span from July 1992 to April 2019 and their time series are plotted in *Figure 16*. Their correlation equals to -0,3309 and it is statistically significant at the 99% level. This is a relevant negative relation, which is furtherly corroborated by the circumstance that both series spike in the opposite direction during the same historical episodes, mainly the Great financial crisis, the European sovereign debt crisis, and the covid-19 pandemics.

The Granger causality analysis signals that GFU and GFC share a strong feedback relationship at 6 and 7 lags: indeed, the series Granger cause each other at a 97.5% significance level. In addition, GFU Granger causes GFC when considering 12 and 24 lags. Therefore, GFU Granger causes GFC at any number of lags. The results are robust to considering the overmentioned subsample.

Preliminarily, GFU appears to be an important driver of GFC, confirming the results of Caggiano and Castelnuovo (2023).

### *4.3.3 GEPU vs GFC*

Their common sample spans from January 1997 to April 2019. Strikingly, GEPU displays the most negative correlation with GFC (-0,6285) among the three uncertainty measures, with a level of significance equal to 99%. In fact, as stressed by *Figure 17*, these two series exhibit opposite time paths, which clearly react in the opposite directions in correspondence of the same events.

However, despite the strong negative correlation, the Granger causality analysis leads to unstable results across different VAR specifications. As a matter of fact, GFC seems to Granger cause GEPU in the VAR settings provided with 6 and 7 lags, whereas GEPU Granger causes GFC in the 12 lags-model. Findings are robust to the previously explained sample variation.

### *4.3.4. Concluding remarks*

All the uncertainty measures show a negative and statistically significant correlation with the Global Financial Cycle, confirming the theoretical negative link argued in the first chapter. However, from the Granger causality analysis, only GFU seems to be a stable determinant of GFC. This is just a preliminary result but might suggest that GFU affects the most GFC among the uncertainty variables. Such a hypothesis will be more formally evaluated in the next chapter through the SVAR analyses outlined in the previous chapter.

## 5. FINDINGS AND RESULTS

The fifth and last chapter of this dissertation will be devoted to illustrating the results of the empirical research based on the econometric specifications described in Chapter 3. The effects of a unitary variance shock to GPR, GEPU and GFC will be investigated, focusing on GFC dynamics. More specifically, the structural IRFs, the structural FEVDs to the uncertainty shocks, the eigen values of the companion matrix, the SACFs, and the charts of the reduced form errors will be commented for all the SVAR models of each econometric specification. Hence, starting from the Chol specification, the stability of the three specification-related reduced form VAR models and the contribution of each different structural uncertainty shock in affecting GFC will be assessed separately for every specification. In addition, comparisons between different specifications will be detailed to investigate the impact of changing econometric tools, techniques, and assumptions on the results.

### *5.1. The characteristics of the structural IRFs and FEVDs*

The IRFs and the FEVDs consider a horizon of 24 months, comprehensive of the month upon the impact and the following 23 months. The first month will be indexed as the month number 0 and the last month as the 23rd one. The confidence bands correspond to the $16^{th}$ and the $84^{th}$ percentiles. Their computation is based on the application of bootstrap algorithms, as regards the Chol specification, whereas it employs the simulation of the posterior distribution by means of the Markov Monte Carlo chain with reference to the remaining specifications. The results about IRFs are always presented in charts, where the confidence bands are represented in coloured - dashed areas. The solid – dotted or just solid black line displays the main response, which corresponds to the mean response, in case of the Chol specification, and the median one for the rest. The charts of the FEVDs follow the same representation scheme just detailed for the IRFs. However, FEVDs will be analysed through tables too, which report the median contributions, exception made for the Chol one, where mean values are considered. Each one of these tables illustrates the overmentioned FEVDs in five different periods: upon impact, 6, 12, 18, and 23 months after the uncertainty shock. They are: *Table 1, Table 2, Table 3, Table 4, Table 5, Table 6, Table 7, Table 8,* and *Table 9*.

Moreover, in order to provide a clearer exposition of the results, a specific colour motif will be assigned to the IRFs and the FEVDs resulting from each econometric specification.

Specifically, a light blue motif will be applied to the results of the Chol specification, while the IRFs and the FEVDs of the PFA – Min and the PFA - Conj specifications will present a yellow motif and a green motif, respectively.

Lastly, it is important to clarify that the economically consistent responses of model variables to a generic uncertainty shock should be the following:

- the uncertainty measures surge and revert to zero some months after the shock occurred;

- the GFC drops due to the reasons explained in the first chapter;

- shadow rate declines, as effect of GFC reduction, as proved by Miranda Agrippino and Rey (2020);

- the reduction in GFC and the rise in uncertainty lead to a drop of WIP growth, since deteriorated financial conditions and higher levels of uncertainty are typically associated to recessions;

-a lower WIP growth and a lower shadow rate should be associated to declining inflation.

### *5.2. Reduced form residuals: an overview of the related time series and SACFs*

Preliminarily, it is worth emphasising that, by considering the SACFs and the time series of the estimated reduced form residuals, all the estimated VAR models return reduced form errors that can be reasonably approximated by zero mean white noises. Indeed, the reduced form residuals do not follow trends over time, on one hand, and their sample autocorrelations are almost never significant after the first lag, on the other one, reverting to zero very quickly. Thus, all the VAR models can be deemed as weakly stationary if they are stable, given that their means are supposed to be constant over time by default. More precisely, the VAR models will be weakly stationary if the eigen values of the companion matrix of the lag coefficients **A** has all the eigen values which, in module, are lower than one.

The charts of the SACFs and the charts of the residuals' time series will be provided only for the Chol specification, since they follow the same pattern across the other specifications. *Figure 29*, *Figure 30*, and *Figure 31* display the SACFs, while *Figure 32*, *Figure 33*, and *Figure 34* show the time series of the reduced form residuals.

### *5.3. The Chol specification*

The specification whose results will be showed firstly is the Chol one, since, as previously explained, the Cholesky decomposition represents the most basic identification strategy and hence the most natural starting point of the current analysis.

The first important result is that, for every uncertainty measure, the estimated companion matrix ***A*** retrieves only eigen values that are lower than one in absolute values. Therefore, the three models are stable and weakly stationary.

#### *5.3.1 The IRFs*

As we can notice from *Figures 24, 25,* and *26*, which depict the structural IRFs resulting from this specification, the space between the mean response and the confidence bands is in a light blue colour. However, only the mean responses, represented with the solid black lines, will be commented in this section. As a clear consequence of the zero restrictions, the responses of all the variables, exception made for the uncertainty measures hit by the shock, of course, are always null upon impact, i.e., at the horizon equal to zero.

The responses of GPR, GEPU and GFU to their own shocks revert completely to zero before the end of the horizon. The IRFs of GPR and GEPU peak upon impact, by taking on values higher than 30% and 15%, respectively, and decline in the following months, by reaching levels below the threshold of 5% at the sixth month. Instead, the response of GFU shows its maximum at the first month after the shock and decreases in the following months. Importantly, it takes on very small values compared to other uncertainty measures: it equals to 0,06% at the sixth month and even its maximum is below 0,2%.

The most striking fact that stands out from the observation of these IRFs is that the responses of the variables to GPR and GEPU shocks are extremely inconsistent with economic theory. The WIP growth rate and shadow rate increase for the most in response to the GPR shock, whereas shadow rate and CPI experience a slight increase and show an overall pattern which is very close to zero in response to the GEPU shock. In addition, GFC generally exhibits a positive response after the occurrence of both shocks. Precisely, its responses take on positive values for all the months after the GPR shock, showing even some persistence and reaching a peak of about 1,7% at the $20^{th}$ month circa. On the other hand, GFC reacts more heterogeneously after GEPU shock, by declining and experiencing a contraction in the first month and in the fifth one

right after the impact and displaying a positive pattern for the remaining months, which reverts almost totally to zero after 24 months. However, the magnitude of the reaction is very limited: its maximum, reported at the 4th month, amounts to approximately 1,3%.

It is worth emphasizing that the responses of the model variables to GEPU shocks are generally insignificant and very uncertain, being surrounded by relatively wide confidence bands.

In stark contrast with the IRFs estimated for GEPU and GPR shocks, all the responses of the economic and financial aggregates to the GFU shock are economically consistent. Especially, GFC declines significantly for all the months following the shock, by reaching the minimum of about 8,5% at the sixth one. Its reaction dies out at the end of the horizon, which confirms the stability of the SVAR model.

Summing up, only GFU shock originates a plausible dynamic for GFC and for the other model variables. As regards the other shocks, the evident inconsistencies found might be due to the circumstance that the zero restrictions imposed by the Cholesky decomposition are generally unrealistic for identifying uncertainty shocks, as explained in Chapter 3. Thus, considering the PFA as identification strategy, which introduces more reasonable assumptions for identifying uncertainty shocks, could be useful for addressing the problem of economically inconsistent IRFs.

### *5.3.2 The FEVDs*

The FEVDs resulting from the Chol specification are illustrated by *Table 3, Table 6, and Table 9*, and they corroborate the hypothesis that the Cholesky decomposition does not identify properly uncertainty shocks and provides just a lower bound. In fact, the contribution of the GEPU and GPR shocks in explaining other variables does not overcome the thresholds of 1% and 2%, respectively, exception made for the FEVD related to CPI that reaches the 4,5% level circa. Specifically, the highest contribution of GPR and GEPU shocks to GFC amounts to 1,86% and 0,735%, respectively. Such low values are quite unplausible and are justified by the application of the Cholesky decomposition. However, the FEVDs referred to GPR and GEPU, especially, are quite high in the first six months after their own shocks. In fact, the first one equals to 96% upon impact and 90% after six months, whereas the second one amounts to 82% and 58% in the same horizons.

The shock to GFU contributes more significantly to explaining the variances of other variables. The FEVD associated to GFC reaches the 21% level at the 12th month after the shock and the

other FEVDs are always higher than the 5% threshold. However, the FEVD concerning GFU equals to 66% upon impact and 71% after six months, which are relatively low values and might signal an incorrect identification strategy.

Therefore, an important result coming from the Chol specification is that GFU shock is associated with the most significant and economically consistent responses and FEVDs related to GFC. On the other hand, the GPR shock originates the least relevant responses of GFC and the GEPU shock contributes the least to the forward variance of GFC among the uncertainty shocks.

### *5.4. The PFA - Min specification*

The use of the PFA and of the Minnesota prior make this econometric specification more reasonable than the Chol one, as explained in Chapter 3. In addition, by maximizing the IRFs of uncertainty measures, it provides an upper bound measure of the effects of uncertainty shocks on the remaining model variables. However, this specification has a quite unpleasant result: for every estimated SVAR model there is at least one eigen value that is higher than one in module. Hence, all the three estimated SVAR models are unstable and their IRFs and FEVDs are hard to die out over the horizon of 24 months after the occurrence of the uncertainty shock, indeed. As regards the three structural IRFs plotted in *Figures 18, 19,* and *20*, only the median responses, which are represented in the solid black lines, will be commented in this section.

#### *5.4.1. The IRFs*

With respect to the Chol specification, the IRFs associated to GEPU and GPR shocks are decidedly more economically significant, in general. In fact, WIP growth rate, shadow rate and GFC exhibit an overall negative pattern in response to both the overmentioned shocks. Only the IRFs of CPI remains inconsistent with economic theory, reporting an overall increase over the horizon. However, its median reaction is very limited and does not overcome the threshold of 0,021%. The response of GFC to GPR shock peaks at the first month, by taking on a value of about -2,5%, and takes on positive values between the $16^{th}$ and the $24^{th}$ month after the shock. The IRF of GFC to GEPU shock shows its minimum of approximately -11,5% at the fifth month after the shock and it does not revert to zero before the end of the horizon.

On the other hand, GFU shock originates all responses that remain economically consistent and acquire more significance relatively to the Chol specification. Specifically, GFC displays an overall negative pattern over time, by peaking at the fifth month after the impact, with a value of -16% circa, and shows some persistency at the end of the horizon. Hence, GFU turns out to be the shock associated with the highest impact on GFC in this specification.

The fact that this specification gives place to economically consistent IRFs signals that the PFA is a more realistic identification strategy for identifying uncertainty shocks compared to the Cholesky decomposition.

Another evident effect of the PFA is the circumstance that the responses of GFU, GEPU and GPR to their own shocks are more relevant compared to the Chol specification, especially in the first six months, of course. Indeed, recall that the PFA maximizes the IRFs of the uncertainty shocks until the sixth month after their happening. The values of the IRFs of GPR, GEPU and GFU upon impact are about 32%, 21%, 0,17% respectively, whereas their values at the sixth month after the shock are around 14%, 11%, 0,12%, respectively. Hence, with respect to the same periods, the responses are always higher or at least equal than those implied by the application of the Cholesky decomposition.

The main drawback of this specification is the fact that almost all the IRFs, including those of GEPU, GFU and GPR, show persistency at the end of the horizon, as a consequence of the instability of their related SVAR models, as previously underlined.

### *5.4.2. The FEVDs*

The FEVDs resulting from this specification have two common traits: they are generally more significant than those implied by the Chol specification and do not revert to zero at the end of the horizon, but, on the contrary, they tend to maintain or increase the levels showed at the sixth month after the shocks occurred. They are displayed by *Tables 1, 4,* and *7.* The first trait is a consequence of the fact that the PFA identified the uncertainty shocks better and hence, as just illustrated, the IRFs are more significant. Specifically, the much higher values of the FEVDs associated to GEPU, GFU and GPR represent one of the main facts in favour of the thesis according to which the PFA outperforms the Cholesky decomposition in identifying such uncertainty shocks. Upon impact, the FEVDs of GFU, GPR and GEPU are about 96.5%, 98.6% and 94%, whereas, at the sixth month after their own shocks, they amount to about 98%, 98.6%

and 96.3%. As concerns the second common characteristic, this is due to SVARs models instability, of course.

Therefore, the capacity of all shocks of explaining GFC has been improved by this specification, compared to the Chol one. In fact, the FEVDs are always higher than those implied by the Chol specification in the same periods. The contributions of GFU, GEPU and GPR are always higher than 25%, 23% and 1.5%, respectively, and their maximums equal to circa 56%, 27.5% and 3%, respectively.

Summing up, GFC displays the most relevant FEVDs and IRFs in response to GFU shock, as in the Chol specification, while it has the least significant IRFs and FEVDs after GPR shock.

### *5.5. The PFA - Conj specification*

As underlined in the last two sections, the PFA combined with the Minnesota prior has proved to have an important drawback in both the two related specifications: it implies unstable estimated SVAR models which map into IRFs and FEVDs that hardly go to zero. In order to address this problem, it could be useful to employ the PFA together with a different prior for the reduced form parameters as well as this specification does, by considering the Conjugate Gaussian inverse Wishart prior. Besides, this choice allows to test whether the results found in the PFA – Min specification are robust to changing prior.

The PFA - Conj identification proves to solve the problem successfully: there is no eigen value which is higher or equal to one in all the three estimated SVAR models. Hence, all the SVAR models are stable and their IRFs and FEVDs should revert to zero. In the following subsections, only the median responses and the median contributions illustrated in *Figure 21*, *Figure 22*, and *Figure 23*, and in *Table 2*, *Table 5*, and *Table 7*, respectively, will be commented.

#### *5.5.1. The IRFs*

Analogously with the PFA - Min specification, the IRFs tend to be more economically consistent and more relevant compared to those associated to the Chol specification, in general, corroborating the thesis according to which the PFA should be a more reasonable strategy for identifying uncertainty shocks. In fact, all the responses show an overall pattern that is economically coherent. However, the IRF of CPI after GEPU shock and the reactions of shadow

rate, WIP growth rate and GFC to GPR shocks are inconsistent for about the half of months after the occurrence of the shocks. In addition, the IRF of GFU is slightly negative for about ten months. Thus, compared to the PFA - Min specification, there is a higher number of responses that are partly or totally economically inconsistent.

GFC exhibits a negative time path from the occurrence of the GPR shock until the 15$^{th}$ month and takes on its lowest value, which equals to circa -4%, at the first month. From the 16$^{th}$ month on, this IRF is positive and does not die out before the end of the horizon. On the contrary, the IRFs of GFC in response to GEPU and GFU shocks are never positive, revert to zero after 23 months and display their minimums at the sixth month, which amount to about -13% and -16%, respectively. Hence, GFU and GPR still trigger the highest and the lowest reduction in GFC, respectively. Notice that the minimums associated with these three IRFs are even lower than their analogous of the PFA - Min specification.

Lastly, as for the PFA - Min specification, the responses of the uncertainty measures after their own shocks are generally more significant than their Chol specification counterparts in the first six months, suggesting the effectiveness of the PFA in maximizing these IRFs in the first half of the first year after the occurrence of the related uncertainty shocks. The values of the IRFs of GPR, GEPU and GFU upon impact are about 30%, 20% and 0.17%, respectively, whereas their values at the sixth month after the shock are 5%, 6% and 0.09%, respectively. So, they are lower or equal to their counterparts in the PFA - Min specification.

### *5.5.2 The FEVDs*

Analogously to the IRFs and the FEVDs of the PFA – Min specification, the FEVDs are characterized by a higher relevance compared to those of the Chol specification, suggesting a higher plausibility of the PFA for identifying uncertainty shocks with respect to the Cholesky decomposition. In fact, GFU, GPR and GEPU contribute to the forward variance of GFC for a value that is always higher than 24%, 5% and 27%, respectively. The maximums of these three FEVDs are 65%, 8% and 39%, respectively, which are higher than their counterparts of the PFA - Min specification. In addition, GFU shock explains the highest percentage of fluctuations in GFC on average and the FEVDs concerning GFC tend to be more significant than those associated to the PFA - Min specification.

Strikingly, uncertainty shocks contribute to the fluctuations of other variables in percentages that are almost always higher than those associated with the PFA - Min specification. Only the contribution of GFU to the CPI fluctuations does not follow this rule.

In addition, for each uncertainty measure, the percentage of movements that is attributed to its own shock is usually higher compared to the Chol specification in the first six months. This confirms the fact that the PFA outperforms the Cholesky identification in identifying such uncertainty shocks and the circumstance that the PFA should bring to upper bound estimates, by construction. The only exception is represented by the FEVD of GPR, which amounts to 95.65% upon impact and hence is lower than its Chol counterpart by 0.4% circa. Upon impact, the FEVDs of GFU, GPR and GEPU are about 94.4%, 95.6% and 84%, whereas, at the sixth month after their own shocks, they amount to about 95%, 90.3% and 80.4%. Notice that these values are less relevant compared to the PFA – Min specification.

Summing up, GFU shock causes the most significant drop in GFC and is associated with the highest contribution to the variance of GFC. On the opposite side, GFC suffers the lowest contraction from the shock to GPR, which in turn explains the lowest percentage of perturbances in GFC. Besides, even if the IRFs and the FEVDs of the uncertainty measures after their own shocks are less relevant relatively to the PFA – Min specification, GFC shows more significant FEVDs and IRFs compared to the overmentioned specification. Overall, the significance of each uncertainty shock in affecting GFC is fairly stable with respect to the PFA – Min specification.

### *5.6. A focus on the effects of the uncertainty shocks on GFC*

To make clearer and more immediate comparisons between the IRFs and the FEVDs of GFC in the three different specifications, *Figure 28* and *Figure 27* will be analysed. They show an overview of the estimated IRFs and the FEVDs with respect to GFC, respectively, by providing a graphical representation to them and assigning to each specification the same colour - motif as in the tables and in the charts of the IRFs previously described in this chapter. Hence, the Chol, PFA - Min, and the PFA - Conj specifications are characterized by confidence bands in the colours of light blue, yellow, and green, respectively. As before, we will refer to mean or median responses unless it is differently specified.

### *5.6.1 The IRFs*

As *Figure 28* clearly points out and as illustrated in the previous subsections, GPR shock originates the least economically consistent and the least significant reactions of GFC in all the specifications. The responses of GFC after this shock are positive for at least seven months and they are not lower than -4,5%. In addition, they are surrounded by very wide confidence bands compared to the remaining variables and take on their minimums upon impact. In contrast, GFU shock gives place to the most relevant IRFs of GFC in every specification; in addition, they are usually the most coherent with economic theory. The reaction of GFC after GFU shock reaches the threshold of -15%. The minimums are reached at the sixth month after the shock, regardless of the specification. Importantly, the IRF of GFC that is denoted by the lowest minimum is the IRF generated by the GFU shock in the PFA - Min specification; nevertheless, this minimum is not so different from the one associated to GFU shock in the PFA - Min specification. Moreover, GFC reacts to GFU shocks by displaying the thickest confidence bands among the uncertainty measures in relative terms. Lastly, the IRFs associated to GEPU shock are usually economically consistent and very significant in the PFA - Min and PFA – Conj specifications, reaching a minimum of -11%. As well as for GFU, the minimums are taken on in correspondence with the sixth month after the uncertainty shock.

On the other hand, *Figure 28* shows that the IRFs linked to the PFA – Conj specification tend to be the most relevant and they are the most realistic, given that they are economically consistent almost in every month and they are not persistent throughout the horizon. In addition, this specification is characterized by the thickest confidence bands and hence by the lowest estimation uncertainty. On the opposite side, the Chol specification is denoted by wide confidence bands and by inconsistent and quite insignificant IRFs. Hence, the PFA has helped the uncertainty shocks to significantly increase their negative influence on GFC.

### *5.6.2. The FEVDs*

*Figure 27* graphically illustrates the FEVDs of uncertainty shocks relatively to GFC. The most outstanding result regarding these charts is the fact that GFU shock is the shock that contributes to the volatility of GFC for the highest percentages in every econometric specification. Remarkably, its contribution amounts even to over 50% and over 60% in the PFA - Min specification and in the PFA – Conj specification, respectively, which are very high values in absolute terms and make GFU the most important driver of the fluctuations of GFC among all

the model variables in these two specifications. Besides, this contribution reaches the 21% threshold in the Chol specification, even if it is estimated at its minimum by construction.

The GEPU shock explains a high portion of the variance of GFC in the PFA - Min specification and in the PFA – Conj specification as well, since both the FEVDs overcome the threshold of 30%. However, these FEVDs are substantially less relevant than those associated with the GFU shock in the same two specifications. The GEPU shock can be reasonably deemed as the second most important determinant of the movements of GFC among the three identified uncertainty shocks, because the related FEVDs are higher or at least almost equal to the FEVDs of the GPR shock in every econometric specification, when they regard GFC. In fact, GPR shock contributes to the 8% of volatility of GFC at most.

Also, *Figure 27* points out that the PFA – Conj specification gives place to the most relevant FEVDs on average, even if they are not remarkably higher than those associated to PFA - Min specification. In both these two specifications, the FEVDs of GFU and GEPU shocks are really significant, reaching values that are higher than 25% almost in each month after the impact. Hence, the PFA allows the three uncertainty shocks to increase their explanatory power for GFC fluctuations with respect to the Cholesky decomposition.

### *5.7. Concluding remarks on the econometric specifications and limitations of the empirical research*

From the results illustrated in this chapter two main conclusions can be drawn about the econometric framework underlying the five overmentioned specifications. First of all, the PFA proves to be effective in retrieving economically consistent responses and IRFs and FEVDs that are more significant than those associated to the Cholesky decomposition.

Secondly, the relevance and the economic consistency of the IRFs and of the FEVDs turn out to be affected by the choice of the prior for the reduced form parameters of the SVAR models. In fact, the Conjugate Gaussian Inverse Wishart prior is generally linked with higher absolute values of FEVDs and of IRFs with respect to the Minnesota prior and less economically consistent IRFs. However, the results concerning GFC do not show significant variations in these two specifications and hence can be deemed as robust to changing prior for the reduced form parameters.

Finally, it is important to stress that this empirical research has the limitation of not taking into account the effects of varying the optimization order of the shocks in the PFA. In fact, results might change a lot when identifying the GFC shock as the first one, since it could lead to less significant and less economically consistent estimated FEVDs and IRFs. Fluctuations that should be attributed to uncertainty shocks could be mistakenly attached to the GFC shock, lowering the importance of uncertainty in affecting GFC. Indeed, financial aggregates, such as GFC, and uncertainty measures – financial uncertainty measures, especially – move in response to the same events typically and, consequently, it is hard to disentangle their respective shocks properly.

### *5.8. Concluding remarks on GFC*

The most outstanding result of this empirical research is the fact that GFU turns out to be the most important driver of GFC among the uncertainty shocks, confirming the conclusion of the Granger causality analysis carried out in Chapter 4. Regardless of the econometric specification, it explains the most relevant percentages of GFC movements - the highest percentage is about 65% - and generates the greatest contractions of GFC - the most significant drop is circa of -16%. In addition, this shock triggers the most economically consistent and accurate estimated responses of GFC among the shocks: the pattern of GFC after GFU shock is substantially negative and displays thin confidence bands in each econometric specification.

GEPU is another important determinant of GFC, triggering reactions of GFC that are often consistent and relevant - the minimum is circa -13% - and FEVDs that can be very high, with a maximum of about 40%. GPR impacts the least on GFC and contributes the least to its movements on average. After this shock, the IRFs of GFC are generally insignificant and at least partly inconsistent and the FEVDs related to GFC are the least relevant in two of the three specifications.

As regards the econometric specifications, the PFA – Conj specification is associated with the most significant reductions in GFC after uncertainty shocks and with the highest contributions of uncertainty shocks to GFC future movements. Moreover, the responses are the most economically consistent among the specifications, since each one shows a pattern that remains negative for the highest number of months and tends to die out over the course of time.

## CONCLUSION

Consistently with theory literature, this thesis provides evidence that global uncertainty measures are able to lead the Global Financial Cycle to a low phase under specific assumptions. By employing a multiperspective approach for the identification of uncertainty shocks, which includes the widely used Cholesky decomposition and the PFA à la Caldara et al. (2016), we have estimated an upper bound and a lower bound for the adverse effects of GPR, GFU and GEPU on GFC. Financial uncertainty, proxied by the GFU index, and economic policies' uncertainty, measured by GEPU, turned out to significantly impact on GFC, since the average responses of GFC to these shocks exhibit a maximum contraction of about -13% and -16%, respectively. By following the same approach, we have showed that global uncertainty measures could be reasonably deemed as important determinants of GFC movements, being GFU and GEPU able to explain even the 65% and the 40% of the forward variance of GFC, respectively. Besides, GFU proved to steadily Granger cause GFC, regardless of the chosen lags, as shown in Chapter 4. Therefore, this empirical research provides evidence of the relevance of global uncertainty measures in affecting GFC, especially for the GFU index, which proves to be the most significant driver of GFC, irrespective of the underlying econometric assumptions.

**REFERENCES**


BAKER, S., R., BLOOM, N., and DAVIS, S., J., 2016. Measuring economic policy uncertainty. *The quarterly journal of economics*, 131(4), 1593–1636.

BAUMESTEIR, C., and HAMILTON, J., D., 2019. Structural interpretation of vector autoregressions with incomplete identification: Revisiting the role of oil supply and demand shocks. *American Economic Review*, 109.5, 1873–1910.

BLOOM, N., 2014. Fluctuations in uncertainty. *Journal of Economic Perspectives*, 28.2, 153–176.

CAGGIANO, G., and CASTELNUOVO, E., 2023. Global Financial Uncertainty. *Journal of Applied Econometrics.* John Wiley & Sons, Ltd., 38(3), 432-449.

CALDARA, D., and M. IACOVIELLO, 2022. Measuring Geopolitical Risk. *American Economic Review*, 112(4), 1194-1225.

CALDARA, D., FUENTES - ALBERO, C., GILCHRIST, S., and ZAKRAJŠEK, E., 2016. The Macroeconomic Impact of Financial and Uncertainty Shocks. *European Economic Review,* 88, 185–207.

CANOVA, F., 2007. *Methods for Applied Macroeconomic Research*. In: CAGGIANO, G., and CASTELNUOVO, E., 2023.

DEL NEGRO, M., and SCHORFHEIDE, F., 2011. Bayesian Macroeconometrics in: *The Oxford Handbook of Bayesian Econometrics*, Chapter 7, 293-389, Oxford University Press, Oxford, J. Geweke, G. Koop, and H. van Dijk (Eds).

DOAN, T., LITTERMAN, R., and SIMS, C., A., 1984. Forecasting and conditional projection using realistic prior distributions. *Econometric Reviews*, 3, 1–100.

FAUST, J., 1998. The robustness of identified VAR conclusions about money. *Carnegie-Rochester Conf. Ser. Public Policy*, 49, 207–244.

GRANGER, C., W., J., 1969. Investigating causal relations by econometric models and cross-spectral methods. In: KILIAN, L., and LÜTKEPOHL, K., 2017.

HAMILTON, J. D., 1994. *Time Series Analysis*. Princeton, NJ: Princeton University Press.

HANSEN, N., MÜLLER, S.D., KOUMOUTSAKOS, P., 2003. Reducing the time complexity of the derandomized evolution strategy with Covariance Matrix Adaption (CMA-ES). *Evolutionary Computation*, 11(1), 1–18.

KILIAN, L., and LÜTKEPOHL, K., 2017. *Structural Vector Autoregressive analysis*. UK: Cambridge University Press.

KNIGHT, F., 1921. *Risk, Uncertainty, and Profit.* Boston and New York: Houghton Mifflin Company, The Riverside Press Cambridge.

KOSE, A., M., PRASAD, E., ROGOFF, K., and WEI, S., 2006. Financial Globalization: A Reappraisal. *IMF Working Paper 06/189*, (Washington: International Monetary Fund).

LUDVIGSON, S. C., MA, S., and NG, S., 2021. Uncertainty and Business Cycles: Exogenous Impulse or Endogenous Response. In: CAGGIANO, G., and CASTELNUOVO, E., 2023.

LYU, Y., TUO, S., WEI, Y., and YANG, M., 2021. Time-varying effects of global economic policy uncertainty shocks on crude oil price volatility : New evidence. *Resources Policy,* 70, 101943.

MIRANDA – AGRIPPINO, S. and REY, H., 2020b. U.S. Monetary Policy and the Global Financial Cycle. *Review of Economic Studies*, 87(6), 2754–2776

MIRANDA – AGRIPPINO, S. and REY, H., 2021. The Global Financial Cycle in: *Handbook of international Economics*, Volume 6, Chapter 1, 1-43, G. Gopinath, E. Helpman, and K. Rogoff (Eds.).

MIRANDA – AGRIPPINO, S., TSEVETELINA, N., and REY, H., 2019. Global Footprints of Monetary Policies. In: MIRANDA – AGRIPPINO, S. and REY, H., 2021.

MOENCH, E., NG, S., and POTTER, S., 2013. Dynamic Hierarchical Factor Models. In: CAGGIANO, G., and CASTELNUOVO, E., 2023.

OZCELEBI, O., 2021. Assessing the impacts of global economic policy uncertainty and the long-term bond yields on oil prices. *Applied Economic Analysis,* 29 (87), 226-244.

REY, H., 2013. Dilemma not Trilemma: The Global Financial Cycle and Monetary Policy Independence. In: *Proceedings - Economic Policy Symposium*. Jackson Hole, Federal Reserve of Kansas City Economic Symposium, 285-333.

STOCK, J., H., and WATSON, M., W., 2001. Vector autoregressions. *Journal of Economic Perspectives*, 15.4, 101–115.

UHLIG, H., 2005. What are the effects of monetary policy on output? Results from an agnostic identification procedure. *Journal of Monetary Economics,* 52, 381–419.

WU, J., C., and XIA, F., D., 2016. Measuring the macroeconomic impact of monetary policy at the zero lower bound. *Journal of Money, Credit and Banking*, 48.2-3, 253–291.

YU, X., and HUANG, Y., XIAO, K., 2021. Global economic policy uncertainty and stock volatility: evidence from emerging economies. *Journal of Applied Economics,* 24 (1), 416–440.

**SITOGRAPHY**

*Globalization | English Meaning*, Cambridge Dictionary, viewed 02/10/2022, available at: https://dictionary.cambridge.org/dictionary/english.

*Handbook of Methods: U.S. Bureau of Labor Statistics*, U.S. Bureau of Labor Statistics, viewed 21/08/2022, available at: https://www.bls.gov/opub/hom/cpi/.

**FIGURES**

*Figure 1: GFC time series*

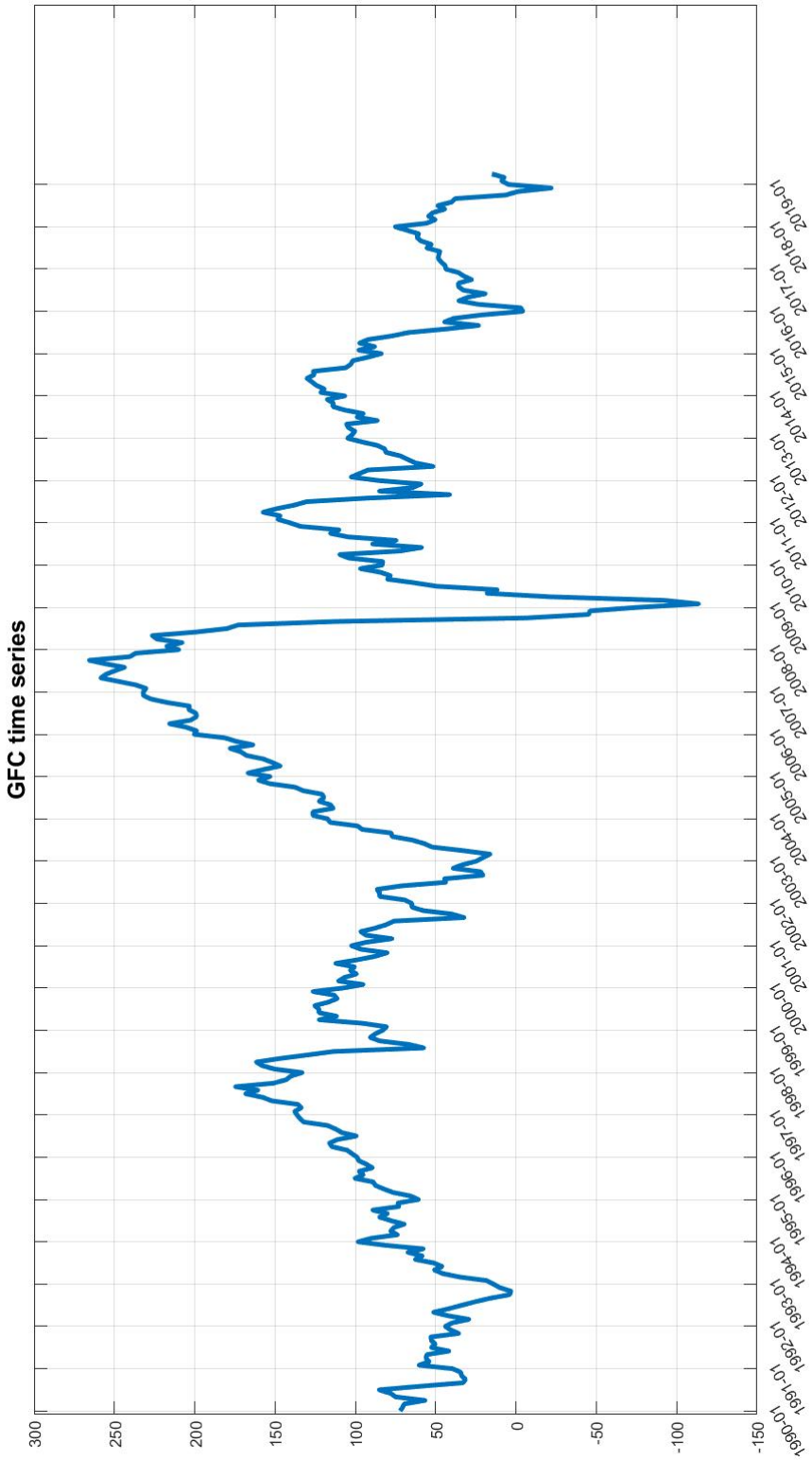

*Figure 2: GPR time series*

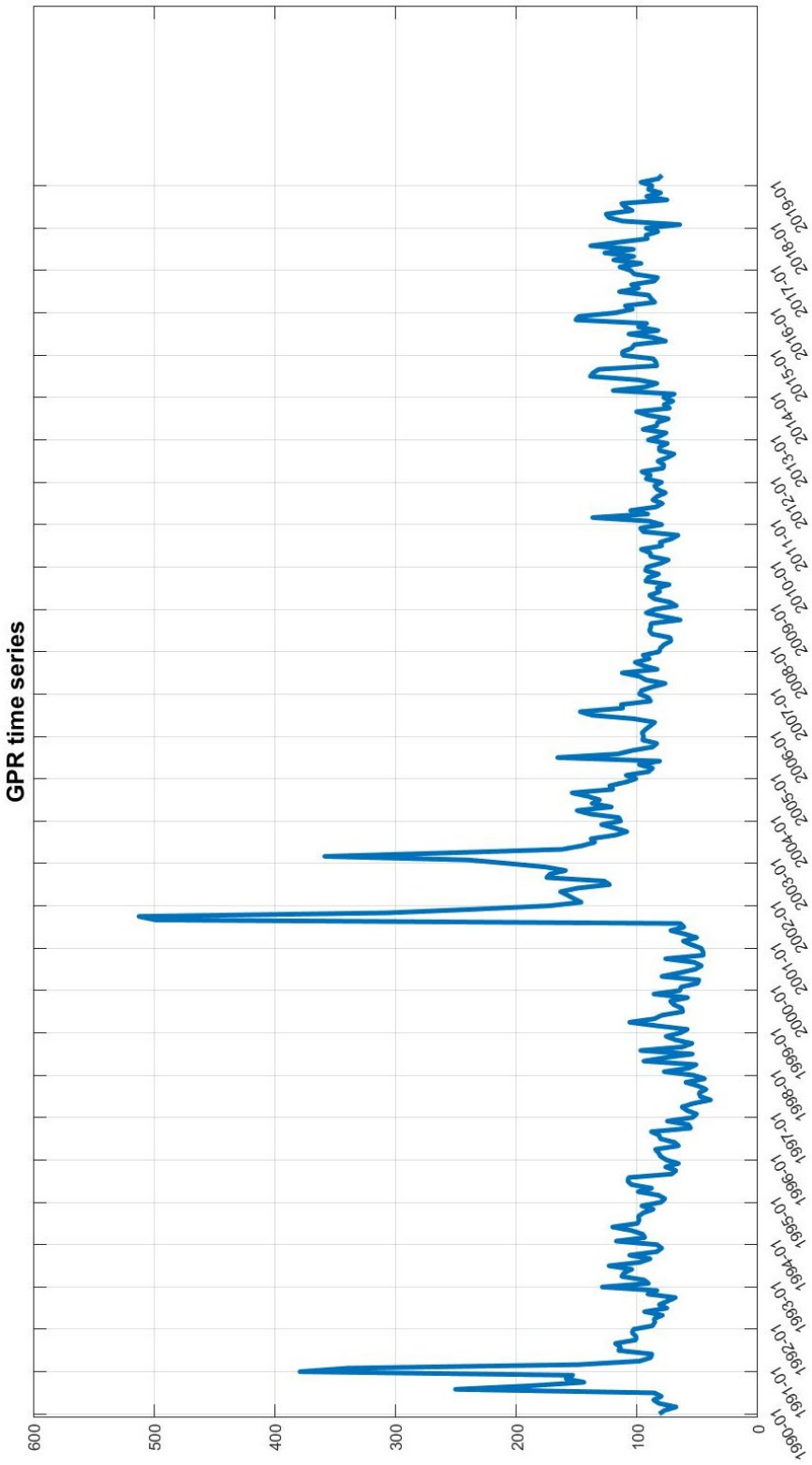

*Figure 3: GFU time series*

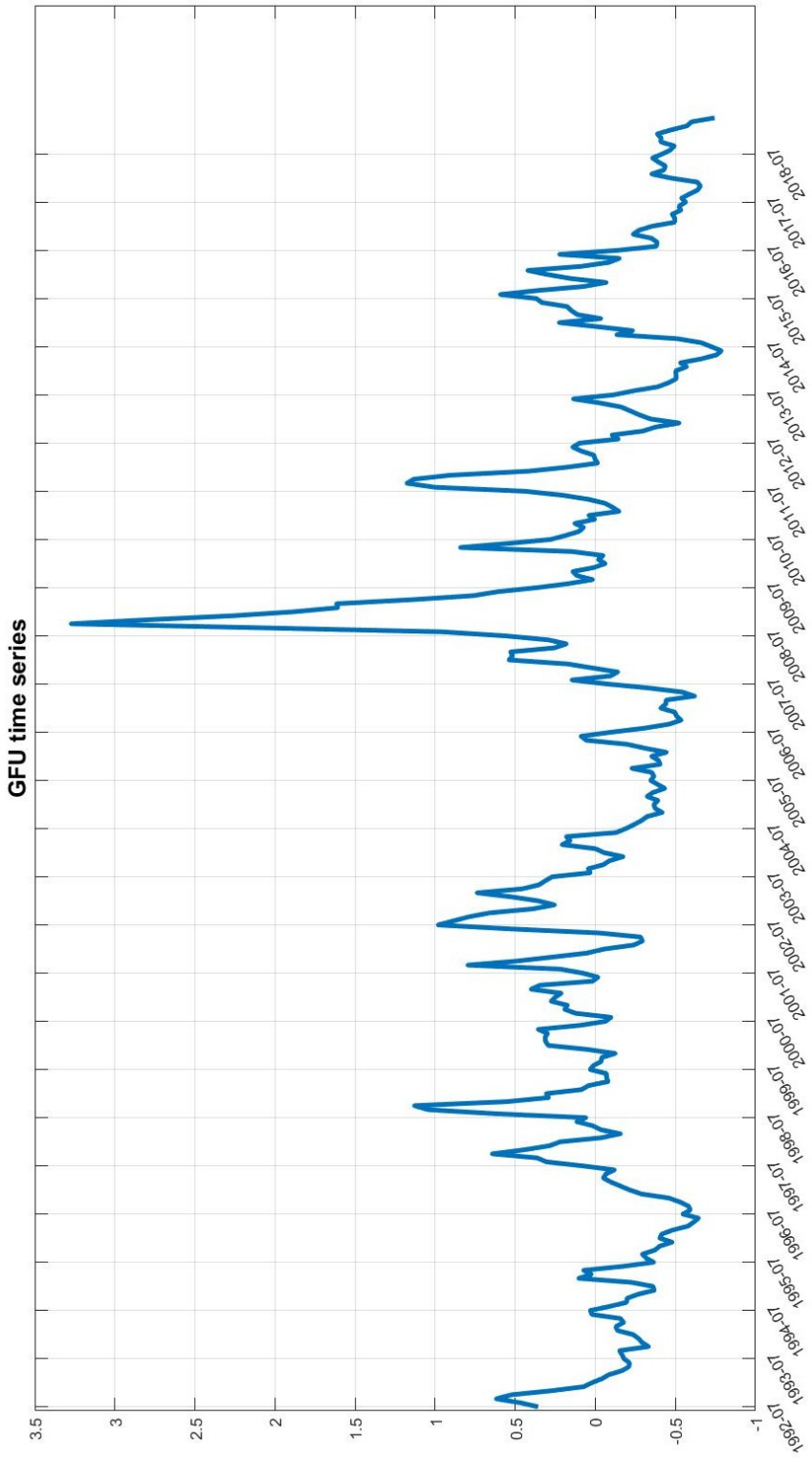

*Figure 4: GEPU time series*

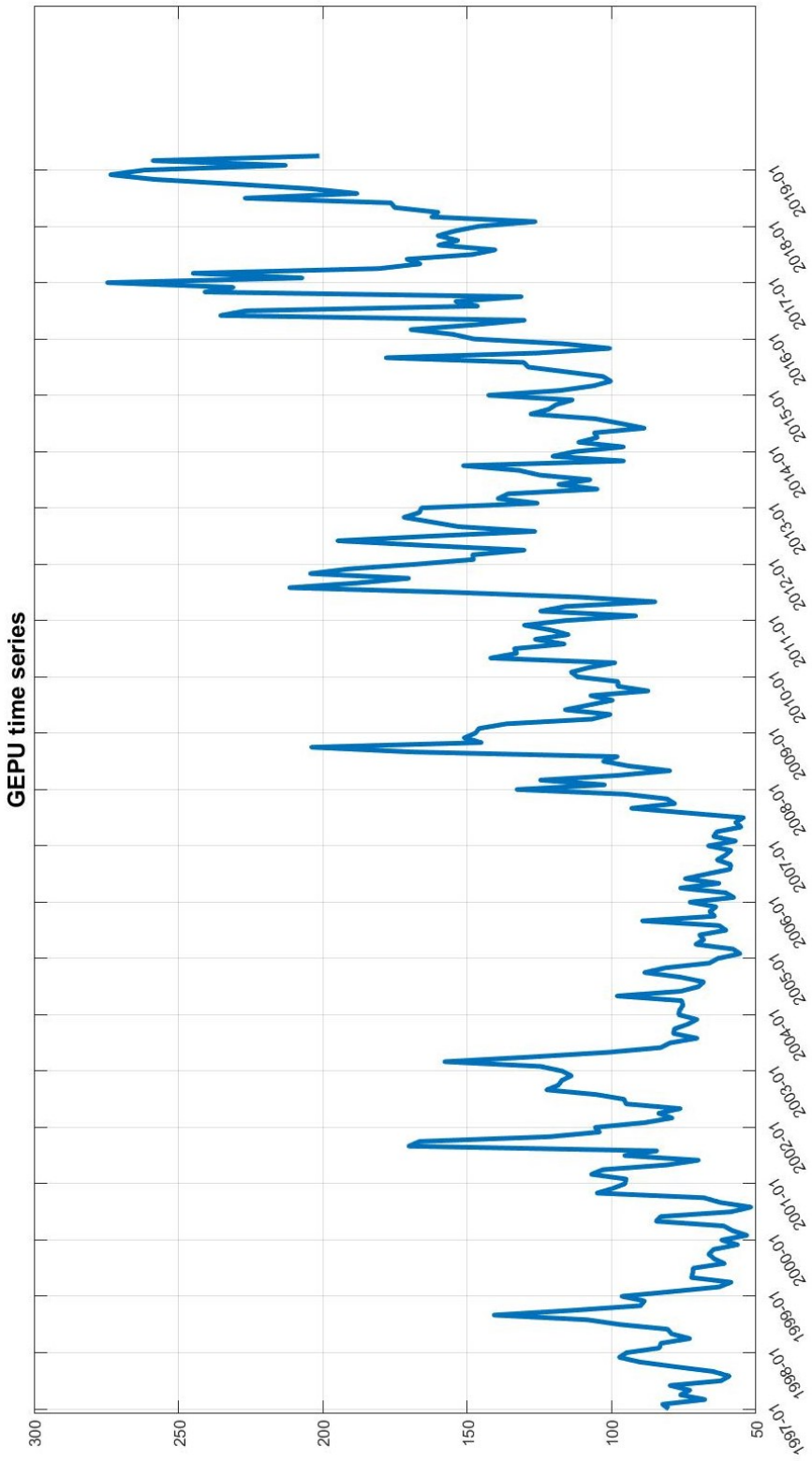

*Figure 5:Shadow rate time series*

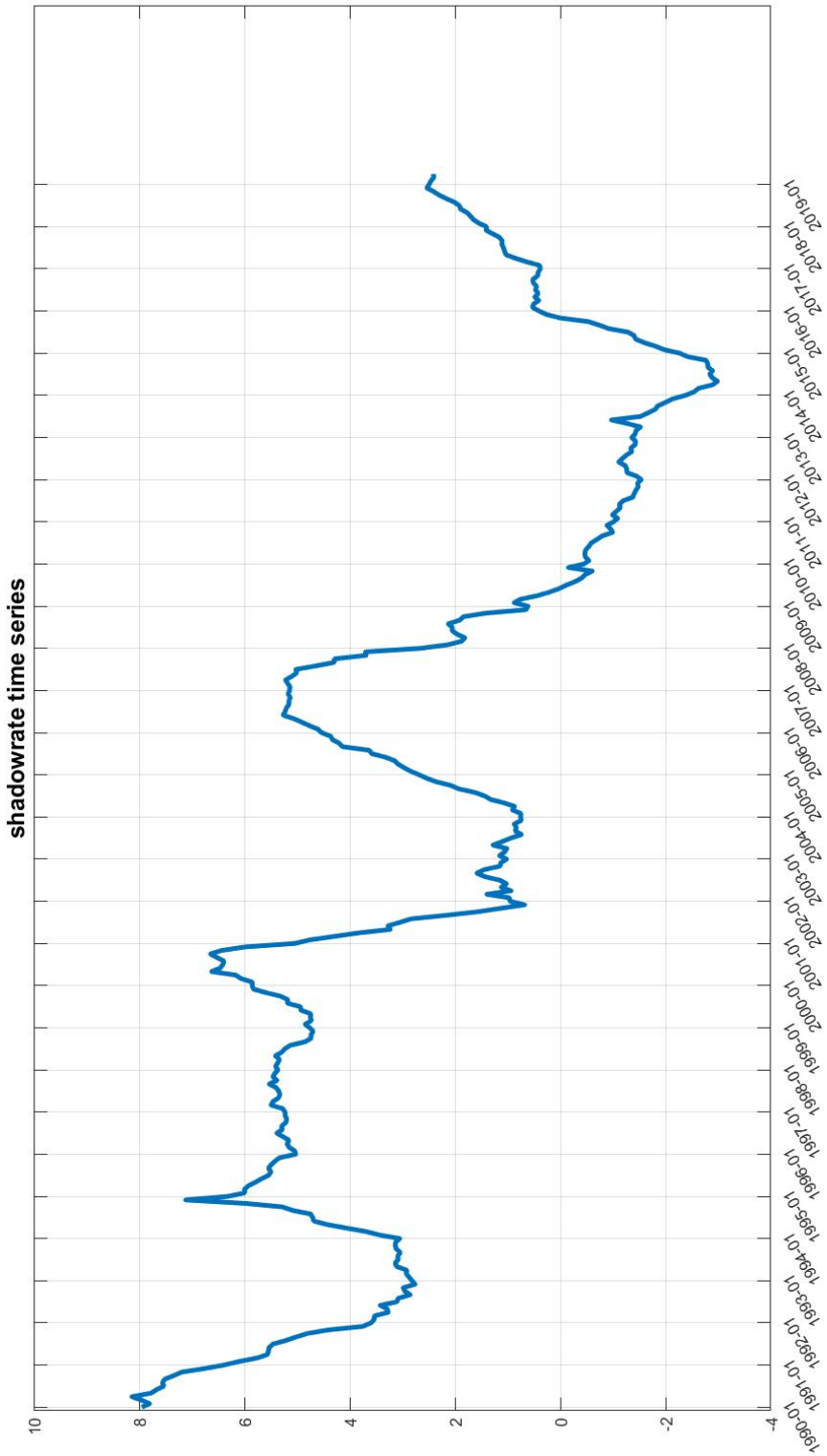

*Figure 6: WIP growth rate time series*

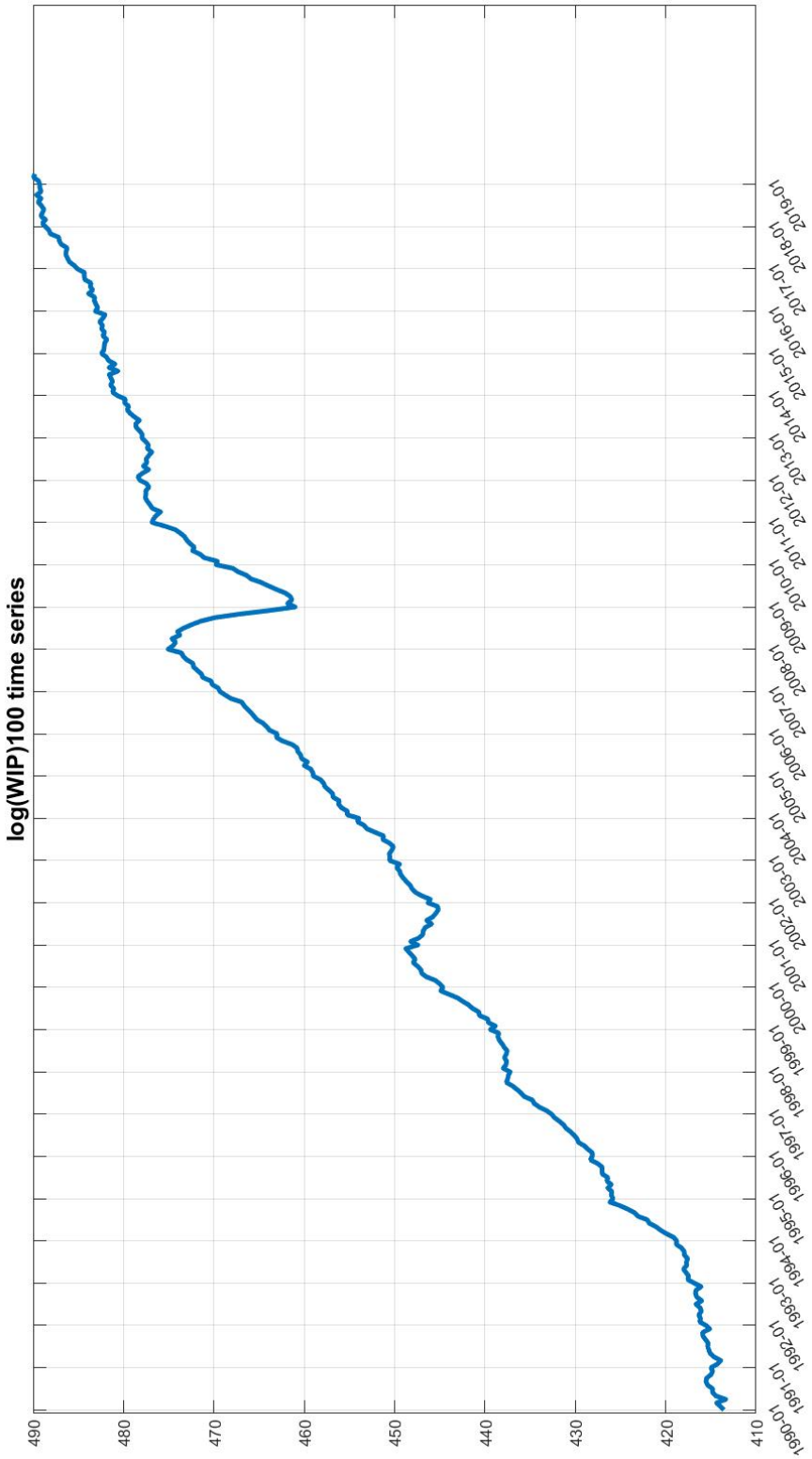

*Figure 7: CPI time series*

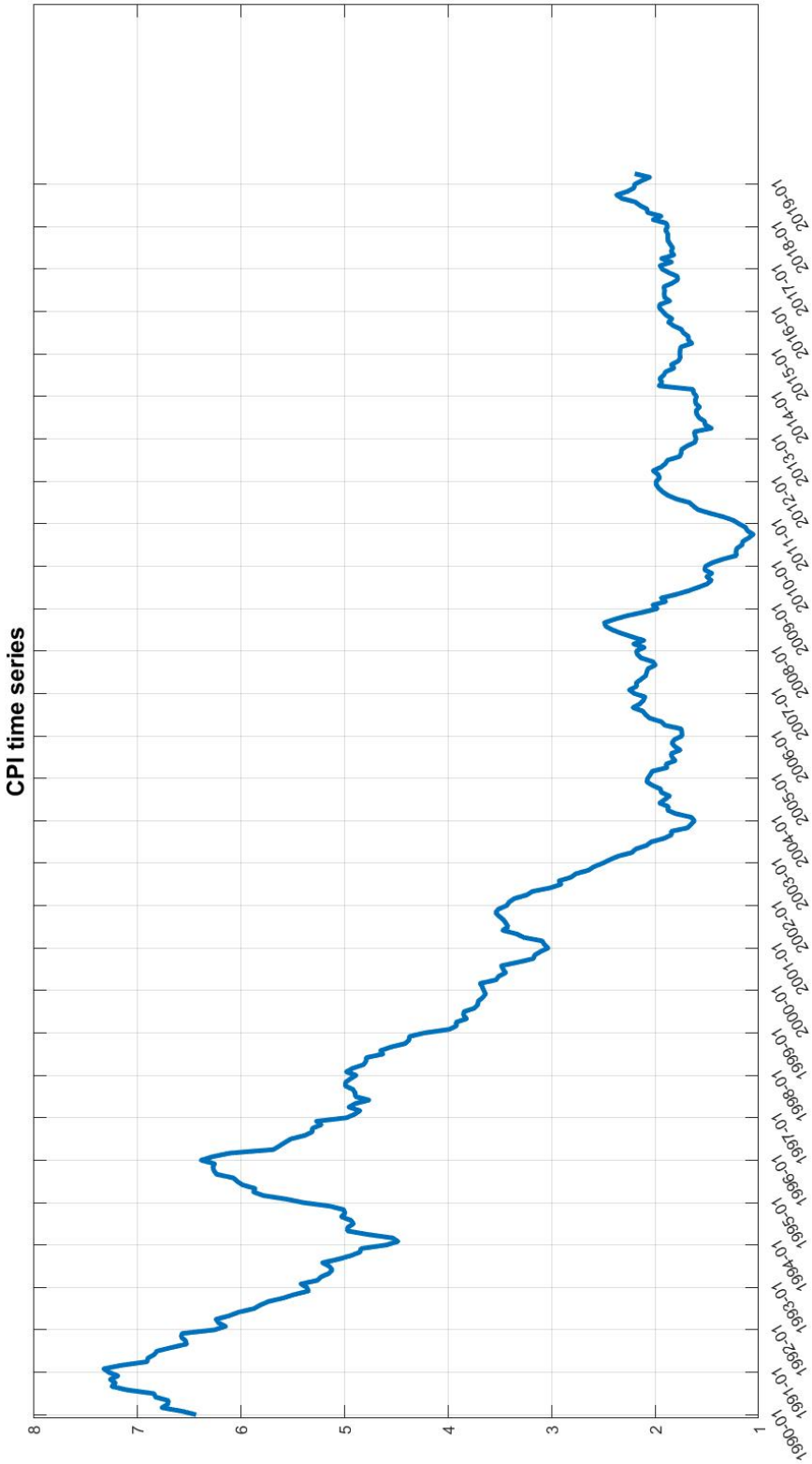

*Figure 8*

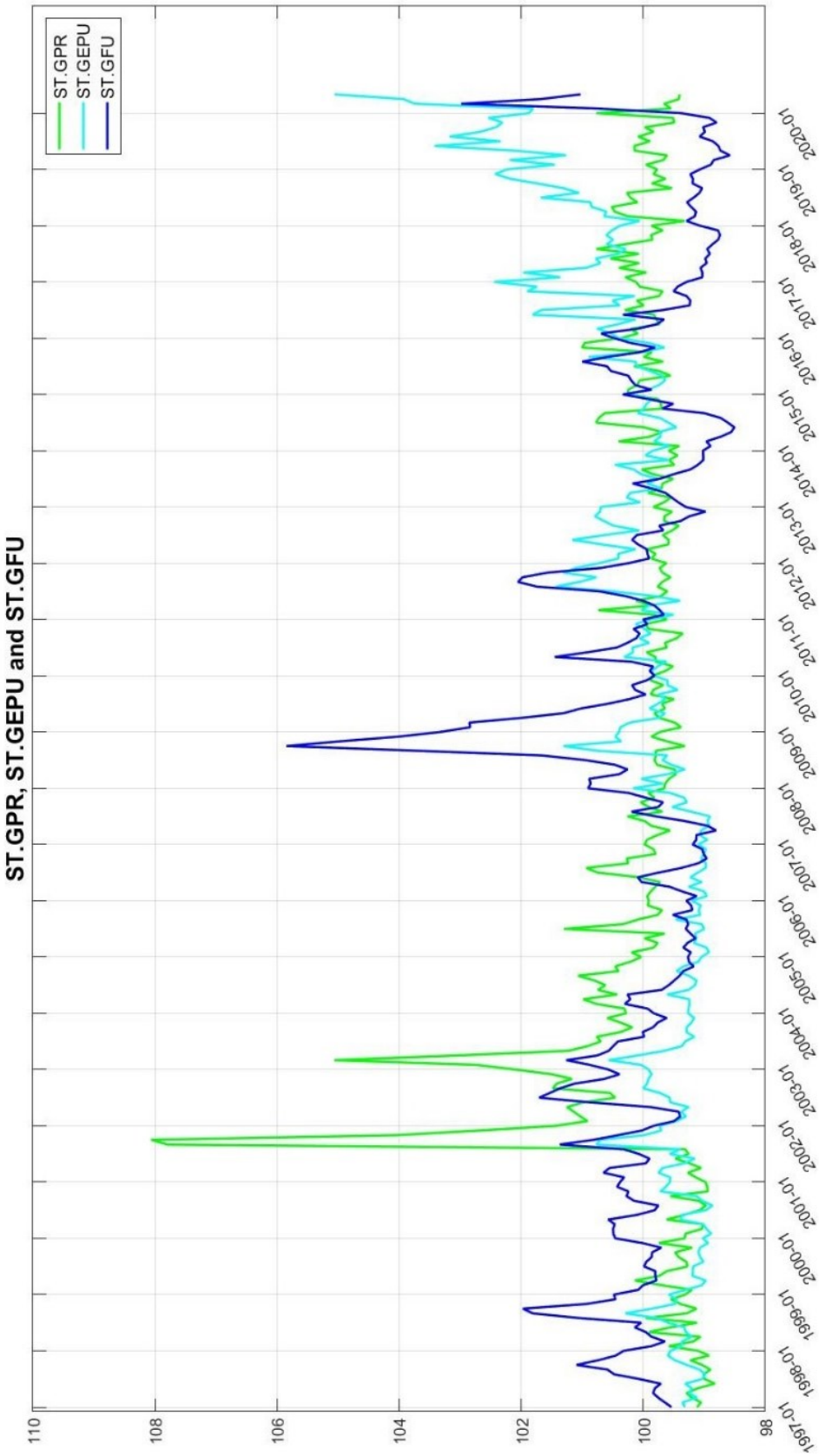
ST.GPR
ST.GEPU
ST.GFU
ST.GPR, ST.GEPU and ST.GFU
110
108
106
104
102
100
98
1997-01
1998-01
1999-01
2000-01
2001-01
2002-01
2003-01
2004-01
2005-01
2006-01
2007-01
2008-01
2009-01
2010-01
2011-01
2012-01
2013-01
2014-01
2015-01
2016-01
2017-01
2018-01
2019-01
2020-01

*Figure 9*

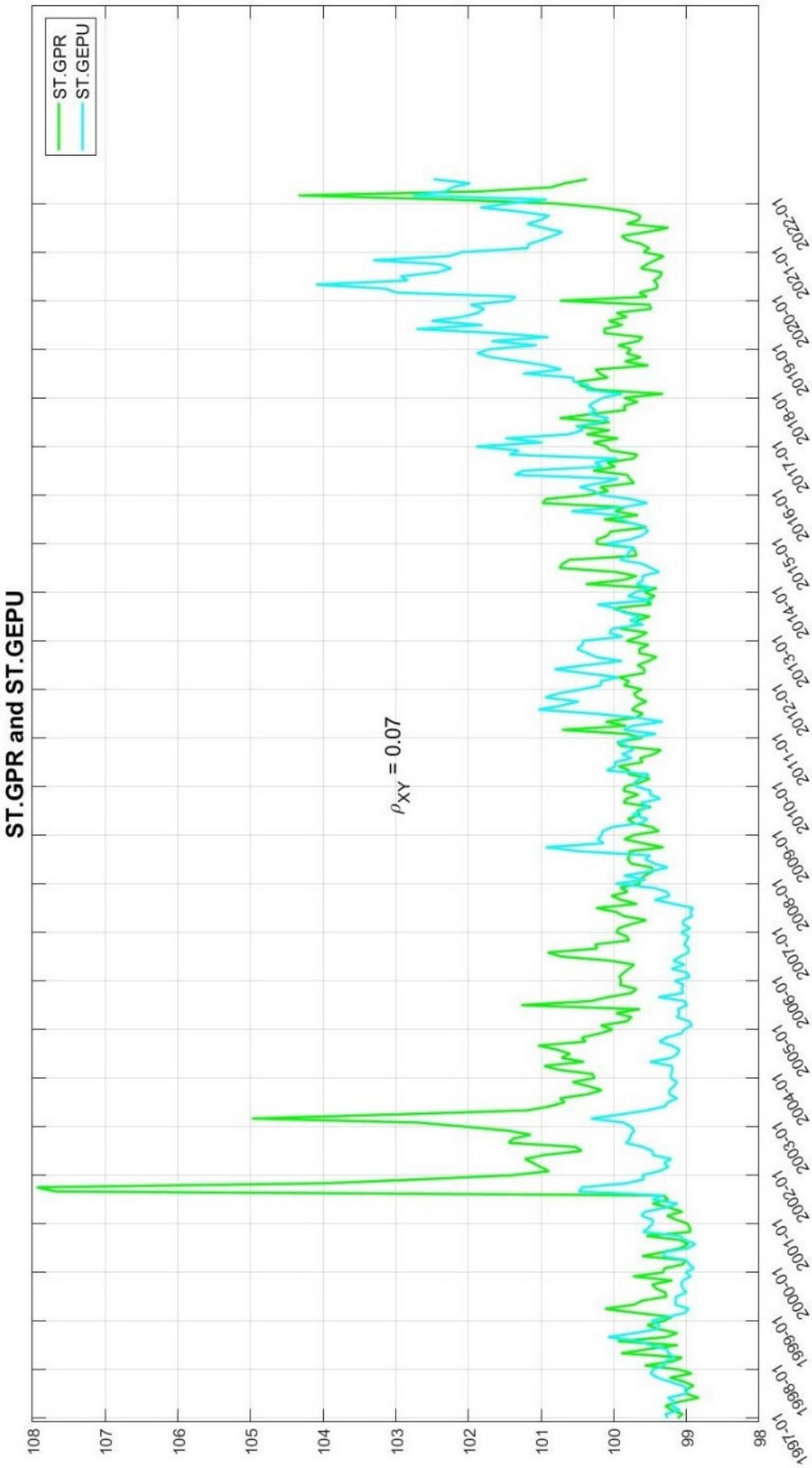
ST.GPR and ST.GEPU
ST.GPR
ST.GEPU
$\rho_{XY}$ = 0.07
108
107
106
105
104
103
102
101
100
99
98
1997-01
1998-01
1999-01
2000-01
2001-01
2002-01
2003-01
2004-01
2005-01
2006-01
2007-01
2008-01
2009-01
2010-01
2011-01
2012-01
2013-01
2014-01
2015-01
2016-01
2017-01
2018-01
2019-01
2020-01
2021-01
2022-01

*Figure 10*

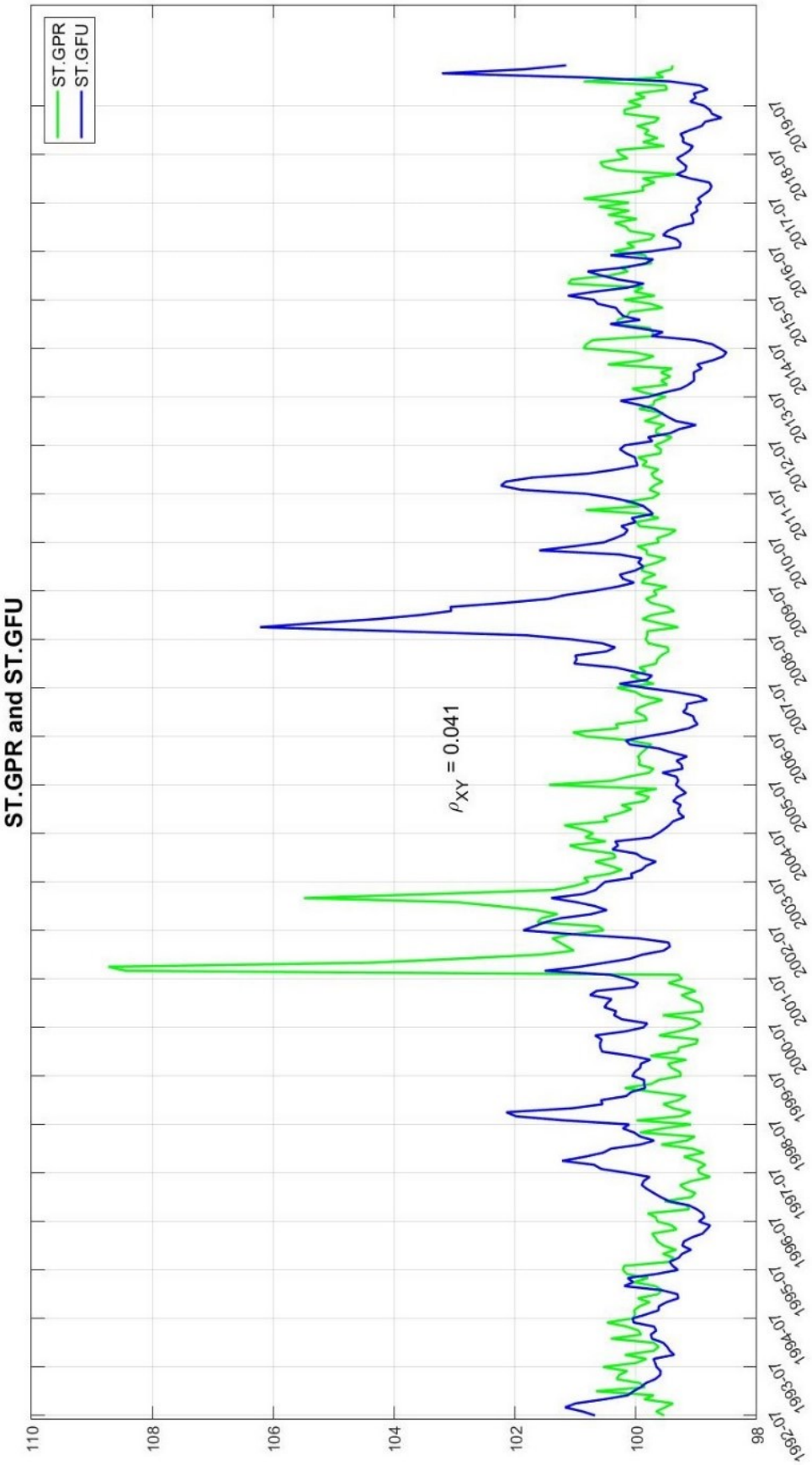
ST.GPR
ST.GFU
ST.GPR and ST.GFU
$\rho_{XY}$ = 0.041
110
108
106
104
102
100
98
1992-07
1993-07
1994-07
1995-07
1996-07
1997-07
1998-07
1999-07
2000-07
2001-07
2002-07
2003-07
2004-07
2005-07
2006-07
2007-07
2008-07
2009-07
2010-07
2011-07
2012-07
2013-07
2014-07
2015-07
2016-07
2017-07
2018-07
2019-07

*Figure 11*

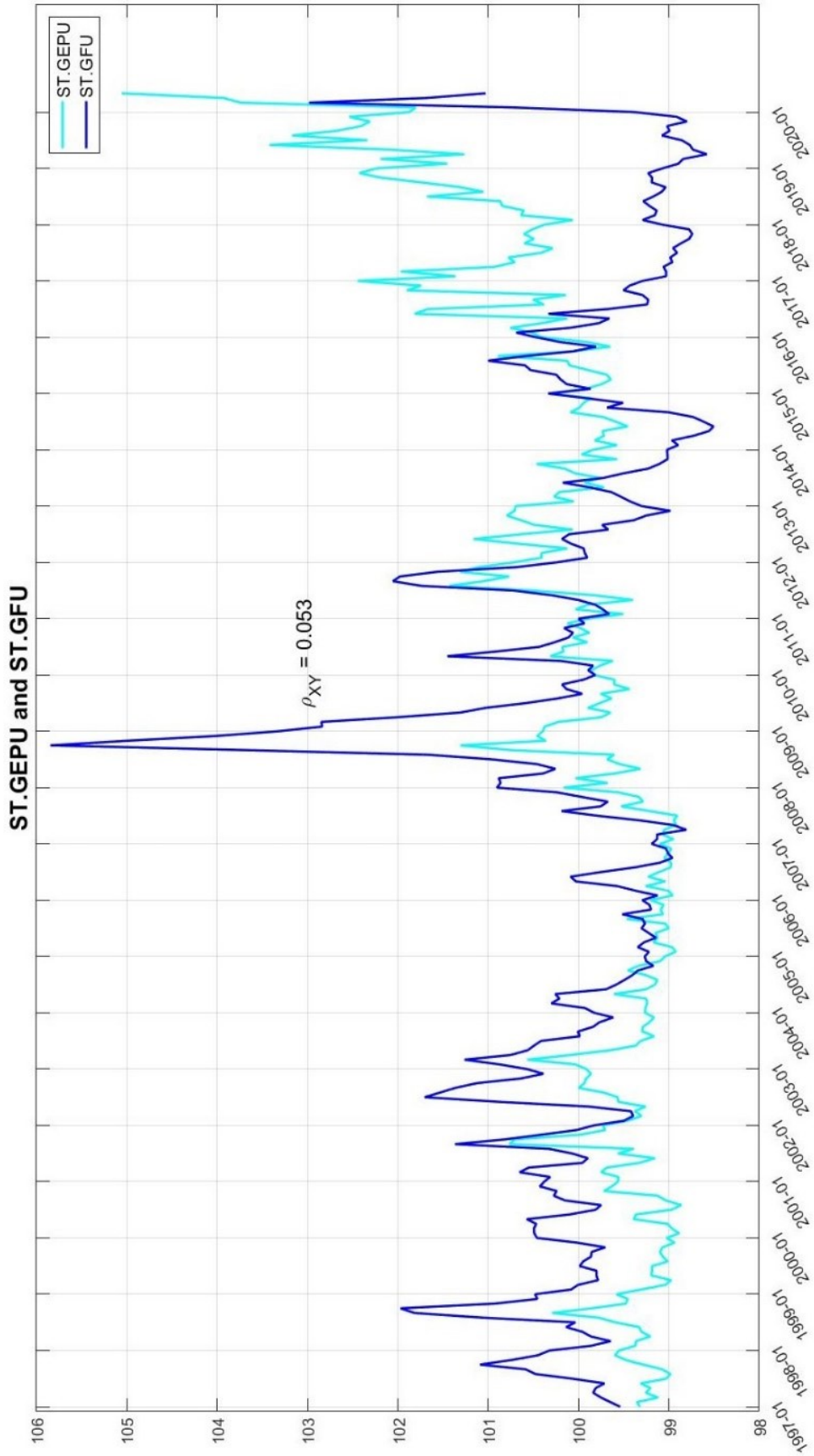
ST.GEPU
ST.GFU
ST.GEPU and ST.GFU
$\rho_{XY}$ = 0.053
106
105
104
103
102
101
100
99
98
1997-01
1998-01
1999-01
2000-01
2001-01
2002-01
2003-01
2004-01
2005-01
2006-01
2007-01
2008-01
2009-01
2010-01
2011-01
2012-01
2013-01
2014-01
2015-01
2016-01
2017-01
2018-01
2019-01
2020-01

*Figure 12*

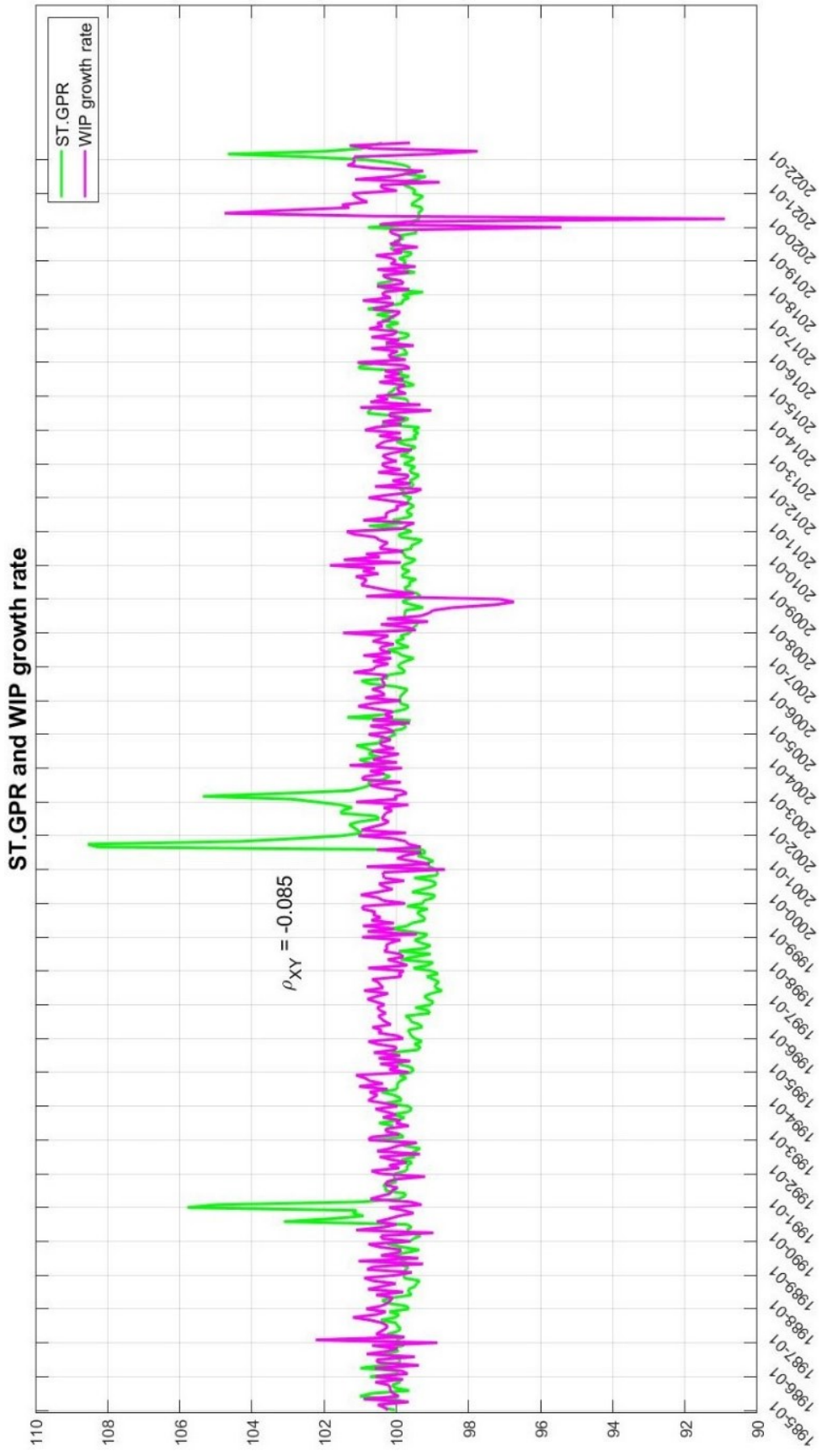
ST.GPR
WIP growth rate
ST.GPR and WIP growth rate
$\rho_{XY}$ = -0.085
110
108
106
104
102
100
98
96
94
92
90
1985-01
1986-01
1987-01
1988-01
1989-01
1990-01
1991-01
1992-01
1993-01
1994-01
1995-01
1996-01
1997-01
1998-01
1999-01
2000-01
2001-01
2002-01
2003-01
2004-01
2005-01
2006-01
2007-01
2008-01
2009-01
2010-01
2011-01
2012-01
2013-01
2014-01
2015-01
2016-01
2017-01
2018-01
2019-01
2020-01
2021-01
2022-01

*Figure 13*

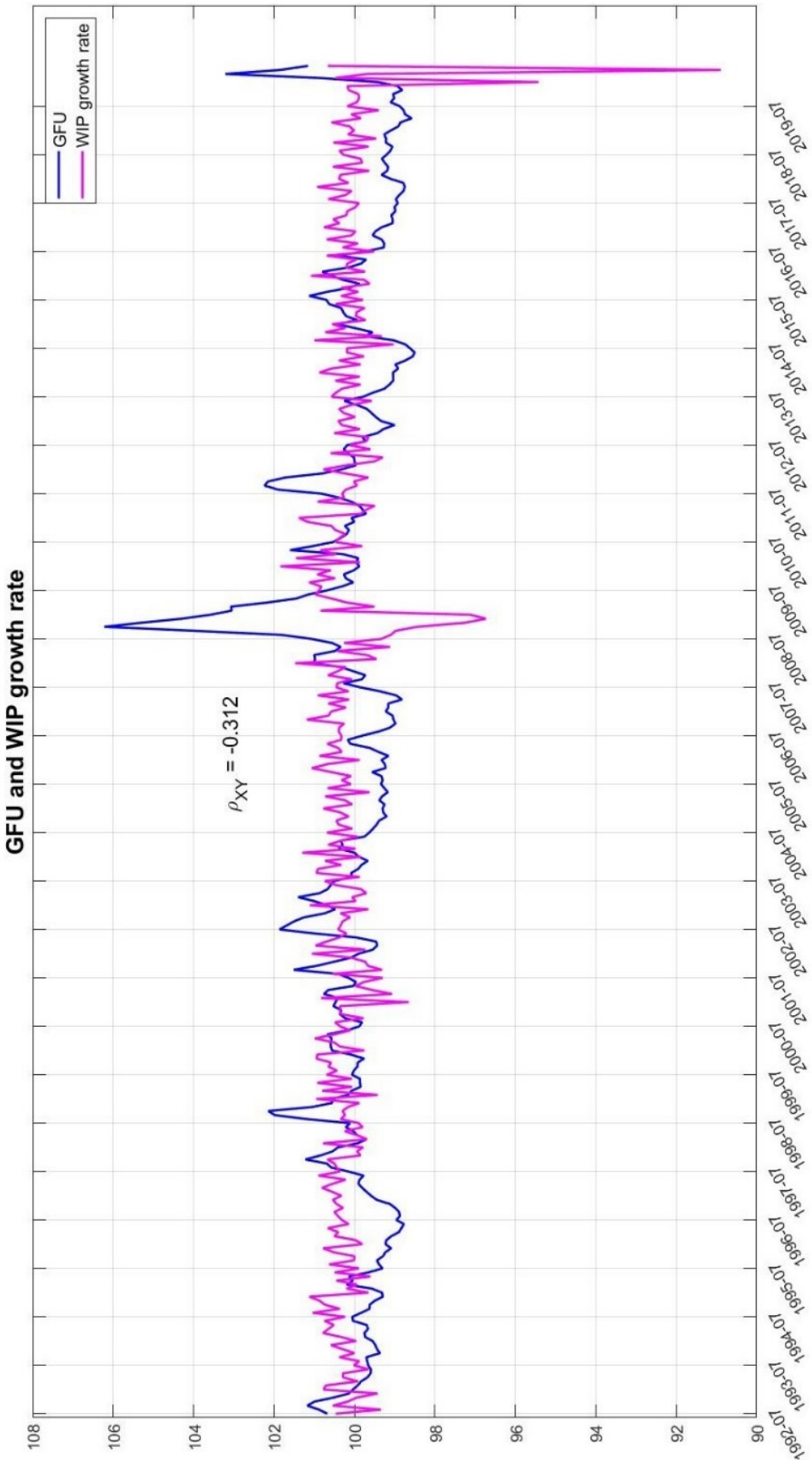
GFU and WIP growth rate
GFU
WIP growth rate
$\rho_{XY}$ = -0.312
108
106
104
102
100
98
96
94
92
90
1992-Q1
1993-Q1
1994-Q1
1995-Q1
1996-Q1
1997-Q1
1998-Q1
1999-Q1
2000-Q1
2001-Q1
2002-Q1
2003-Q1
2004-Q1
2005-Q1
2006-Q1
2007-Q1
2008-Q1
2009-Q1
2010-Q1
2011-Q1
2012-Q1
2013-Q1
2014-Q1
2015-Q1
2016-Q1
2017-Q1
2018-Q1
2019-Q1

*Figure 14*

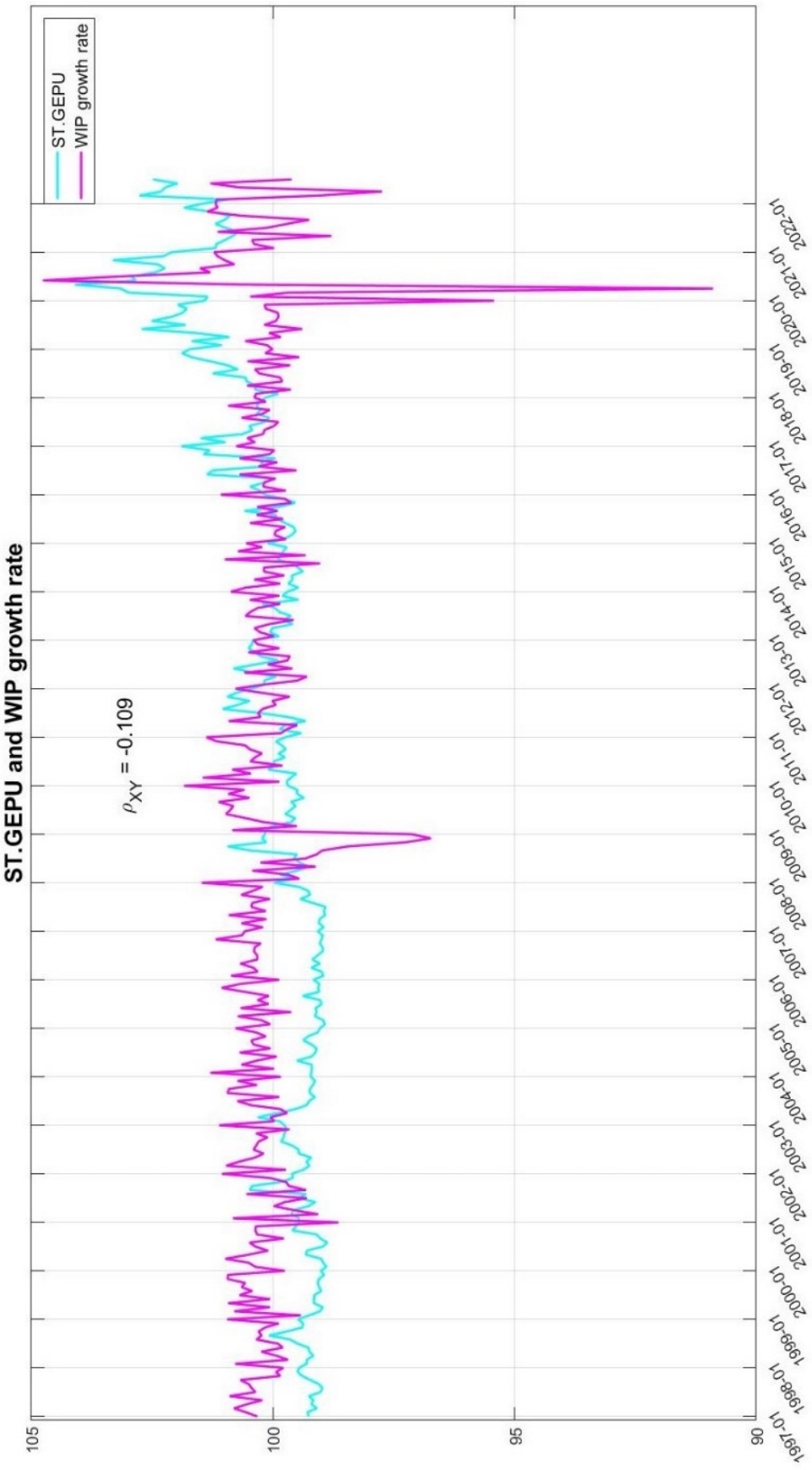
ST.GEPU and WIP growth rate
ST.GEPU
WIP growth rate
$\rho_{XY}$ = -0.109
105
100
95
90
1997-01
1998-01
1999-01
2000-01
2001-01
2002-01
2003-01
2004-01
2005-01
2006-01
2007-01
2008-01
2009-01
2010-01
2011-01
2012-01
2013-01
2014-01
2015-01
2016-01
2017-01
2018-01
2019-01
2020-01
2021-01
2022-01

*Figure 15*

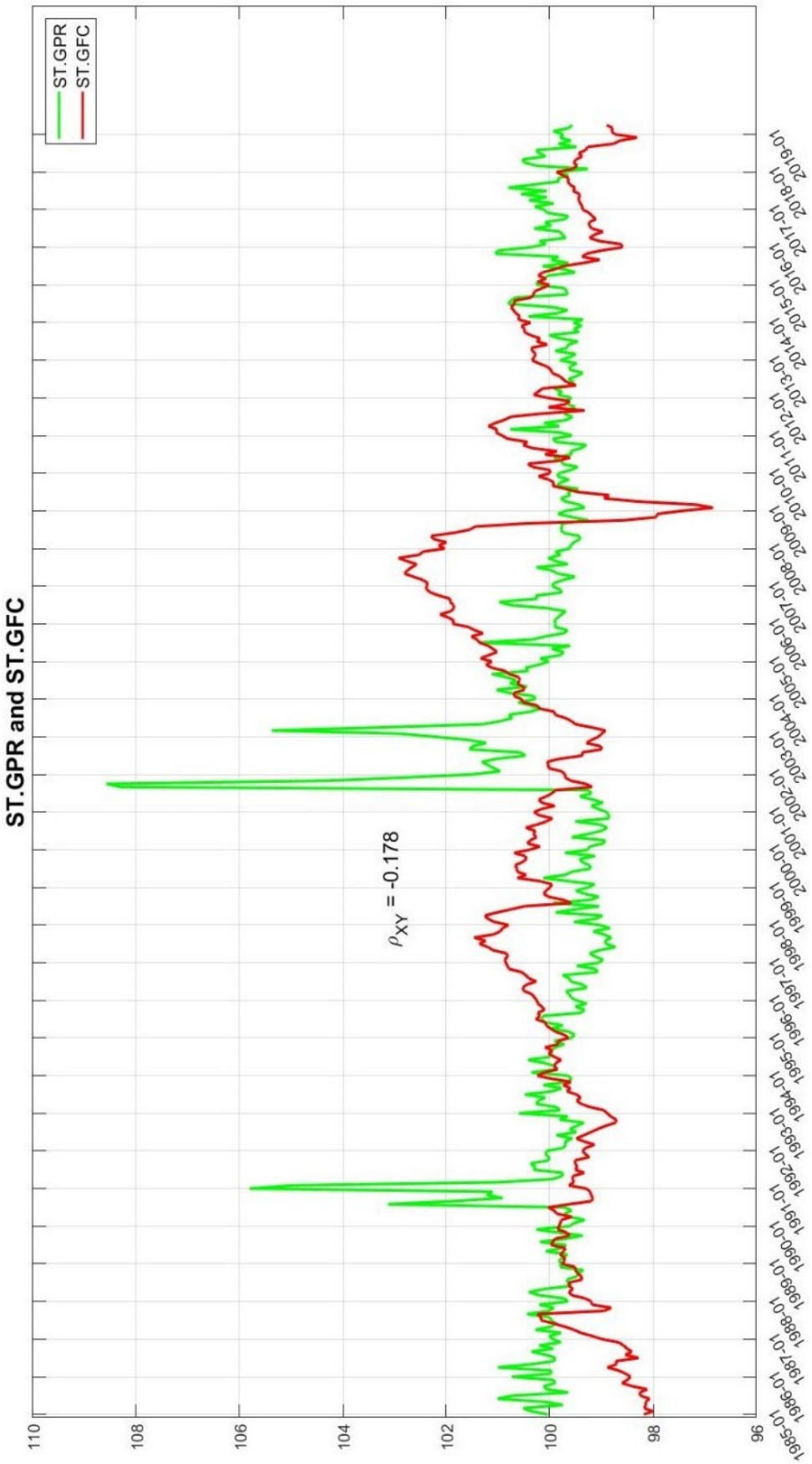
ST.GPR and ST.GFC
ST.GPR
ST.GFC
$\rho_{XY}$ = -0.178
110
108
106
104
102
100
98
96
1985-01
1986-01
1987-01
1988-01
1989-01
1990-01
1991-01
1992-01
1993-01
1994-01
1995-01
1996-01
1997-01
1998-01
1999-01
2000-01
2001-01
2002-01
2003-01
2004-01
2005-01
2006-01
2007-01
2008-01
2009-01
2010-01
2011-01
2012-01
2013-01
2014-01
2015-01
2016-01
2017-01
2018-01
2019-01

*Figure 16*

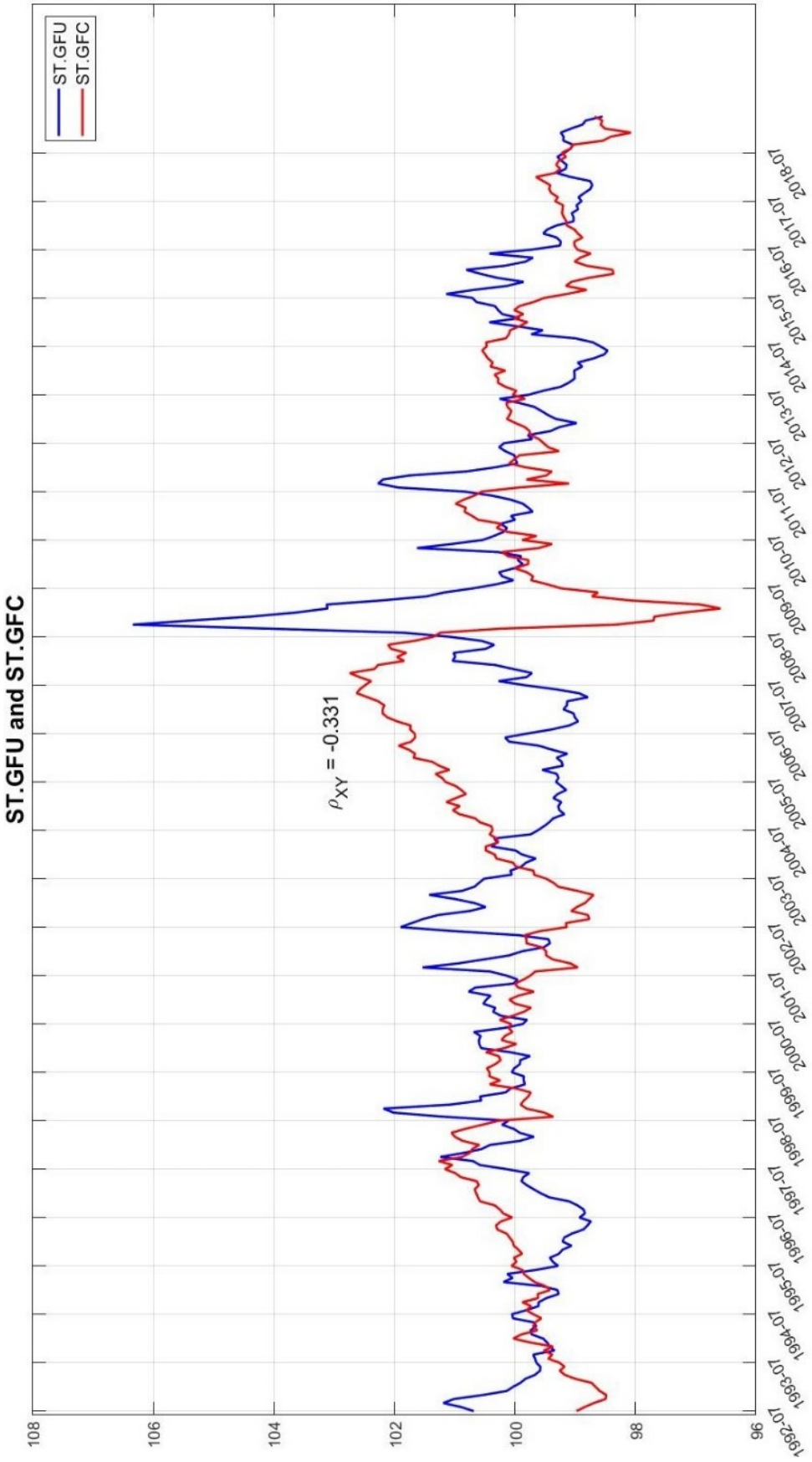
ST.GFU
ST.GFC
ST.GFU and ST.GFC
$\rho_{XY}$ = -0.331
108
106
104
102
100
98
96
1992-07
1993-07
1994-07
1995-07
1996-07
1997-07
1998-07
1999-07
2000-07
2001-07
2002-07
2003-07
2004-07
2005-07
2006-07
2007-07
2008-07
2009-07
2010-07
2011-07
2012-07
2013-07
2014-07
2015-07
2016-07
2017-07
2018-07

*Figure 17*

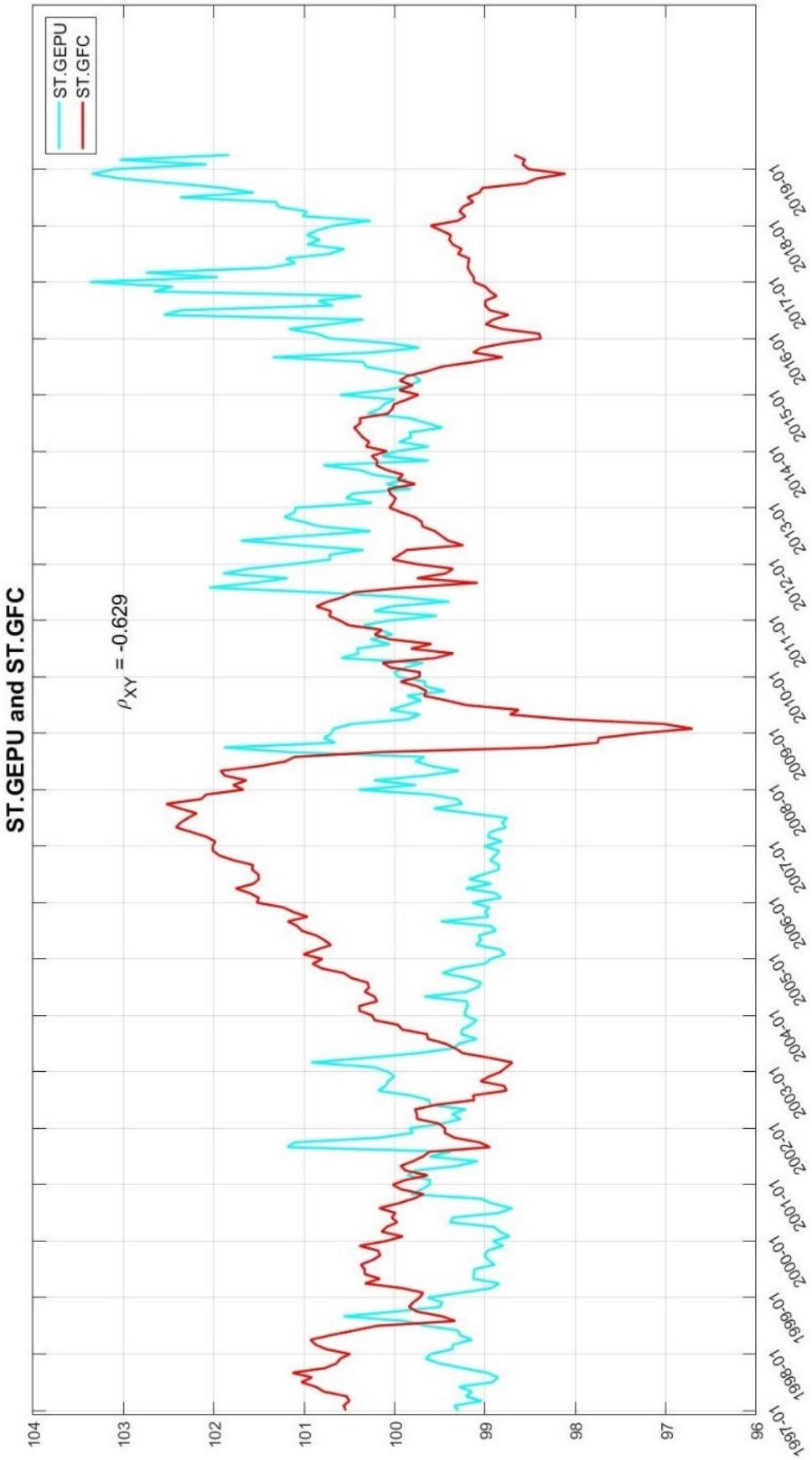
ST.GEPU and ST.GFC
ST.GEPU
ST.GFC
$\rho_{XY}$ = -0.629
104
103
102
101
100
99
98
97
96
1997-01
1998-01
1999-01
2000-01
2001-01
2002-01
2003-01
2004-01
2005-01
2006-01
2007-01
2008-01
2009-01
2010-01
2011-01
2012-01
2013-01
2014-01
2015-01
2016-01
2017-01
2018-01
2019-01

*Figure 18: IRFs of PFA - Min specification (GPR shock)*

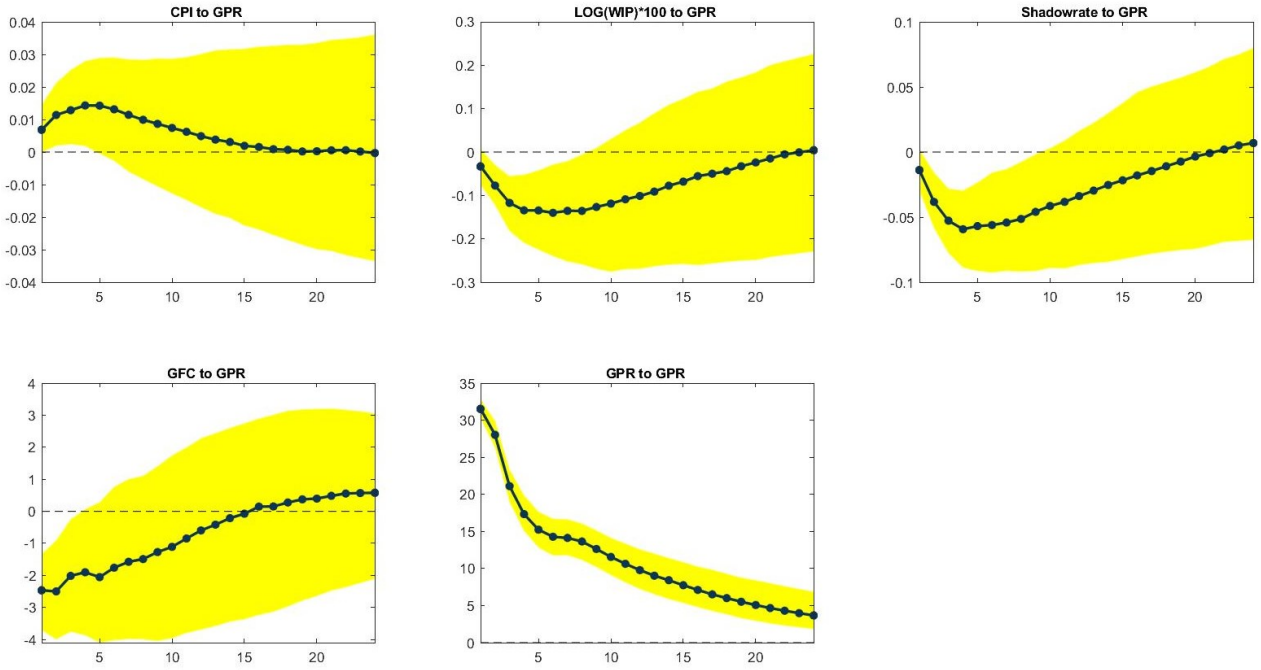


*Figure 19: IRFSs of PFA - Min specification (GFU shock)*

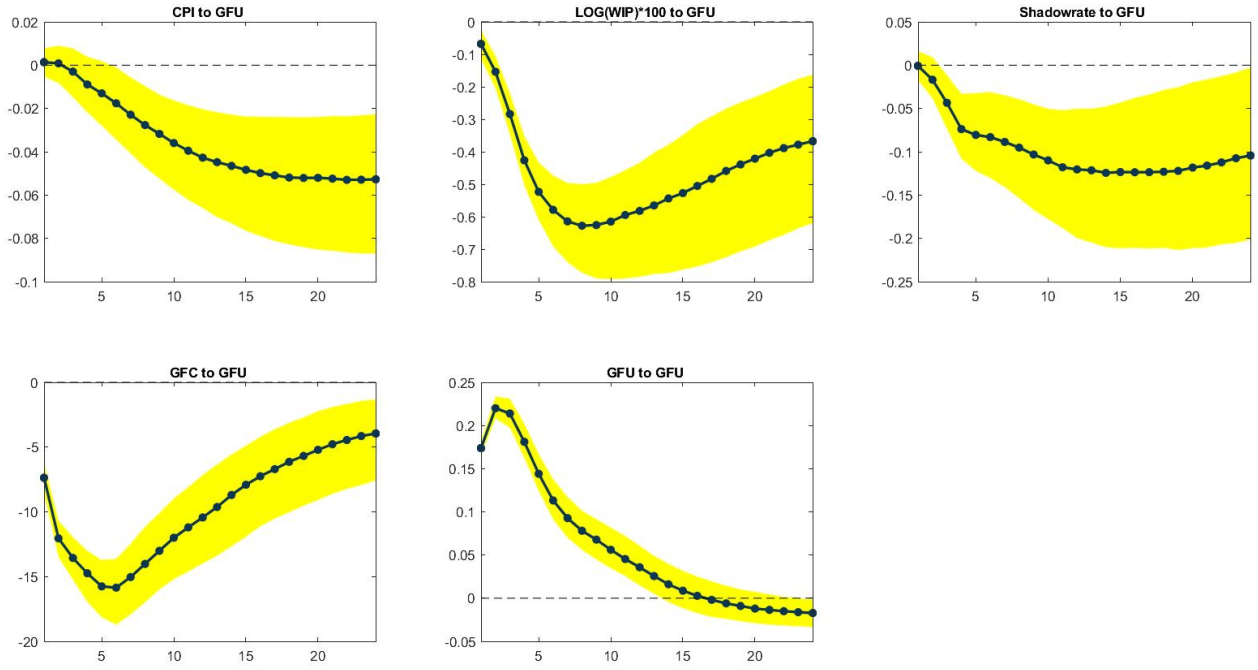

*Figure 20: IRFs of PFA - Min specification (GEPU shock)*

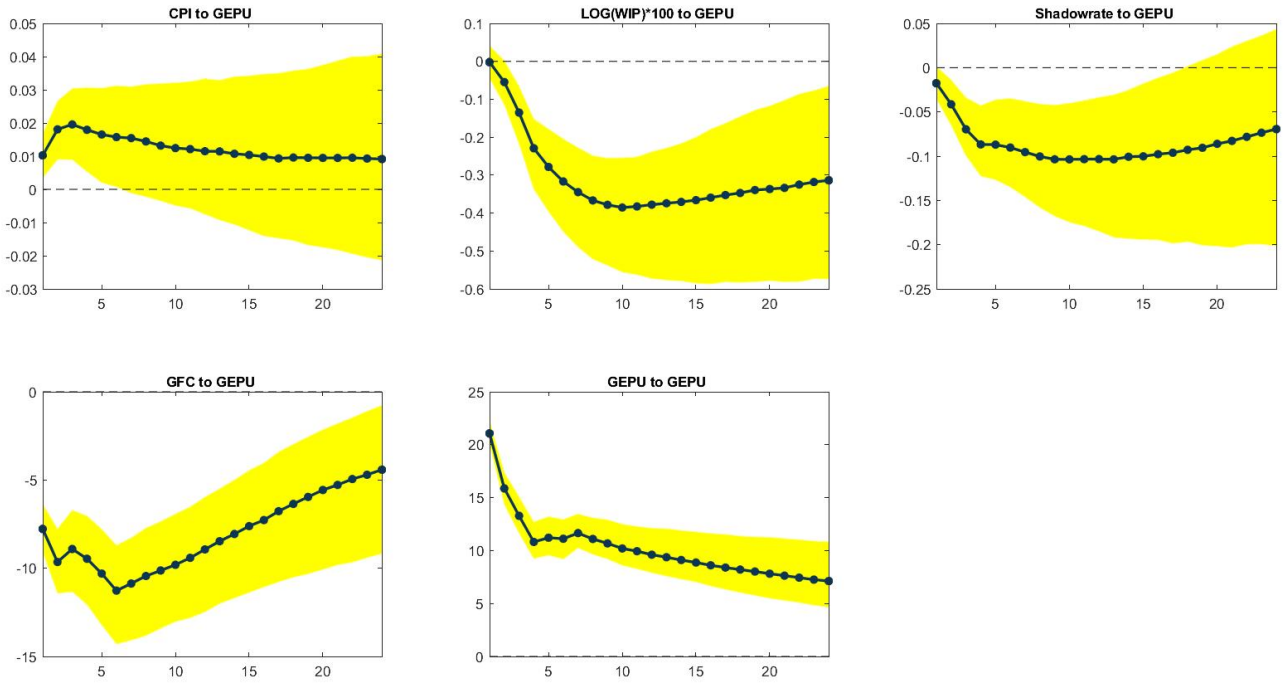


*Figure 21: IRFs of PFA - Conj specification (GEPU shock)*

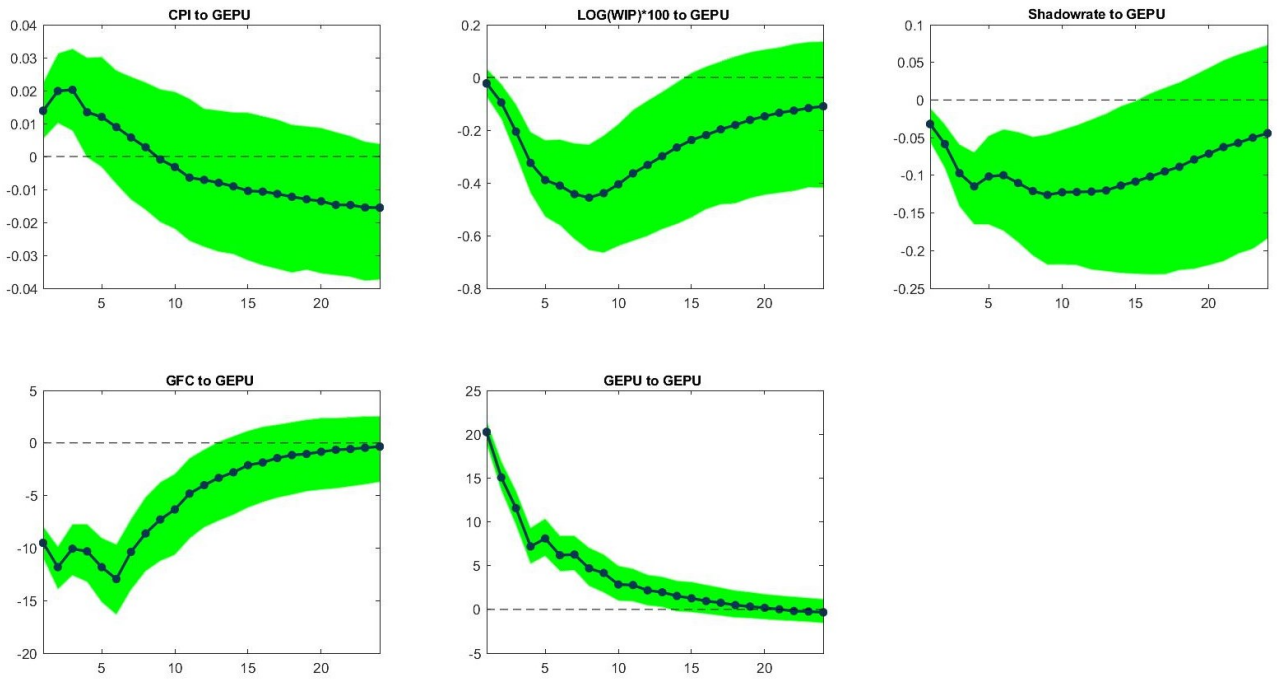

*Figure 22: IRFs of PFA - Conj specification (GFU shock)*

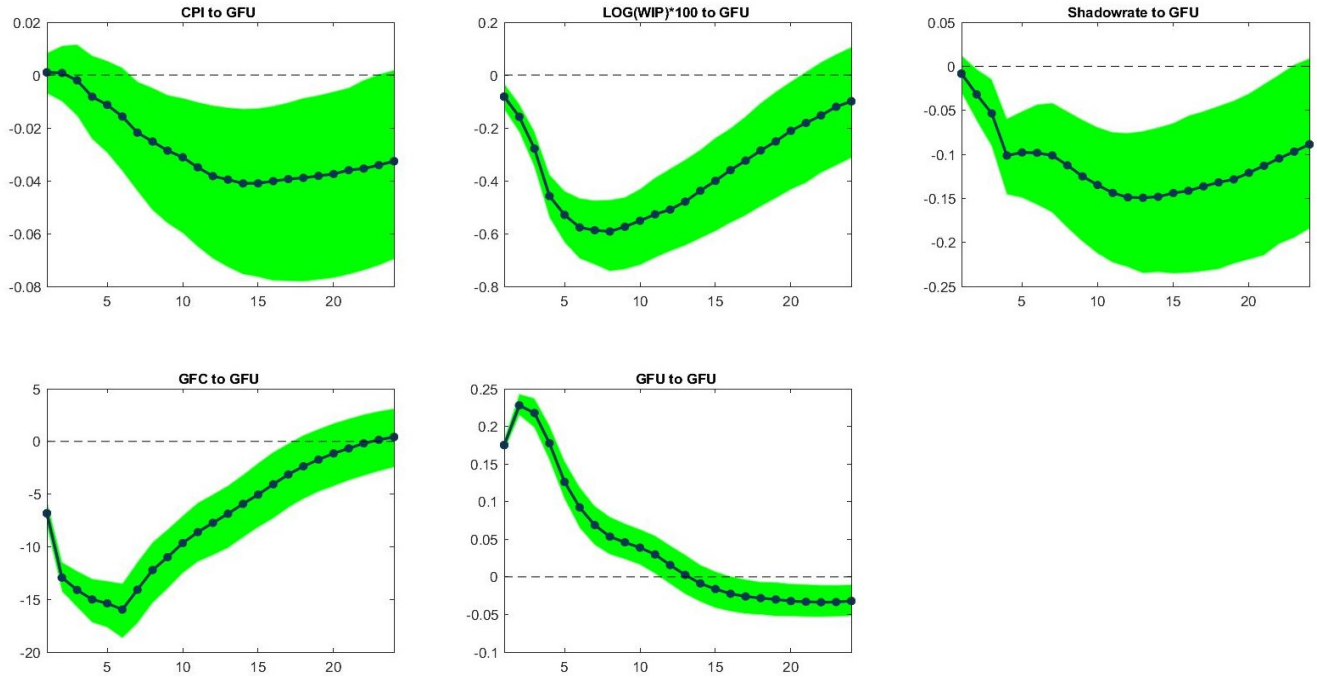


*Figure 23: IRFs of PFA - Conj specification (GPR shock)*

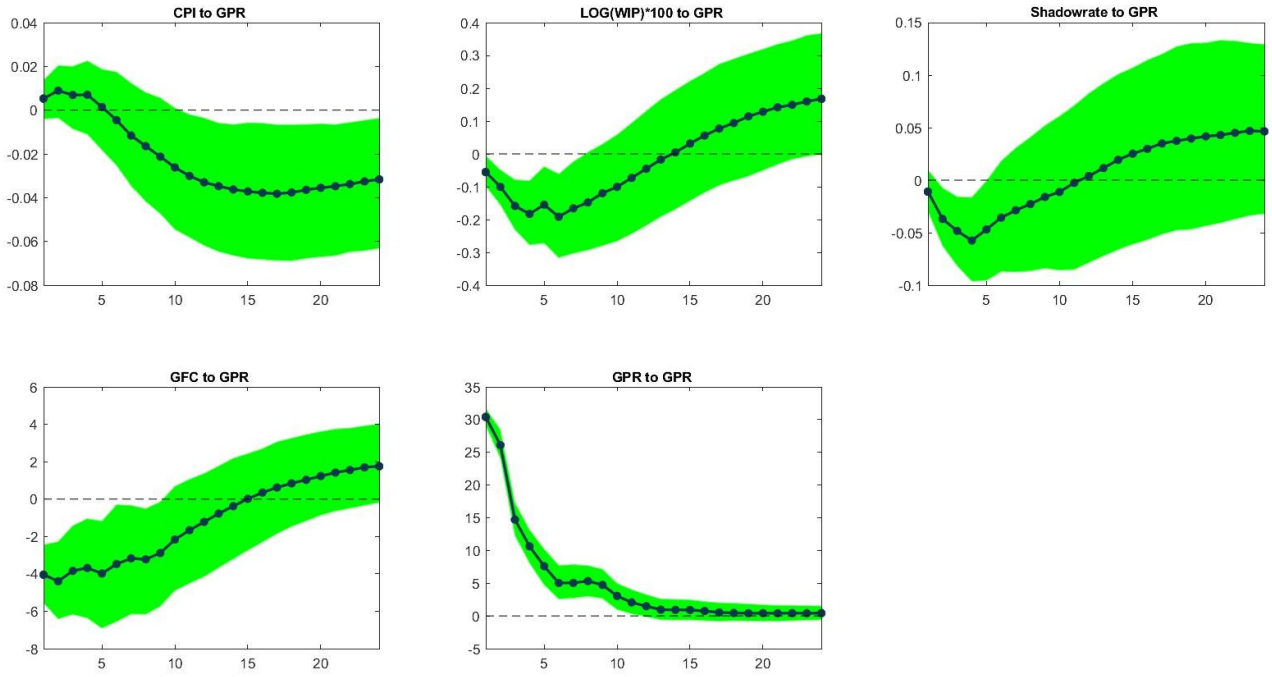

*Figure 24: IRFs of Chol specification (GEPU shock)*

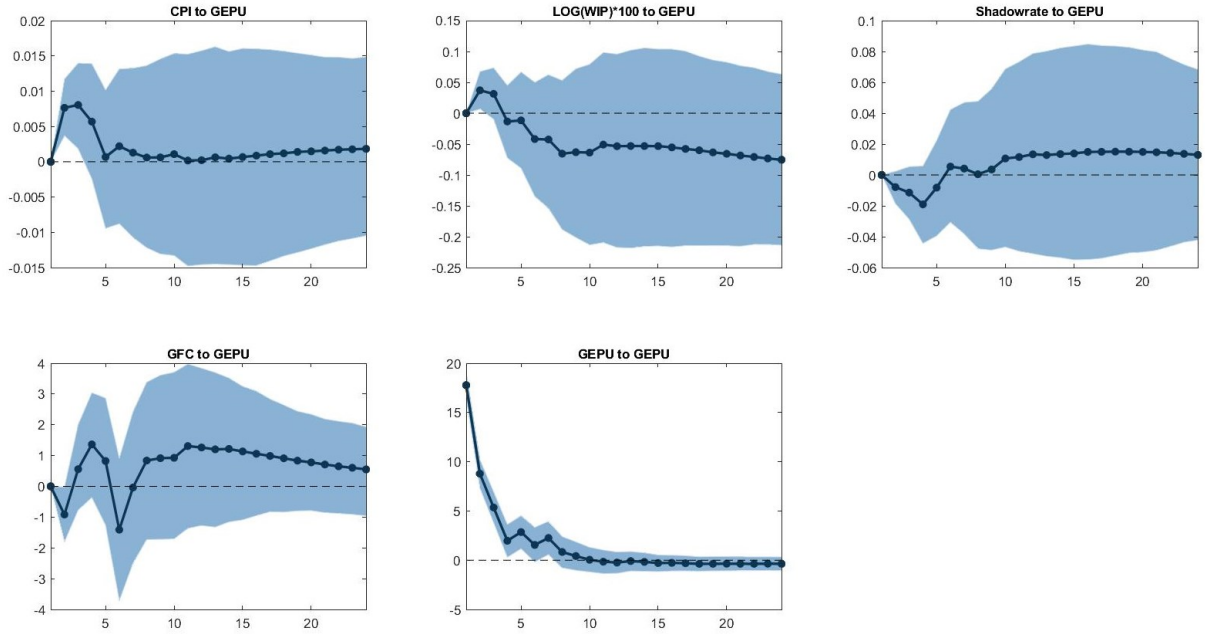


*Figure 25: IRFs of Chol specification (GPR shock)*

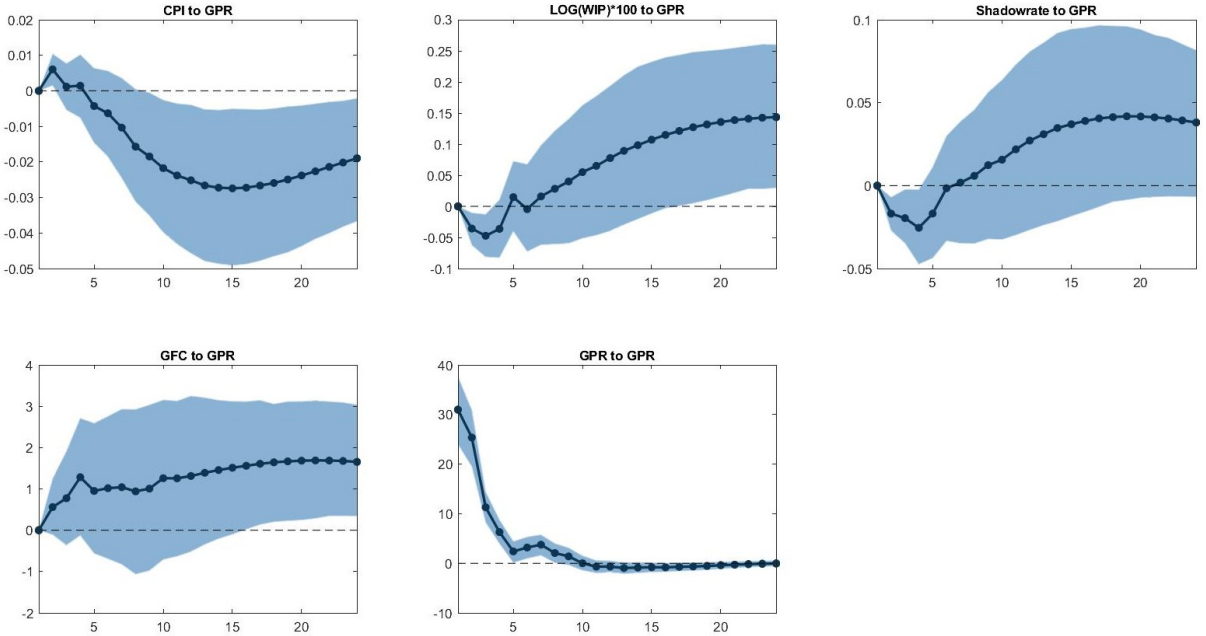

*Figure 26: IRFs of Chol specification (GFU shock)*

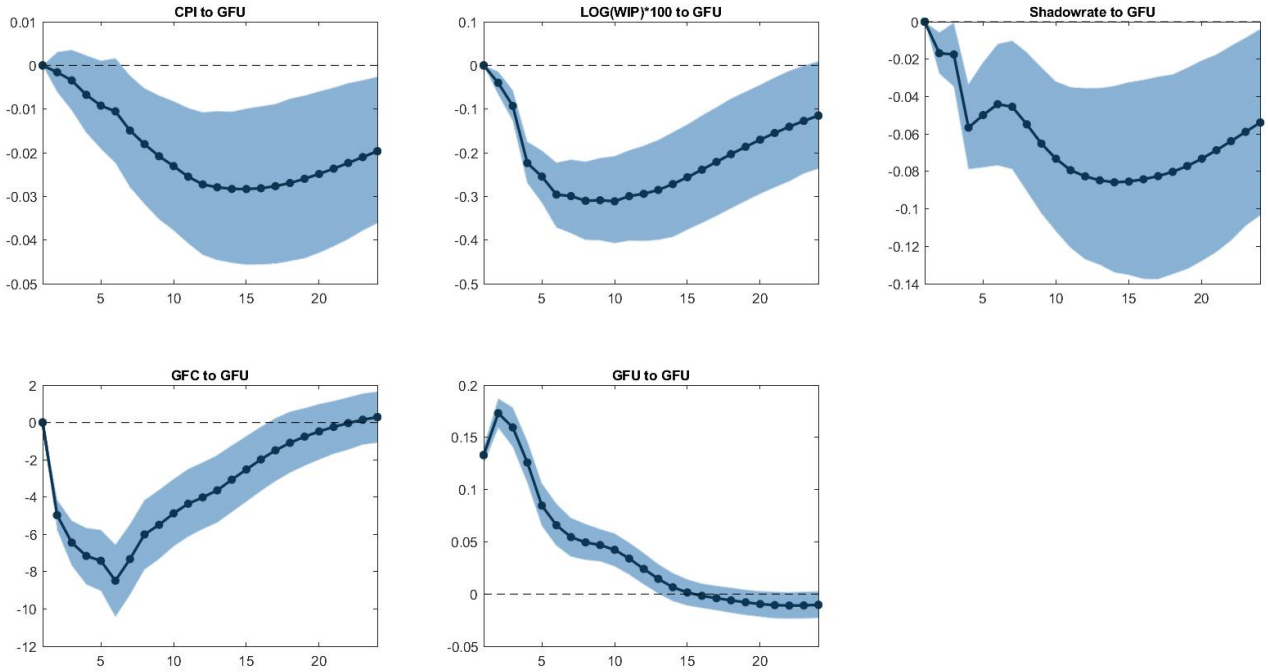

*Figure 27: FEVDs of uncertainty shocks with respect to GFC*

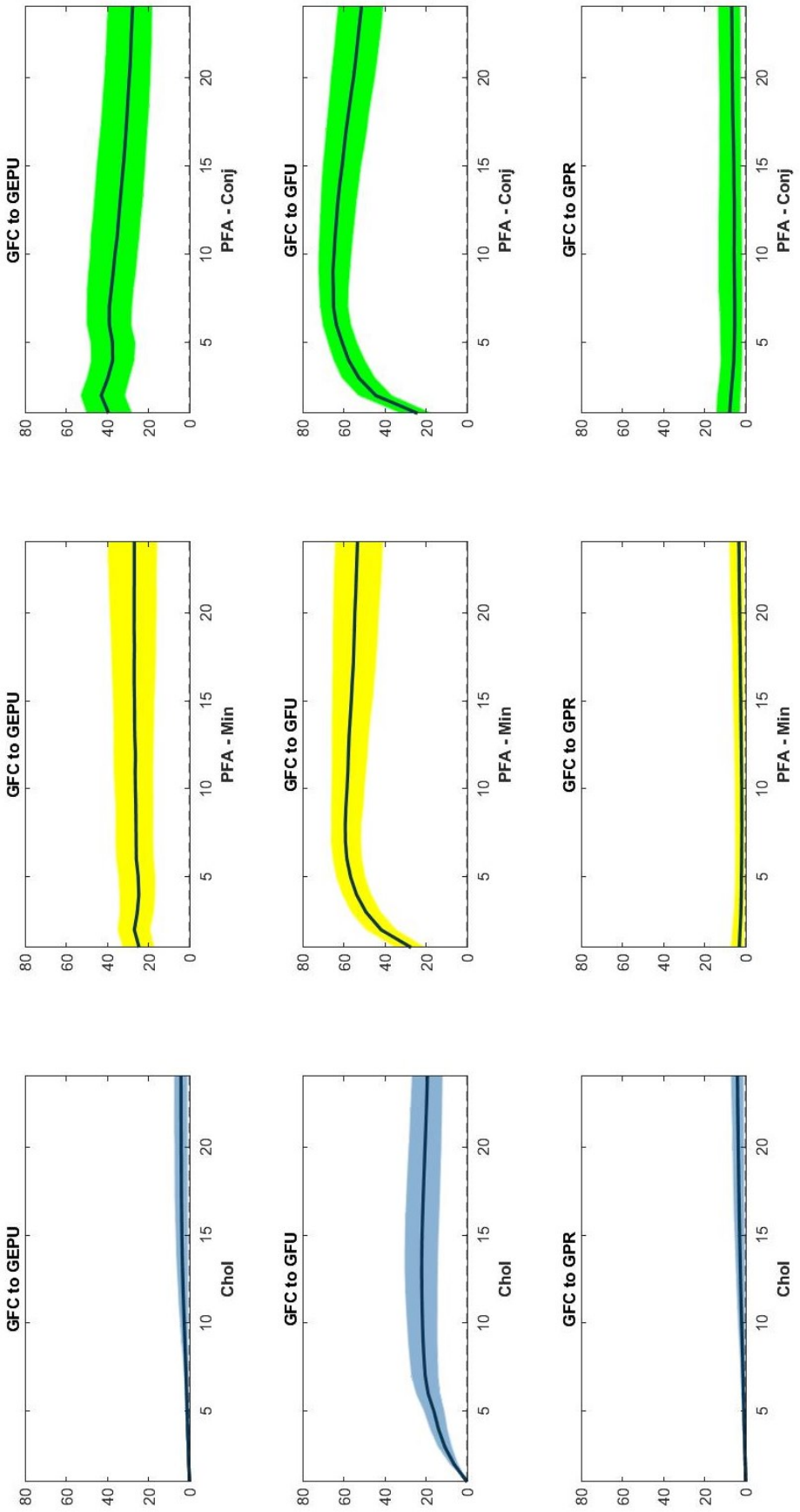

*Figure 28: IRFs of GFC*

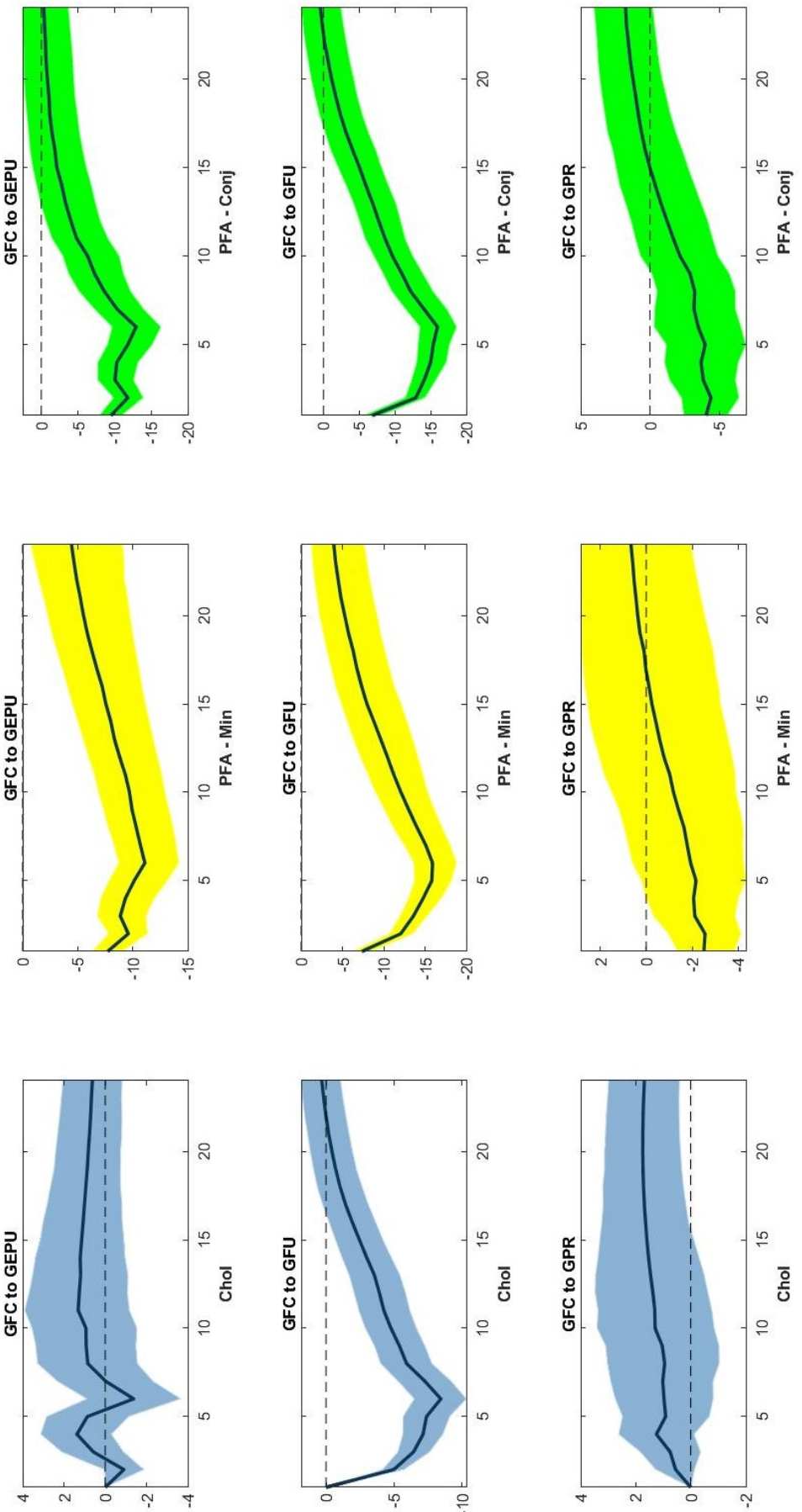

*Figure 29: the SACF of the reduced form residuals of the SVAR model with GEPU (Chol specification)*

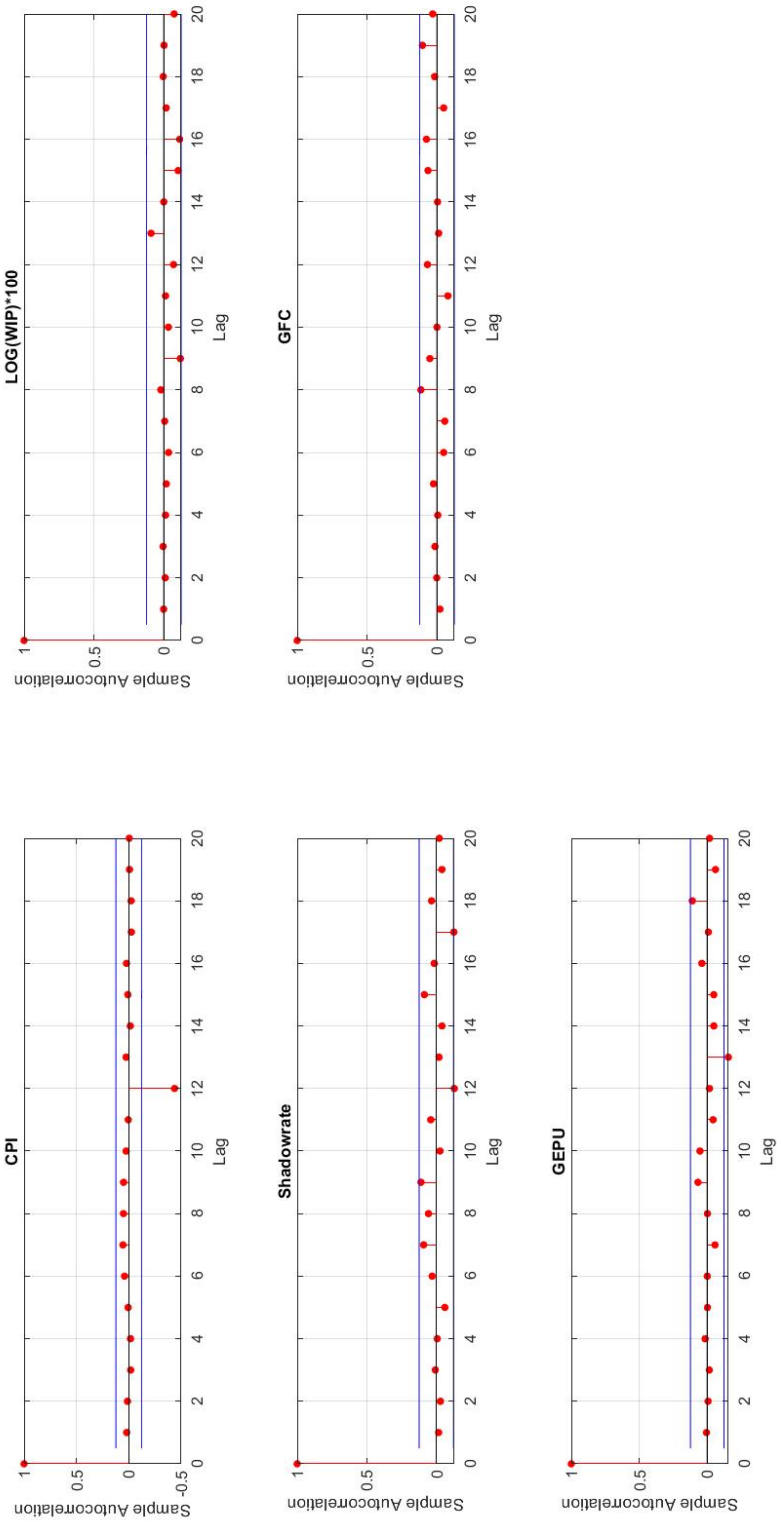

*Figure 30: the SACF of the reduced form residuals of the SVAR model with GFU (Chol specification)*

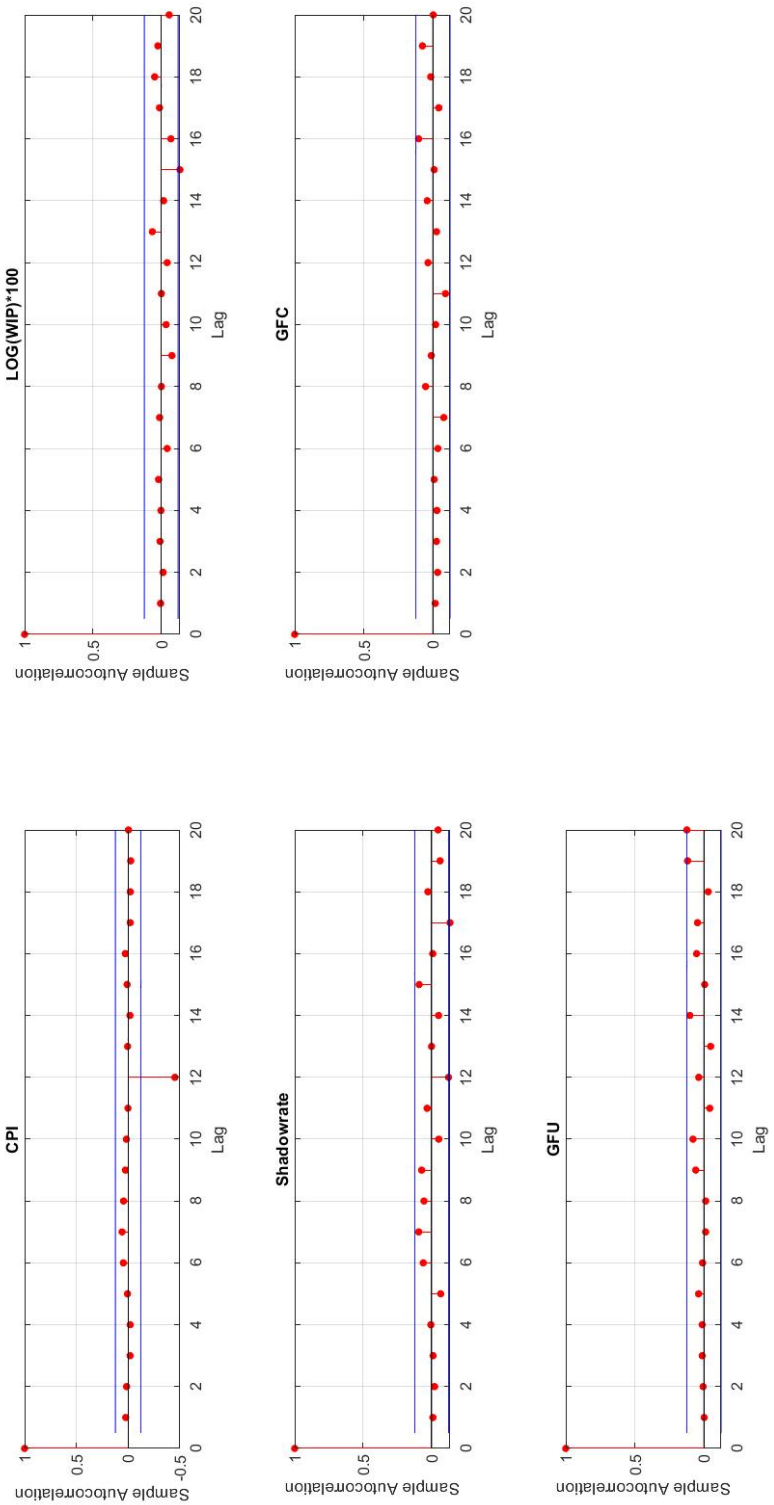

*Figure 31: the SACF of the reduced form residuals of the SVAR model with GPR (Chol specification)*

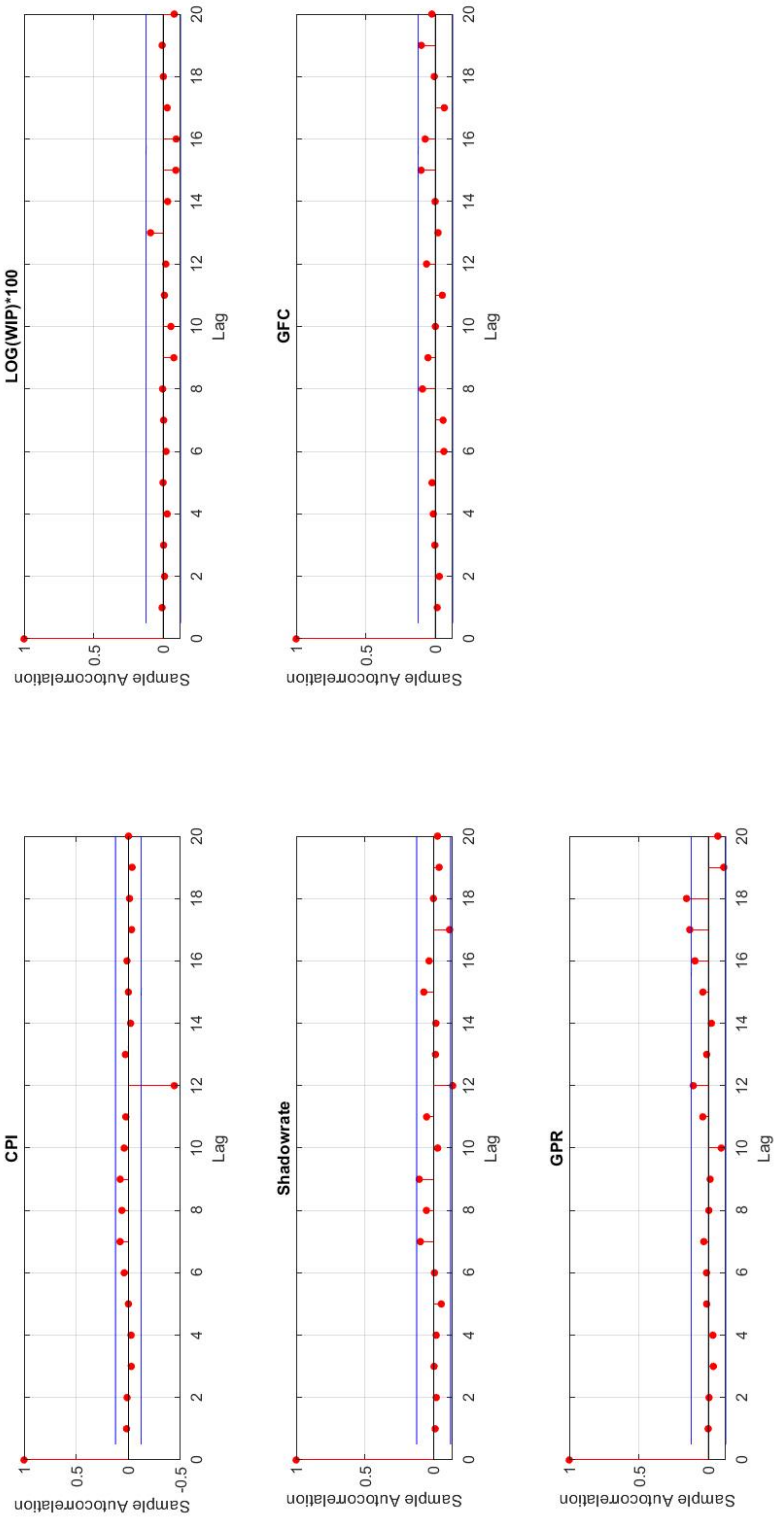

*Figure 32: the time series of the reduced form residuals of the SVAR model with GPR (Chol specification)*

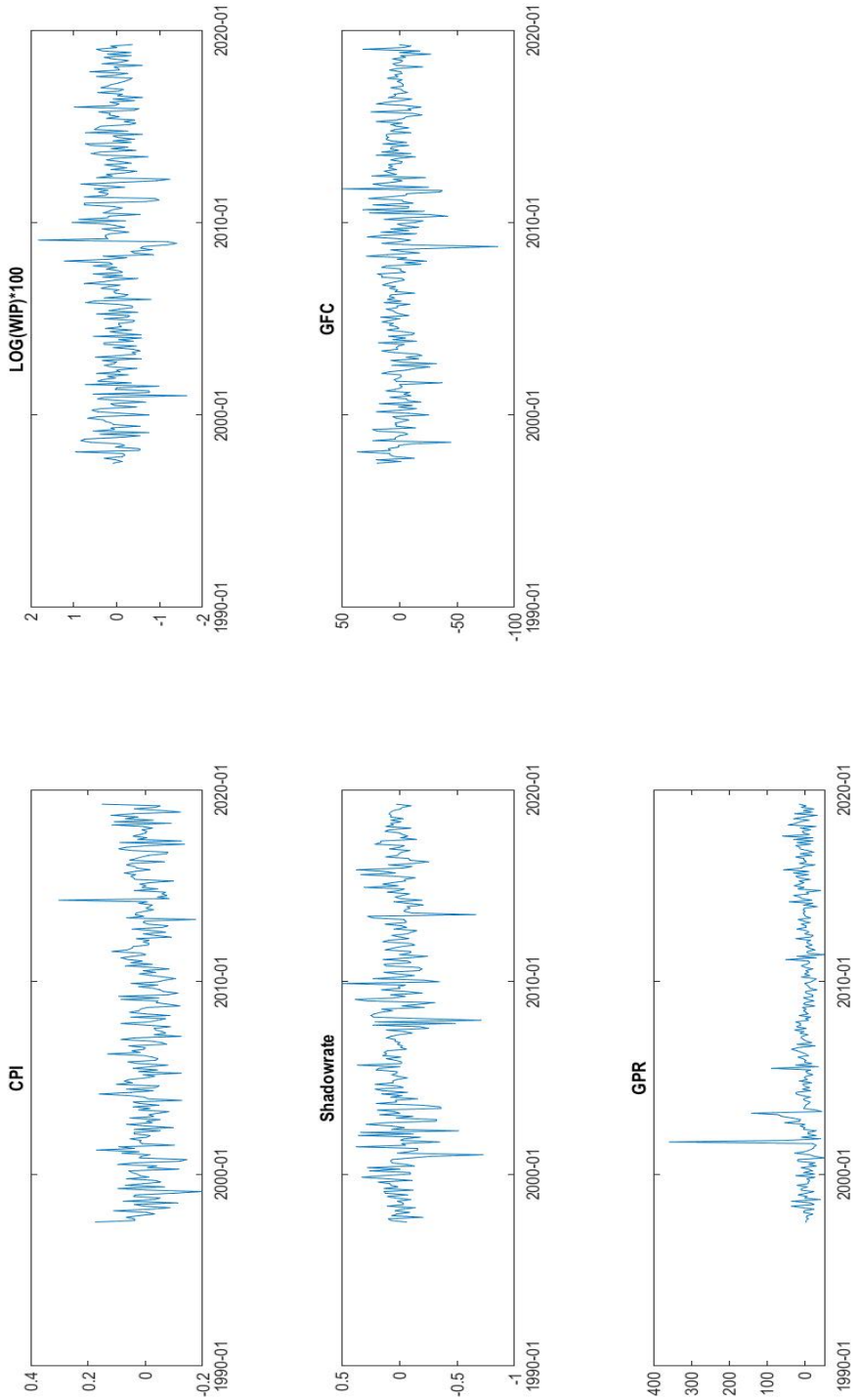

*Figure 33: the time series of the reduced form residuals of the SVAR model with GPR (Chol specification)*

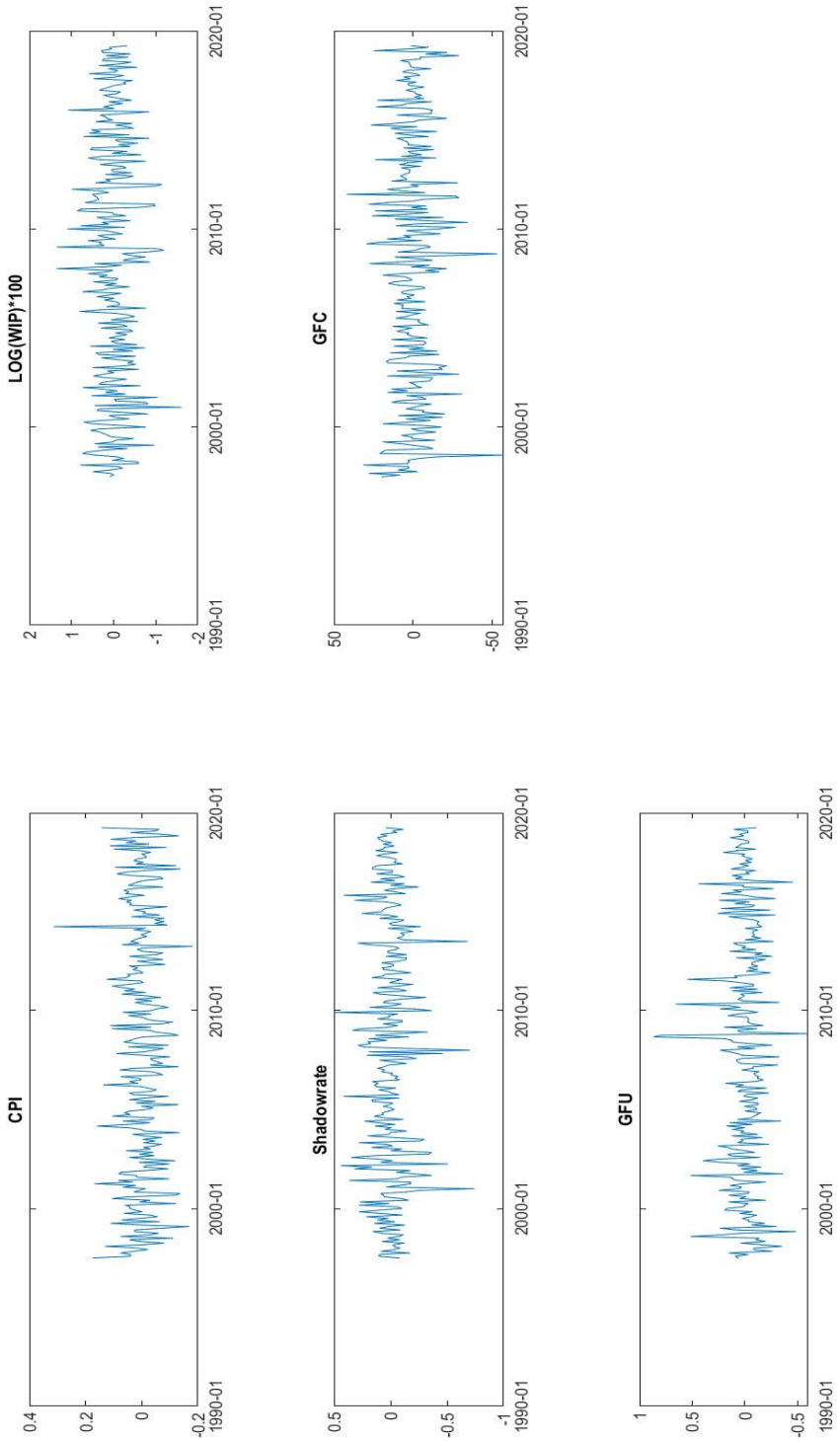

*Figure 34: the time series of the reduced form residuals of the SVAR model with GPR (Chol specification)*

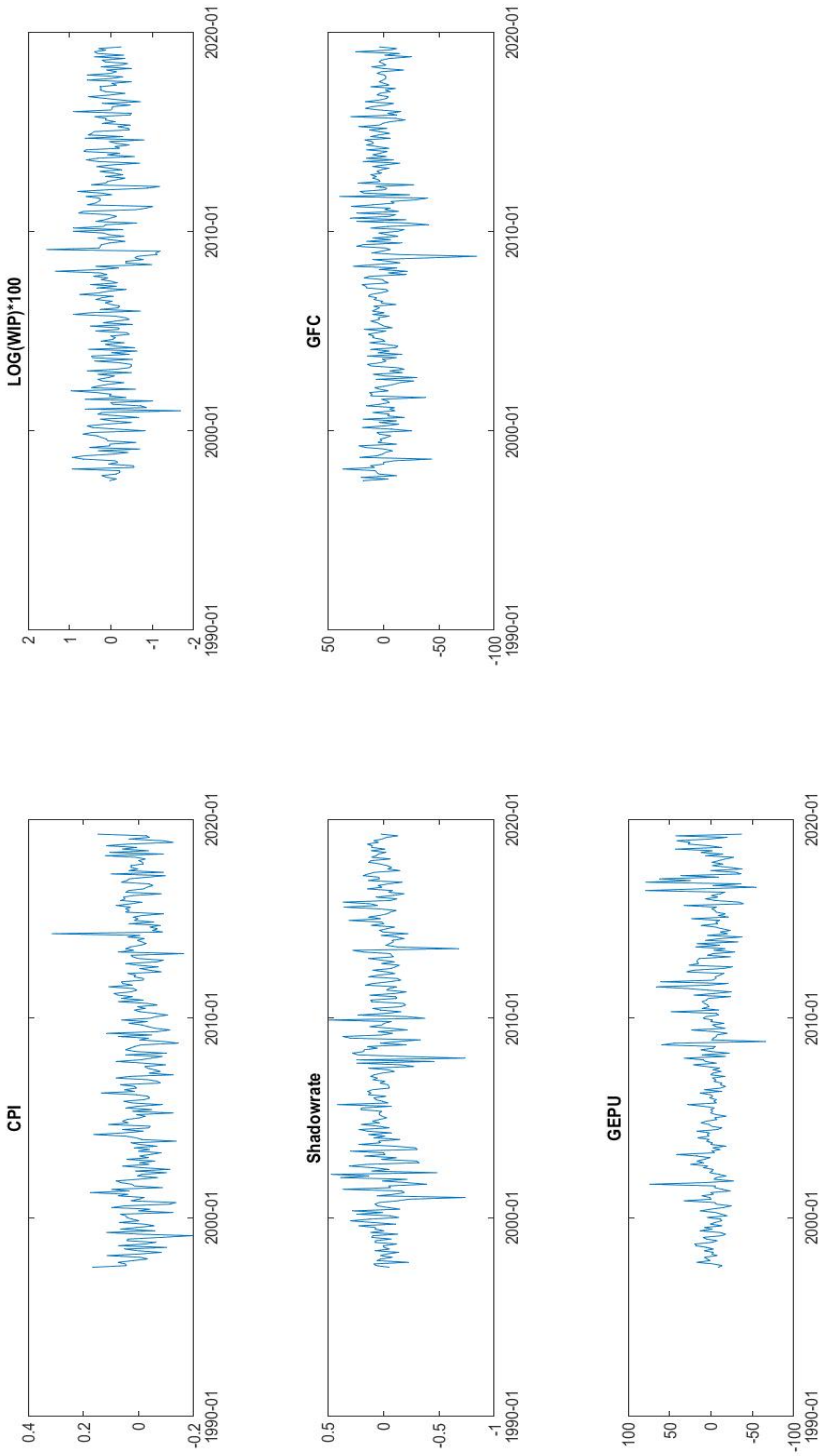

## TABLES

*Table 1: FEVDs of GPR shock (PFA- Min specification)*

| Horizon/variable | Upon impact | 6 months | 12 months | 18 months | 23 months |
|---|---|---|---|---|---|
| **CPI** | 0,72% | 1,42% | 1,49% | 1,63% | 1,83% |
| **WIP growth rate** | 0,63% | 2,50% | 2,10% | 2,40% | 2,74% |
| **Shadow rate** | 0,53% | 3,23% | 2,66% | 2,59% | 2,61% |
| **GFC** | 3,04% | 1,76% | 2,20% | 2,90% | 3,31% |
| **GPR** | 98,42% | 98,07% | 97,16% | 96,27% | 95,39% |

*Table 2: FEVDs of GPR shock (PFA- Conj specification)*

| Horizon/variable | Upon impact | 6 months | 12 months | 18 months | 23 months |
|---|---|---|---|---|---|
| **CPI** | 0,75% | 1,41% | 3,01% | 4,43% | 5,12% |
| **WIP growth rate** | 1,38% | 4,16% | 3,00% | 3,79% | 4,25% |
| **Shadow rate** | 0,61% | 2,12% | 2,12% | 2,62% | 2,95% |
| **GFC** | 7,76% | 5,33% | 5,52% | 6,39% | 6,78% |
| **GPR** | 95,65% | 90,29% | 85,25% | 80,61% | 77,89% |

*Table 3: FEVDs of GPR shock (Chol specification)*

| Horizon/variable | Upon impact | 6 months | 12 months | 18 months | 23 months |
|---|---|---|---|---|---|
| **CPI** | 0,00% | 0,26% | 2,07% | 3,88% | 4,70% |
| **WIP growth rate** | 0,00% | 0,20% | 0,29% | 0,98% | 1,75% |
| **Shadow rate** | 0,00% | 0,29% | 0,31% | 0,80% | 1,22% |
| **GFC** | 0,00% | 0,29% | 0,51% | 1,15% | 1,86% |
| **GPR** | 96,06% | 87,42% | 83,07% | 80,90% | 79,84% |

*Table 4: FEVDs of GEPU shock (PFA- Min specification)*

| Horizon/variable | Upon impact | 6 months | 12 months | 18 months | 23 months |
|---|---|---|---|---|---|
| **CPI** | 2,22% | 3,25% | 2,75% | 2,84% | 3,17% |
| **WIP growth rate** | 0,33% | 8,96% | 12,11% | 12,39% | 12,54% |
| **Shadow rate** | 1,04% | 5,64% | 5,73% | 5,63% | 5,21% |
| **GFC** | 24,80% | 26,65% | 26,82% | 27,32% | 27,08% |
| **GEPU** | 93,83% | 96,08% | 95,29% | 93,92% | 92,49% |

*Table 5: FEVDs of GEPU shock (PFA- Conj specification)*

| Horizon/variable | Upon impact | 6 months | 12 months | 18 months | 23 months |
|---|---|---|---|---|---|
| **CPI** | 4,12% | 3,35% | 4,10% | 5,11% | 6,02% |
| **WIP growth rate** | 0,61% | 14,65% | 14,35% | 12,17% | 11,52% |
| **Shadow rate** | 2,76% | 7,50% | 7,30% | 7,09% | 7,33% |
| **GFC** | 39,38% | 39,01% | 33,74% | 29,82% | 27,67% |
| **GEPU** | 84,07% | 84,36% | 77,69% | 72,65% | 69,40% |

*Table 6: FEVDs of GEPU shock (Chol specification)*

| Horizon/variable | Upon impact | 6 months | 12 months | 18 months | 23 months |
|---|---|---|---|---|---|
| **CPI** | 0,00% | 0,39% | 0,21% | 0,16% | 0,13% |
| **WIP growth rate** | 0,00% | 0,21% | 0,53% | 0,69% | 0,85% |
| **Shadow rate** | 0,00% | 0,13% | 0,08% | 0,11% | 0,15% |
| **GFC** | 0,00% | 0,33% | 0,40% | 0,62% | 0,73% |
| **GEPU** | 82,15% | 57,54% | 52,35% | 49,35% | 47,03% |

*Table 7: FEVDs of GFU shock (PFA- Min specification)*

| Horizon/variable | Upon impact | 6 months | 12 months | 18 months | 23 months |
|---|---|---|---|---|---|
| **CPI** | 0,34% | 1,62% | 5,08% | 8,05% | 9,85% |
| **WIP growth rate** | 2,01% | 30,91% | 33,28% | 30,78% | 28,77% |
| **Shadow rate** | 0,32% | 4,38% | 6,67% | 7,84% | 8,10% |
| **GFC** | 27,27% | 59,06% | 57,24% | 54,87% | 53,35% |
| **GFU** | 97,05% | 97,92% | 95,28% | 91,46% | 88,19% |

*Table 8: FEVDs of GFU shock (PFA- Conj specification)*

| Horizon/variable | Upon impact | 6 months | 12 months | 18 months | 23 months |
|---|---|---|---|---|---|
| **CPI** | 0,38% | 1,55% | 3,70% | 5,35% | 5,85% |
| **WIP growth rate** | 2,89% | 35,02% | 35,34% | 29,81% | 25,35% |
| **Shadow rate** | 0,68% | 6,17% | 9,45% | 11,22% | 11,40% |
| **GFC** | 24,14% | 64,93% | 62,81% | 56,50% | 51,36% |
| **GFU** | 94,43% | 95,04% | 85,34% | 75,01% | 68,65% |

*Table 9: FEVDs of GFU shock (Chol specification)*

| Horizon/variable | Upon impact | 6 months | 12 months | 18 months | 23 months |
|---|---|---|---|---|---|
| **CPI** | 0,00% | 0,68% | 2,75% | 4,63% | 5,54% |
| **WIP growth rate** | 0,00% | 10,16% | 12,73% | 12,27% | 10,97% |
| **Shadow rate** | 0,00% | 1,93% | 3,70% | 5,46% | 6,30% |
| **GFC** | 0,00% | 19,69% | 21,41% | 20,30% | 18,69% |
| **GFU** | 65,90% | 71,92% | 71,16% | 61,64% | 54,90% |

## MATLAB CODES

In this section the most important MATLAB codes used to retrieve the results of this empirical research will be displayed. More specifically, five MATLAB files will be reported. The first one refers to the codes required to run the Granger Causality tests and to get the figures described in Chapter 4. The second and the third ones contain the codes employed to achieve the results illustrated in Chapter 5. The fourth one is comprehensive of all the codes used to plot IRFs and to write the tables of FEVDs. Finally, the fifth one allows to generate *Figure 27* and *Figure 28.*

Notice that we have made use of two main sources: the third version of the VAR toolbox elaborated by Ambrogio Cesa-Bianchi and the codes employed by Caldara et al. (2016). The VAR toolbox can be freely downloaded at: "https://sites.google.com/site/ambropo/MatlabCodes". Some adjustments have been applied to both these sets of codes in order to produce the overmentioned results, of course.

```
%=========================================================================
%% A PRELIMINARY ANALYSIS OF THE RELATIONSHIPS BETWEEEN UNCERTAINTY MEASURES
AND GFC: GRANGER CAUSALITY TESTS AND CORRELATIONS
%=========================================================================

%% PRELIMINARIES
%=========================================================================
clear all; clear session; close all; clc
warning off all

for i=1:10
model_vec                                                                =
{'GPRvsGEPU','GPRvsGFU','GEPUvsGFU','GPRvsGFC','GEPUvsGFC','GFUvsGFC','GPR
vsWIP','GEPUvsWIP', 'GFUvsWIP', 'GFCvsWIP'};
% Load data
[xlsdata, xlstext] = xlsread('DATI_tesi4.xlsx',model_vec{i});
X = xlsdata;
dates = xlstext(2:end,1);
vnames = xlstext(1,2:end);
nvar = length(vnames);
D=datenum(dates,'yyyy-mm');

%pairwise correlations
[rho,pval] = corr(X,X)
correl= num2str(round(rho(2,1),3));

%% PLOT UNCERTAINTY MEASURES
%=========================================================================
%plot time series, displaying pairwise correlations
figure
if i==1
plot(X(:,1),'LineWidth',1.5,'Color','g');
hold on
plot(X(:,2),'LineWidth',1.5, 'Color','c');
elseif i==2
plot(X(:,1),'LineWidth',1.5,'Color','g');
hold on
```

```
plot(X(:,2),'LineWidth',1.5, 'Color','b');
elseif i==3
plot(X(:,1),'LineWidth',1.5,'Color','c');
hold on
plot(X(:,2),'LineWidth',1.5, 'Color','b');
elseif i==4
plot(X(:,1),'LineWidth',1.5,'Color','g');
hold on
plot(X(:,2),'LineWidth',1.5, 'Color','r');
elseif i==5
plot(X(:,1),'LineWidth',1.5,'Color','c');
hold on
plot(X(:,2),'LineWidth',1.5, 'Color','r');
elseif i==6
plot(X(:,1),'LineWidth',1.5,'Color','b');
hold on
plot(X(:,2),'LineWidth',1.5, 'Color','r');
elseif i==7
plot(X(:,1),'LineWidth',1.5,'Color','g');
hold on
plot(X(:,2),'LineWidth',1.5, 'Color','m');
elseif i==8
plot(X(:,1),'LineWidth',1.5,'Color','c');
hold on
plot(X(:,2),'LineWidth',1.5, 'Color','m');
elseif i==9
plot(X(:,1),'LineWidth',1.5,'Color','b');
hold on
plot(X(:,2),'LineWidth',1.5, 'Color','m');
elseif i==10
plot(X(:,1),'LineWidth',1.5,'Color','r');
hold on
plot(X(:,2),'LineWidth',1.5, 'Color','m');
end

h=size(D,1);
SelectedDates=datestr(D(1:12:end),'yyyy-mm');
```

```
ax=gca;
set(ax,'XTick',(1:12:h),'XTickLabel',SelectedDates);
txt = {['\rho_{XY} = ' correl]};
if i==10
text(150,102,txt,'FontSize',13)
else
text(150,103,txt,'FontSize',13)
end
title([vnames{1} ' and ' vnames{2}],'FontSize',15);
legend(vnames{1},vnames{2},'FontSize',11);
grid on
savefig(['./results/comparisons/' model_vec{i} '.fig']);
hold off

%% GRANGER CAUSALITY TESTS
%=========================================================================
%Granger causality test 6 lags
causedata = X(:,1);
EffectsData = X(:,2);
[hgc(1),pvalue(1),stat(1),cvalue(1)] = gctest(causedata,EffectsData,...
    NumLags=6)

%Granger causality test 6 lags
causedata = X(:,2);
EffectsData = X(:,1);
[hgc_1(1),pvalue_1(1),stat_1(1),cvalue_1(1)]                              =
gctest(causedata,EffectsData,...
    NumLags=6)

%Granger causality test 7 lags
causedata = X(:,1);
EffectsData = X(:,2);
[hgc_2(1),pvalue_2(1),stat_2(1),cvalue_2(1)]                              =
gctest(causedata,EffectsData,...
    NumLags=7)

%Granger causality test 7 lags
```

```
causedata = X(:,2);
EffectsData = X(:,1);
[hgc_3(1),pvalue_3(1),stat_3(1),cvalue_3(1)]                                =
gctest(causedata,EffectsData,...
    NumLags=7)

%Granger causality test 12 lags
causedata = X(:,1);
EffectsData = X(:,2);
[hgc_2(1),pvalue_2(1),stat_2(1),cvalue_2(1)]                                =
gctest(causedata,EffectsData,...
    NumLags=12)

%Granger causality test 12 lags
causedata = X(:,2);
EffectsData = X(:,1);
[hgc_3(1),pvalue_3(1),stat_3(1),cvalue_3(1)]                                =
gctest(causedata,EffectsData,...
    NumLags=12)

%Granger causality test 24 lags
causedata = X(:,1);
EffectsData = X(:,2);
[hgc_4(1),pvalue_4(1),stat_4(1),cvalue_4(1)]                                =
gctest(causedata,EffectsData,...
    NumLags=24)

%Granger causality test 24 lags
causedata = X(:,2);
EffectsData = X(:,1);
[hgc_5(1),pvalue_5(1),stat_5(1),cvalue_5(1)]                                =
gctest(causedata,EffectsData,...
    NumLags=24)

%% FEEDBACK TESTS
%=========================================================================
%Feedback test at lag 6
```

```
causedata = X(:,1);
EffectsData = X(:,2);
[hgc_f1(1),pvalue_f1(1),stat_f1(1),cvalue_f1(1)]                    =
gctest(causedata,EffectsData, Alpha=0.025,...
    NumLags=6)
causedata = X(:,2);
EffectsData = X(:,1);
[hgc_f1(2),pvalue_f1(2),stat_f1(2),cvalue_f1(2)]                    =
gctest(causedata,EffectsData, Alpha=0.025,...
    NumLags=6)

%Feedback test at lag 7
causedata = X(:,1);
EffectsData = X(:,2);
[hgc_f2(1),pvalue_f2(1),stat_f2(1),cvalue_f2(1)]                    =
gctest(causedata,EffectsData, Alpha=0.025,...
    NumLags=7)
causedata = X(:,2);
EffectsData = X(:,1);
[hgc_f2(2),pvalue_f2(2),stat_f2(2),cvalue_f2(2)]                    =
gctest(causedata,EffectsData, Alpha=0.025,...
    NumLags=7)

%Feedback test at lag 12
causedata = X(:,1);
EffectsData = X(:,2);
[hgc_f2(1),pvalue_f2(1),stat_f2(1),cvalue_f2(1)]                    =
gctest(causedata,EffectsData, Alpha=0.025,...
    NumLags=12)
causedata = X(:,2);
EffectsData = X(:,1);
[hgc_f2(2),pvalue_f2(2),stat_f2(2),cvalue_f2(2)]                    =
gctest(causedata,EffectsData, Alpha=0.025,...
    NumLags=12)

%Feedback test at lag 24
causedata = X(:,1);
```

```
EffectsData = X(:,2);
[hgc_f3(1),pvalue_f3(1),stat_f3(1),cvalue_f3(1)]                              =
gctest(causedata,EffectsData, Alpha=0.025,...
    NumLags=24)
causedata = X(:,2);
EffectsData = X(:,1);
[hgc_f3(2),pvalue_f3(2),stat_f3(2),cvalue_f3(2)]                              =
gctest(causedata,EffectsData, Alpha=0.025,...
    NumLags=24)

save(['./results/comparisons/' model_vec{i} '.mat'])

clear
end

%% PLOT ALL THE UNCERTAINTY MEASURES IN THE SAME FIGURE
%=========================================================================
% Load data
[xlsdata, xlstext] = xlsread('DATI_tesi4.xlsx','GPRvsGEPUvsGFU');
X = xlsdata;
dates = xlstext(2:end,1);
vnames = xlstext(1,2:end);
nvar = length(vnames);
D=datenum(dates,'yyyy-mm');

figure
plot(X(:,1),'LineWidth',1.5, 'Color','g');
hold on
plot(X(:,2),'LineWidth',1.5, 'Color','c');
hold on
plot(X(:,3),'LineWidth',1.5, 'Color','b');
h=size(D,1);
SelectedDates=datestr(D(1:12:end),'yyyy-mm');
ax=gca;
set(ax,'XTick',(1:12:h),'XTickLabel',SelectedDates);
title([vnames{1} ', ' vnames{2} ' and ' vnames{3}],'FontSize',15);
legend(vnames{1},vnames{2},vnames{3},'FontSize',11);
```

```
grid on
savefig('./results/comparisons/GPRvsGEPUvsGFU.fig');
hold off



%=========================================================================
%% CHOLESKY SPECIFICATION: ESTIMATION, IRFS AND FEVDS
%=========================================================================
%% PRELIMINARIES
%=========================================================================
clear all; clear session; close all; clc
warning off all
% Determine where your m-file's folder is
folder = fileparts(mfilename);
% Add that folder plus all subfolders to the path
addpath(genpath(folder));
addpath(genpath('./v3dot0'))

model_vec = {'GEPU','GPR','GFU'};

for i=1:3
% Load data
[xlsdata, xlstext] = xlsread('DATI_tesi.xlsx',model_vec{i});
X = xlsdata;
dates = xlstext(2:end,1);
vnames = xlstext(1,2:end);
nvar = length(vnames);
D = datenum(dates,'yyyy-mm');
% Observations
nobs = size(X,1);

%% TIME SERIES AND SACFs
%=========================================================================
%Plot GEPU
if i==1
figure
```

```
FigSize(26,18)
    plot(X(:,5),'LineWidth',3,'Color',cmap(1));
    title(['GEPU time series'],'FontSize',15);
    h=size(D,1);
    SelectedDates=datestr(D(1:12:end),'yyyy-mm');
    ax=gca;
    set(ax,'XTick',(1:12:h),'XTickLabel',SelectedDates);
    grid on;
    savefig(['./results/Cholesky/GEPU time series.fig']);
end
hold off

%Plot WIP, CPI, shadowrate, GPR and GFC
model_variables = {'CPI','log(WIP)100','shadowrate','GFC','GPR'};
if i==2
    for ii = 1:5
    figure
    FigSize(26,18)
    plot(X(:,ii),'LineWidth',3,'Color',cmap(1));
    title([model_variables{ii} ' time series'],'FontSize',15);
    h=size(D,1);
    SelectedDates=datestr(D(1:12:end),'yyyy-mm');
    ax=gca;
    set(ax,'XTick',(1:12:h),'XTickLabel',SelectedDates);
    grid on;
    savefig(['./results/Cholesky/'      model_variables{ii}      '      time
series.fig']);
    hold off
    end
end
hold off

%Plot GFU
hold off
if i==3
    figure
    FigSize(26,18)
```

```
    plot(X(:,5),'LineWidth',3,'Color',cmap(1));
    title(['GFU time series'],'FontSize',15);
    h=size(D,1);
    SelectedDates=datestr(D(1:12:end),'yyyy-mm');
    ax=gca;
    set(ax,'XTick',(1:12:h),'XTickLabel',SelectedDates);
    grid on;
    savefig(['./results/Cholesky/GFU time series.fig']);
end
hold off

%Plot series together
figure
FigSize(26,18)
title(['Variables time series - ' model_vec{i}],'FontSize',15);
for ii=1:nvar
    subplot(3,2,ii)
    H(ii) = plot(D,X(:,ii),'LineWidth',3,'Color',cmap(1));
    title(vnames(ii));
    datetick('x', 'yyyy-mm');
    grid on;
end
savefig(['./results/Cholesky/Variables time series - ' model_vec{i}
'.fig']);
hold off

%compute SACF of time series
figure
title(['Time series SACF - ' model_vec{i}],'FontSize',15);
for ii=1:nvar
subplot(3,2,ii);
autocorr(X(:,ii));
title(vnames(ii));
end
savefig(['./results/Cholesky/Time series SACF - ' model_vec{i} '.fig']);

%% VAR ESTIMATION
```

```
%=========================================================================
% Set deterministics for the VAR
det = 1;
% Set number of nlags
nlags = 6;
% Estimate VAR
[VAR, VARopt] = VARmodel(X,nlags,det);
% Print estimation on screen
VARopt.vnames = vnames;
[TABLE, beta] = VARprint(VAR,VARopt,4);
VARopt.frequency = 'm';

% white noise test for residuals. As a first step, display residuals time
series. If they are not white noises, we have to
% add lags
figure
title(['Residuals overview - ' model_vec{i}]);
for ii=1:nvar
subplot(3,2,ii);
plot(D(7:end,:),VAR.resid(:,ii));
title(vnames(ii));
datetick('x', 'yyyy-mm');
end
savefig(['./results/Cholesky/Residuals overview - ' model_vec{i} '.fig']);

%Second, plot residuals ACF
figure
title(['Residuals ACF - ' model_vec{i}]);
for ii=1:nvar
subplot(3,2,ii);
autocorr(VAR.resid(:,ii));
title(vnames(ii));
end
savefig(['./results/Cholesky/Residuals ACF - ' model_vec{i} '.fig']);

%% COMPUTE IR and VD
%=========================================================================
```

```
% Set some options for IRF calculation
VARopt.nsteps = 24;
VARopt.ident = 'short';
VARopt.vnames = vnames;
VARopt.FigSize = [26,12];
VARopt.pctg  = 68;      % confidence level for bootstrap
% Compute IRF
[IRF, VAR] = VARir(VAR,VARopt);
% Compute error bands
[IRinf,IRsup,IRmed,IRbar] = VARirband(VAR,VARopt);
% Plot
VARirplot(IRbar,VARopt,IRinf,IRsup);

% Compute VD
[VD, VAR] = VARvd(VAR,VARopt);
% Compute VD error bands
[VDinf,VDsup,VDmed,VDbar] = VARvdband(VAR,VARopt);

% Retrieve Forecast Error Variance Decomposition on an excel file
FEVD_Table(1, :) = VD(1:24,5,1);
FEVD_Table(2, :) = VD(1:24,5,2);
FEVD_Table(3, :) = VD(1:24,5,3);
FEVD_Table(4, :) = VD(1:24,5,4);
FEVD_Table(5, :) = VD(1:24,5,5);

filename = 'FEVD_thesis.xlsx';
writematrix(FEVD_Table,filename,'Sheet', [model_vec{i}]);

%% SAVE RESULTS
%=========================================================================
model_vec_1=strcat('./results/Cholesky/',model_vec{i},'_Chol.mat');
model_vec_2=strcat('./results/Cholesky/',model_vec{i},'_Chol_results.mat')
;
save(model_vec_1,"IRbar","IRmed","IRsup","IRinf","VDbar","VDmed","VDsup","
VDinf"); %to save only the IRFs and FEVDs
save(model_vec_2) % save all
end
```

```
%=========================================================================
%% PFA SPECIFICATIONS: ESTIMATION, IRFS AND FEVDS
%This is a modified version of the code elaborated by Caldara et al.(2016)
to estimate the SVAR models applying the PFA
%=========================================================================
%----------------------
%% Maximization of Marginal Density functions for Minnesota prior
%----------------------

MAIN_MAX_MDD_1

%----------------------
%% Housekeeping
%----------------------

clear all;
clc;
close all;


addpath(genpath('./thesis_codes/EER-D-16-00143_replication_files/EER-D-16-
00143_replication_files/results'))
addpath(genpath('./thesis_codes/EER-D-16-00143_replication_files/EER-D-16-
00143_replication_files/auxfiles'))
addpath(genpath('./v3dot0'))

%----------------------
%% Specify Settings
%----------------------

for minn_prior= 0:1 % Minnesota Prior (0= natural conjugate gaussian inverse-
wishart prior)
model_vec       = {'GPR','GFU','GEPU'}; % Select models to be estimated (see
model_spec_1.m)

p    = 6;          % Number of lags
```

```
T0  = 24;          % Pre-sample for Minnesota Prior
nex = 1;           % Deterministic terms (1: constant)

nd    = 1000;    % Number of draws in MC chain
bburn = 0.2*nd;   % Burn-in, i.e. the number of draws from MC chain that we
discard intentionally starting from the first draw. This should ensure more
accurate estimates from MC

Horizon = 23;     % Horizon for impulse responses and forecast
                  % error variance decomposition
pctg=68;          %Confidence band for irf and fevd.
pctg_inf = (100-pctg)/2;           %16 for pctg=68;
pctg_sup = 100 - (100-pctg)/2;     %84 for pctg=68


ptileVEC  = [pctg_inf 50 pctg_sup]; % Percentiles of posterior distributions
to be stored

randn('state',294015341); % Seed for random number generator (create a square
matrix 294015341 by 294015341 whose elements are numbers drawn randomly and
independently from a normal distribution).
                          % This works as pseudo casual number generator for
Monte Carlo chain in the sense that it provides draws of numbers to seed the
MC chain
%----------------------
%% Load database
%----------------------

data_file = 'Dati_tesi1';

newData1 = importdata(strcat(data_file,'.xlsx'),' ');

% Create new variables in the base workspace from those fields.

vars = fieldnames(newData1);
for i = 1:length(vars)
    assignin('base', vars{i}, newData1.(vars{i}));
```

```
end
YYdata = data;

clear data
nDate = datenum(textdata(2:end,1));

for iii = 1:size(model_vec,2)
    mmodel = model_vec(:,iii);
    model_spec_1
    n = size(i_var_str,2);  % Number of Endogenous variables

    %------------------------------------------------
    %% Generate dummy observations for prior
    %------------------------------------------------

    vm_dummy_1

    %------------------------------------------------
    %% Generate settings for penalty function algorithm
    %------------------------------------------------

    RR =zeros(nv);
         RR(1,1) = 1; % Selection matrix of variables entering the penalty
function (see uhligpenalty.m)
         RR(2,2) = 1;
         nper = 6;    % Include impulse responses from period 1 to nper in
the PF
         nshocks=2;   % Number of shocks to be identified

    %------------------------------------------------------------
    %%     DEFINITION OF DATA, LAG STRUCTURE AND POSTERIOR SIMULATION
    %------------------------------------------------------------

    if minn_prior ==0
        X          = XXact;
        Y          = YYact;
        T          = nobs;
```

```
    elseif minn_prior ==1
        X           = [XXact; XXdum];
        Y           = [YYact; YYdum];
        T           = nobs+Tdummy;
    end

    %--------------------------
    %% Estimation Preliminaries
    %--------------------------


    % Define matrices to compute IRFs

    J = [eye(n);repmat(zeros(n),p-1,1)];
    F = zeros(n*p,n*p);    % Matrix for Companion Form
    I  = eye(n);
    for i=1:p-1
        F(i*n+1:(i+1)*n,(i-1)*n+1:i*n) = I;
    end

    % Compute OLS estimates

    B = (X'*X)\(X'*Y); % Point estimates
    U = Y-X*B;      % Residuals
    Sigmau = U'*U/(T-p*n-1);   % Covariance matrix of residuals

% white noise test for residuals. Display residuals of VAR model and the
related SACFs for each time series. If they are not white noises, we have to
% add lags
init=sample_init_row+T0;
if minn_prior==0
ndate1=nDate;
elseif minn_prior==1
ndate2= (nDate(end)+1:30:nDate(end)+(Tdummy*30));
ndate1=[nDate;ndate2'];
end
```

```
figure('Name','Residuals overview');
for i=1:5
subplot(3,2,i);
plot(ndate1(init:end,:),U(:,i));
title(i_var_str_names(i));
datetick('x', 'yyyy-mm');
end
savefig(strcat('./results/Residuals
Overview_',model_vec{iii},'_',num2str(minn_prior),'.fig'));

figure('Name','Residuals ACF');
for i=1:5
subplot(3,2,i);
autocorr(U(:,i));
title(i_var_str_names(i));
end
savefig(strcat('./results/Residuals
ACF_',model_vec{iii},'_',num2str(minn_prior),'.fig'));

    % Identification of shocks at OLS estimates
    s = sqrt(diag(Sigmau));
    LC = chol(Sigmau)';

    % initialize Omega1 for calculation of impulse responses

    Omega1 = [LC;zeros((p-1)*n,size(LC,2))];
    A0 = (LC')\eye(size(LC,1));
    F(1:n,1:n*p)    = B(1:n*p,:)';
    Fols = F;
    eigen           = eig(F);
    eigen           = max(eigen);
    largeeig        = abs(eigen);   % Compute the largest eigenvalue

    [mufactorOLS, fflag] = uhligpenalty(LC,Fols,s,RR,nper,nshocks);

    %--------------------------
```

```
    %% Bayesian Estimation
    %-------------------------
    % Define objects that store the draws
    nCalc=0;
    i_transf=[];

    LtildeAdd    = zeros(nd-bburn,Horizon+1,n,nshocks); % Array that stores
impulse responses
    Ltilde       = zeros(nd-bburn,Horizon+1,n,nshocks);  % Array that stores
impulse responses from model variables
    W            = zeros(nd-bburn,Horizon+1,n,nshocks); % Array that stores
forecast error variance decomposition

    % Set preliminaries for priors
    %The general formulae to retrieve the parameters that
    %describe the posterior distribution for Sigma and B, that is supposed
to be a normal-Wishart one, are provided. According to the
    %hypotheses that they applied, the parameters are simply equal to:
nnuT=T, NT=X'*X, BbarT=OLS
    %estimate for B, ST= the OLS estimate for Sigma.
    if minn_prior ==0
        N0=zeros(size(X',1),size(X,2));
        nnu0=0;
        nnuT = T +nnu0;
        NT = N0 + X'*X;
        Bbar0=B;
        S0=Sigmau;
        BbarT = NT\(N0*Bbar0 + (X'*X)*B);
        ST    =    (nnu0/nnuT)*S0    +    (T/nnuT)*Sigmau    +    (1/nnuT)*((B-
Bbar0)')*N0*(NT\eye(n*p+nex))*(X'*X)*(B-Bbar0); %This is equal to Sigmau,
i.e. the OLS estimate for var cov matrix
        STinv = ST\eye(n); %the inverse matrix of ST
        m=size(B,1);
        R=zeros(n,nnuT);
    end

%Here, we are starting the loop for Bayesian estimation based on MC Direct
```

```
%sampling. Record goes from 0 to 1000, the number of draws that we have set.
    record=0;
    counter = 0;

    disp('                                                              ');
    disp('       BAYESIAN ESTIMATION OF VAR: DIRECT SAMPLING...         ');
    disp('                                                              ');

    while record<nd

        if minn_prior == 1
            %Monte Carlo chain sampling starts, when supposing Minnesota
prior
            % Draws from the density Sigma | Y
            Sigmadraw   = iwishrnd(Sigmau*(T-n*p-1),T-n*p-1);
            % Draws from the density vec(Phi) |Sigma(j), Y
            B_new                                                       =
mvnrnd(reshape(B,n*(n*p+1),1),kron(Sigmadraw,inv(X'*X)));
            % Rearrange vec(Phi) into Phi
            Bdraw     = reshape(B_new,n*p+1,n);

        elseif minn_prior == 0

            %Monte Carlo chain sampling starts, when supposing Conjugate
Gaussian Inverse Wishart prior
            % Step 1: Draw from the marginal posterior for Sigmau
p(Sigmau|Y,X)
            R=mvnrnd(zeros(n,1),STinv/nnuT,nnuT)';
            %   It returns a N-by-D matrix R of random vectors
            %   chosen from the multivariate normal distribution with 1-by-
D mean
            %   vector MU, and D-by-D covariance matrix SIGMA. This is the
            %   first draw for R, that is the matrix used to retrieve a draw
for Sigma from its posterior.
            Sigmadraw=(R*R')\eye(n); %this is the inverse of squared R and
a draw for the var cov matrix from its posterior.
```

```
            % Step 2: Taking newSigma as given draw for B using a
multivariate normal
            bbeta = B(:); %reshape B as column vector
            SigmaB = kron(Sigmadraw,NT\eye(n*p+nex)); %we are making the
kronocker product, i.e. we are multiplyng each element of the inverse of
squared R by the matrix NT\eye(n*p+nex)
            SigmaB = (SigmaB+SigmaB')/2;
            Bdraw = mvnrnd(bbeta,SigmaB); %draw B from its posterior, that
we assume to follow a mvrnd with mean equal to sample OLS estimates of
coefficients and variance-coviariance matrix
            %equal to SigmaB
            Bdraw     = reshape(Bdraw,n*p+1,n);

        end

        Bdraw= reshape(Bdraw,n*p+nex,n); % Reshape Bdraw from vector to
matrix
        LC =chol(Sigmadraw,'lower');
        F(1:n,1:n*p)    = Bdraw(1:n*p,:)';

        record=record+1; %in such a way, the procedure of sampling restarts
for each posterior parameter
        counter = counter +1;

        if counter==0.05*nd
            disp(['         DRAW NUMBER:   ', num2str(record)]);
            disp('                                                        ');
            disp(['     REMAINING DRAWS:   ', num2str(nd-record)]);
            disp('                                                        ');
            counter = 0;
        end

        if record > bburn  %when we have drawn a number of observations
higher than bburn, i.e.200, we can use each draw to compute IRFs and FEVDs
            s = sqrt(diag(Sigmadraw));
            [mufactor, fflag] = uhligpenalty(LC,F,s,RR,nper,nshocks);
```

```
            Utildedraw = YYact-XXact*Bdraw;

            IRF_T = vm_irf(F,J,mufactor,Horizon+1,n,Omega1);
            IRF_T = IRF_T(:,:,1:nshocks);

            Ltilde(record-bburn,:,:,:) = IRF_T;

            if fflagFEVD ==1
                W(record-
bburn,:,:,:)=variancedecompositionFD(F,J,Sigmadraw,mufactor(:,1:nshocks),n
,Horizon,i_transf);
            end
        end

    end

    LtildeAdd(:,:,1:n,:) = Ltilde;
    LtildeFull = prctile(LtildeAdd(bburn+1:end,: ,:,:),ptileVEC);
    VAR.LtildeFull = permute(LtildeFull,[3,2,1,4]);

    WhFull = prctile(W(bburn+1:end,:,:,:),ptileVEC);
    VAR.WhFull = permute(WhFull,[3 2 1 4]);

    VAR.i_var_str_names = i_var_str_names;

    %% Plot IRFs and store FEVDs into an excel file
    IRF_plots

%save FEVD and IRF for each model and prior in different mat files

save(strcat('./results/PFAspec_',char(mmodel),'Iden_1_PF',num2str(nper),'.
mat'),'VAR');
end
end

%=========================================================================
%% IRFS AND FEVDS OF UNCERTAINTY SHOCKS
```

```
%It is the MATLAB file IRF_plots.m
%=========================================================================

%% PRELIMINARIES
%=========================================================================
h=size(VAR.LtildeFull,2);
% Define a timeline
steps = 1:1:h;
x_axis = zeros(1,h);
LtildeFull1=VAR.LtildeFull([5 4 3 2 1],:,:,:); %reorder rows of matrix of
IRF in a way that the order of variables will be the same as that of the
Cholesky specification
i_var_str_names1=VAR.i_var_str_names(:,[5 4 3 2 1]); %reorder variables'
names in a way that the order will be the same as that of the Cholesky
specification

%% IRFs to uncertainty shocks
%=========================================================================
figure;
FigSize(26,12)
SwatheOpt = PlotSwatheOption;
SwatheOpt.marker = '*';
SwatheOpt.trans = 1;
if minn_prior==1
SwatheOpt.swathecol= 'yellow';
else
SwatheOpt.swathecol= 'green';
end
for i=1:size(LtildeFull1,1)
    subplot(2,3,i);
    plot(steps,LtildeFull1(i,:,2,1),'LineStyle','-
','Color','k','LineWidth',2,'Marker',SwatheOpt.marker); hold on
    PlotSwathe(LtildeFull1(i,:,2,1),[LtildeFull1(i,:,1,1);
LtildeFull1(i,:,3,1)],SwatheOpt); hold on;
    plot(x_axis,'--k','LineWidth',0.5); hold on
    xlim([1 h]);
```

```
    title([i_var_str_names1{i}      '      to      '      model_vec{iii}],
'FontWeight','bold','FontSize',10);
    set(gca, 'Layer', 'top');
    savefig(['./results/IRF    to    a    '    model_vec{iii}    '    shock_'
num2str(minn_prior)]);
end

%% FEVDs of uncertainty shocks
%=========================================================================
WhFull1=VAR.WhFull([5 4 3 2 1],:,:,:); %reorder rows of matrix of FEVD in a
way that the order of variables will be the same as that of the Cholesky
specification
%display FEVDs in a table
FEVD_Table = WhFull1(:,:,2,1);
disp(' ')
disp(['Percentage Variance due to a ' model_vec{iii} ' shock (t= from 0 to
23)'])
disp('-------------------------------------------------')
filename = 'FEVD_thesis.xlsx';
%store FEVDs into a specific excel file
writematrix(FEVD_Table,filename,'Sheet',strcat('PFA_',num2str(minn_prior),
'_',model_vec{iii}));

%save IRFs and FEVDs
if minn_prior==1
   result_str={'Minn'};
else
   result_str={'Conj'};
end
result_name=strcat('./results/',model_vec{iii},'_',result_str,'.mat');
save(char(result_name),"LtildeFull1","WhFull1");


%=========================================================================
%% IRFS AND FEVDS OF GFC: AN OVERVIEW
%=========================================================================
%% PRELIMINARIES
```

```
%=========================================================================
clear all; clear session; close all; clc
warning off all

addpath(genpath('./EER-D-16-00143_replication_files/EER-D-16-
00143_replication_files/results'))
addpath(genpath('./EER-D-16-00143_replication_files/EER-D-16-
00143_replication_files/auxfiles'))
addpath(genpath('./v3dot0'))

variable_vec={'GEPU','GEPU','GEPU','GFU','GFU','GFU','GPR','GPR','GPR'};
spec_vec={'Chol','PFA - Min','PFA - Conj','Chol','PFA - Min','PFA -
Conj','Chol','PFA - Min','PFA - Conj'};

h=24;
% Define a timeline
steps = 1:1:h;
x_axis = zeros(1,h);

%% IRFs TO UNCERTAINTY SHOCKS
%=========================================================================
figure;
FigSize(26,12)
for i=1:9
if i==1
load ./results/Cholesky/GEPU_Chol.mat
elseif i==2
load ./results/GEPU_Minn.mat
elseif i==3
load ./results/GEPU_Conj.mat
elseif i==4
load ./results/Cholesky/GFU_Chol.mat
elseif i==5
load ./results/GFU_Minn.mat
elseif i==6
load ./results/GFU_Conj.mat
elseif i==7
```

```
load ./results/Cholesky/GPR_Chol.mat
elseif i==8
load ./results/GPR_Minn.mat
else
load ./results/GPR_Conj.mat
end
spec_vec_1= spec_vec(:,i);
SwatheOpt = PlotSwatheOption;
SwatheOpt.trans = 1;
if strcmp(spec_vec_1,'PFA - Min')
    SwatheOpt.swathecol= 'yellow';
elseif strcmp(spec_vec_1,'PFA - Conj')
    SwatheOpt.swathecol= 'green';
end
if strcmp(spec_vec_1,'Chol')
    subplot(3,3,i);
    plot(steps,IRbar(:,4,5),'LineStyle','-
','Color','k','LineWidth',2,'Marker',SwatheOpt.marker); hold on
    PlotSwathe(IRbar(:,4,5),[IRinf(:,4,5)  IRsup(:,4,5)],SwatheOpt);  hold
on;
    plot(x_axis,'--k','LineWidth',0.5); hold on
    xlim([1 h]);
    xlabel(spec_vec_1,'FontWeight','bold','FontSize',10);
    title(['GFC to ' variable_vec{i}], 'FontWeight','bold','FontSize',10);
    set(gca, 'Layer', 'top');
 else
    subplot(3,3,i);
    plot(steps,LtildeFull1(4,:,2,1),'LineStyle','-
','Color','k','LineWidth',2,'Marker',SwatheOpt.marker); hold on
    PlotSwathe(LtildeFull1(4,:,2,1),[LtildeFull1(4,:,1,1);
LtildeFull1(4,:,3,1)],SwatheOpt); hold on;
    plot(x_axis,'--k','LineWidth',0.5); hold on
    xlim([1 h]);
    xlabel(spec_vec_1,'FontWeight','bold','FontSize',10);
    title(['GFC to ' variable_vec{i}], 'FontWeight','bold','FontSize',10);
    set(gca, 'Layer', 'top');
end
```

```
end
savefig("IRF of GFC to uncertainty shocks");
hold off

%% FEVDs of uncertainty shocks with respect to GFC
%=========================================================================
figure;
FigSize(26,12)
for i=1:9
if i==1
load ./results/Cholesky/GEPU_Chol.mat
elseif i==2
load ./results/GEPU_Minn.mat
elseif i==3
load ./results/GEPU_Conj.mat
elseif i==4
load ./results/Cholesky/GFU_Chol.mat
elseif i==5
load ./results/GFU_Minn.mat
elseif i==6
load ./results/GFU_Conj.mat
elseif i==7
load ./results/Cholesky/GPR_Chol.mat
elseif i==8
load ./results/GPR_Minn.mat
else
load ./results/GPR_Conj.mat
end
spec_vec_1= spec_vec(:,i);
SwatheOpt = PlotSwatheOption;
SwatheOpt.trans = 1;
if strcmp(spec_vec_1,'PFA - Min')
    SwatheOpt.swathecol= 'yellow';
    WhFull1=WhFull1*100;
elseif strcmp(spec_vec_1,'PFA - Conj')
    SwatheOpt.swathecol= 'green';
    WhFull1=WhFull1*100;
```

```
end
if strcmp(spec_vec_1,'Chol')
    subplot(3,3,i);
    plot(steps,VDbar(:,5,4),'LineStyle','-
','Color','k','LineWidth',2,'Marker',SwatheOpt.marker); hold on
    PlotSwathe(VDbar(:,5,4),[VDinf(:,5,4)  VDsup(:,5,4)],SwatheOpt);  hold
on;
    plot(x_axis,'--k','LineWidth',0.5); hold on
    xlim([1 h]);
    ylim([0 80]);
    xlabel(spec_vec_1,'FontWeight','bold','FontSize',10);
    title(['GFC to ' variable_vec{i}], 'FontWeight','bold','FontSize',10);
    set(gca, 'Layer', 'top');
 else
    subplot(3,3,i);
    plot(steps,WhFull1(4,:,2,1),'LineStyle','-
','Color','k','LineWidth',2,'Marker',SwatheOpt.marker); hold on
    PlotSwathe(WhFull1(4,:,2,1),[WhFull1(4,:,1,1);
WhFull1(4,:,3,1)],SwatheOpt); hold on;
    plot(x_axis,'--k','LineWidth',0.5); hold on
    ylim([0 80]);
    xlim([1 h]);
    xlabel(spec_vec_1,'FontWeight','bold','FontSize',10);
    title(['GFC to ' variable_vec{i}], 'FontWeight','bold','FontSize',10);
    set(gca, 'Layer', 'top');
end
end
savefig("FEVD of GFC to uncertainty shocks");
```